LIPOSOMAL CO-ENCAPSULATION OF QUERCETIN WITH SYNERGISTIC CHEMOTHERAPEUTIC DRUGS FOR BREAST CANCER TREATMENT

WONG MAN YI
(B.Sc. (Pharmacy) (Hons), National University of Singapore)

A THESIS SUBMITTED

FOR THE DEGREE OF DOCTOR OF PHILOSOPHY

DEPARTMENT OF PHARMACY

NATIONAL UNIVERSITY OF SINGAPORE

2010

ACKNOWLEDGEMENTS

I would like to thank my supervisor, Dr Gigi Chiu for her invaluable support; Dr Giorgia Pastorin, thesis committee member for her advice on the project; Associate Professor Chui Wai Keung for taking the time to be my PhD qualifying examination examiner and Associate Professor Chan Sui Yung for her encouragement to pursue graduate studies.

In addition, I am grateful for Ms Tan Bee Jen's laboratory management so that it is conducive for conducting research, Ms Ng Swee Eng and Ms Ng Sek Eng for their help in handling administrative matters pertaining to chemical orders.

Last but not least, I would like to thank my laboratory mates, Mr Shaikh Mohammed Ishaque, Ms Anumita Chaudhury, Ms Ling Leong Uung and Mr Tan Kuan Boone for their insightful discussions and companionship.

TABLE OF CONTENTS

SUMMARY

Quercetin is a flavonoid commonly found in fruits and vegetables which exerts selective cytotoxicity on cancer cells and synergizes with chemotherapeutic drugs. However, its clinical usage has been hampered by low water solubility. Therefore, the objectives of this thesis were to (i) develop a liposomal formulation to solubilize quercetin, (ii) identify chemotherapeutic drugs that synergize with quercetin in breast cancer cells, (iii) co-encapsulate quercetin/drug combinations into liposomes, and (iv) evaluate the co-encapsulated formulation *in vitro* and *in vivo*. Liposomal encapsulation of quercetin was around 100%, increased its solubility by 10-fold, reduced quercetin degradation and the formulation was also physically stable. Quercetin synergized with (i) irinotecan and (ii) vincristine in the JIMT-1 and MDA-MB-231 breast cancer cell lines. Irinotecan could be encapsulated in DPPC/DSPE-PEG_{2000}/Quercetin (90:5:5 mole ratio) liposomes with around 80% efficiency and vincristine could be encapsulated in ESM/Cholesterol/PEG_{2000}-ceramide/Quercetin (72.5:17.5:5:5 mole ratio) liposomes with around 70% efficiency. Both formulations displayed controlled and co-ordinated release of the two agents. *In vitro* evaluation of liposomal vincristine/quercetin formulation comprising of ESM/Cholesterol/PEG_{2000}-ceramide/Quercetin 72.5:17.5:5:5 mole ratio demonstrated the

highest anti-cancer activity; thus, this formulation was further evaluated *in vivo*. Through liposomal co-encapsulation, plasma half lives of quercetin and vincristine were increased, and the synergistic ratio of the two drugs maintained. The formulation exhibited significant anti-tumor activity at two-thirds of the maximum tolerated dose of vincristine in a human epidermal growth factor 2 overexpressing, trastuzumab-resistant breast tumor xenograft model.

LIST OF TABLES

LIST OF FIGURES

A	Additive effect
ANOVA	Analysis of variance
AUC	Area under the curve
BEH	Bridged Ethyl Hybrid
CV	Coefficient of variation
CI	Combination index
CL	Total body clearance
C_{max}	Maximum plasma concentration of drug
D	Dose
D:L	Drug: Lipid ratio
D_m	Median effect concentration
DMPC	1,2-Dimyristoyl-sn-Glycero-3-Phosphocholine
DMPC	1,2-Dimyristoyl-sn-Glycero-3-Phosphocholine
DPPC	1,2-Dipalmitoyl-sn-Glycero-3-Phosphocholine
DPPH	2,2-diphenyl-1-picrylhydrazyl
DSC	Differential scanning calorimetry
DSPC	1,2-Distearoyl-sn-Glycero-3-Phosphocholine
DSPE-PEG_{2000}	1,2-Distearoyl-sn-Glycero-3-Phosphoethanolamine-N-[Amino(Polyethylene Glycol)$_{2000}$]
D_x	Dose of a drug that inhibits "x" percent of cells
EC_{50}	Median effective concentration
ED	Effective dose
EDTA	Ethylenediamminetetraacetic acid
EGFR	Epidermal growth factor receptor
EPC	Egg phosphatidylcholine
EPR	Enhanced permeability and retention effect
ER	Estrogen receptor
ESM	Egg sphingomyelin
f_a	Fraction of cells affected by treatment
FDA	Food and Drug Administration
HBS	4-(2-hydroxyethyl)-1-piperazineethanesulfonic acid buffered saline
HEPES	4-(2-hydroxyethyl)-1-piperazineethanesulfonic acid
HER2	human epidermal growth factor receptor 2
HPLC	High performance liquid chromatography

LC	Liquid chromatography
LLOQ	Lower limit of quantification
MAPT	microtubule-associated protein tau
MPS	Mononuclear phagocyte system
MRT	Mean residence time
MS	Mass spectrometry
MTD	Maximum tolerated dose
MTT	3-(4,5-diethylthiazoyl-2-yl)-2,5-diphenyltetrazolium bromide
O	Dose of drug A to attain the observed effect
PC	Phosphatidylcholine
PEG	Polyethylene Glycol
PR	Progesterone receptor
QELS	Quasi-elastic light scattering
r	Linear correlation coefficient
R^2	Coefficient of determination
r_a	Ratio of Drug A to B
RES	Reticuloendothelial system
R_f	Flory radius
RNA	Ribonucleic acid
SEM	Standard error of mean
SN-38	7-ethyl-10-Hydroxycamptothecin
T_c	Transition temperature
UPLC	Ultra performance liquid chromatography
V	Volume of distribution
α	Interaction index

LIST OF PUBLICATIONS, PRESENTATIONS AND AWARDS

Journal Publications

1. Man-Yi Wong, Gigi N.C. Chiu "Liposome formulation of co-encapsulated vincristine and quercetin enhanced antitumor activity in a trastuzumab-insensitive breast tumor xenograft model" Nanomedicine: Nanotechnology, biology and nanomedicine. (Accepted)
2. Man-Yi Wong, Gigi N.C. Chiu "Rapid and simultaneous determination of vincristine and quercetin in plasma by ultra performance liquid chromatography" Journal of Pharmaceutical and Biomedical Sciences (Accepted)
3. Bee Jen Tan, Kiah Shen Quek, Man-Yi Wong, Wai Keung Chui, Gigi N.C. Chiu. "Liposomal M-V-05: Formulation development and activity testing of a novel dihydrofolate reductase inhibitor for breast cancer therapy" International Journal of Oncology, 2010, 37, pp 211-218.
4. Wong, Man-Yi, Gigi N.C. Chiu. "Simultaneous liposomal delivery of quercetin and vincristine for enhanced estrogen-receptor negative breast cancer" Anti-Cancer Drugs, 2010, 21 (4), pp. 401-410.
5. Chiu, Gigi N.C., Wong, Man-Yi; Ling, Leong-Uung; Shaikh, Ishaque M., Tan, Kuan-Boone, Chaudhury, Anumita; Tan, Bee-Jen "Lipid-Based Nanoparticulate Systems for the Delivery of Anti-Cancer Drug Cocktails: Implications on Pharmacokinetics and Drug Toxicities" Current Drug Metabolism, 2009, 10 (8), pp. 861-874.
6. Wong, Man-Yi, Chiu, G.NC. "Development and characterization of a nanocarrier for quercetin" International Journal of Nanoscience, 2009, 8 (1-2), pp. 175-179.

Oral conference presentations

1. Man-Yi Wong, Tan Bee Jen, Amy Leo, Gigi N. Chiu "The use of natural compounds to enhance conventional chemotherapeutic drugs for breast cancer therapy" 19th Singapore Pharmacy Congress, 19th -21st October 2007, Singapore.

Conference abstracts

1. Wong, M.-Y., Chiu, G.N.C "Liposomal co-encapsulation of vincristine and quercetin enhances *in vivo* antitumor efficacy in a HER-2 overexpressing, trastuzumab-resistant breast tumor xenograft model" Accepted for presentation in 2010 FIP PSWC/AAPS Annual Meeting & Exposition, 14th–18th November 2010, New Orleans, United States of America.

2. Wong, M.-Y., Chiu, G.N.C "Simultaneous Determination of Vincristine and Quercetin in Plasma by Ultra Performance Liquid Chromatography" Accepted for presentation in 39th American College of Clinical Pharmacology Annual Meeting, 12th–14th September 2010, Baltimore, United States of America.
3. Wong, M.-Y., Chiu, G.N.C. "Co-encapsulation of quercetin and vincristine in liposomes for breast cancer therapy" 2009 AAPS Annual Meeting & Exposition, 8th–12th November 2009, Los Angeles, United States of America.
4. Man Yi Wong, Gigi N. Chiu "Assessment of synergistic activity of natural products with conventional chemotherapeutics on breast cancer cell lines" 20th Singapore Pharmacy Congress, 25th–26th July 2009, Singapore.
5. Man Yi Wong, Siew Jin Chen, Gigi Chiu "Co-encapsulation of apigenin and synergistic conventional chemotherapeutics in liposome formulations" 7th Globalization of Pharmaceutics Education Network Conference, 9th–12th September 2008, Leuven, Belgium.
6. Man Yi Wong, Gigi N. Chiu "Development & characterization of a combination chemotherapy formulation comprising quercetin & irinotecan" AACR Centennial Conference, 4th–8th November 2007, Singapore.
7. Kiah Shen Quek, Bee Jen Tan, Man Yi Wong, Wai Keung Chui, Gigi N. Chiu "Formulation development and *in vitro* efficacy study of a novel dihydrofolate reductase inhibitor" AACR Centennial Conference, 4th–8th November 2007, Singapore.

Awards

1. American Association of Pharmaceutical Scientists Annual Meeting 2009 Travel ship Award, Formulation Design and Development Section.
2. American College of Clinical Pharmacology Student Award 2010.

Chapter 1

BACKGROUND

1.1 Introduction

Drug delivery systems have been shown to improve the pharmacological properties of many drugs, resulting in increased circulation lifetimes, enhanced efficacy and reduced toxicity (Papahadjopoulos, Allen et al. 1991). Recently, drug delivery systems, such as liposomes (Zamboni 2005; Lee, Kim et al. 2006; Fanciullino and Ciccolini 2009), micelles (Koo, Rubinstein et al. 2006; Kedar, Phutane et al. 2010), and nanoparticles (Langer, Balthasar et al. 2003; Wang, Sui et al. 2010) have been used for systemic delivery of anti-cancer agents, enhancing the efficacy and ameliorating the toxicity of chemotherapeutic drugs. Therefore, this project aims to develop and characterize a drug delivery system for a natural product, quercetin, and to co-encapsulate conventional chemotherapeutic agents exhibiting synergism with quercetin so as to develop effective and novel treatment regimens against cancer.

1.2 Cancer overview

The National Cancer Institute defines cancer as a disorder in which abnormal cells divide without control and are able to

invade other tissues. Cancer development is a multi-step process which involves a series of gene mutations leading to gradual increases in tumor size, disorganization and malignancy (Vogelstein and Kinzler 1993). Due to the many different possible gene mutations, cancer is not a single disease but a group of diseases that differ in prognosis and response to treatment. Nevertheless, cancer cells have seven common characteristics, which are self-sufficiency in growth signals, insensitivity to antigrowth signals, evasion of apoptosis, limitless replicative potential, sustained angiogenesis, tissue invasion and metastasis (Hanahan and Weinberg 2000).

Globally, cancer is the leading cause of death, accounting for 7.9 million deaths, which constitute approximately 13% of all deaths (World Health Organization, Global cancer statistics, 2007). In addition, deaths from cancer are projected to continue rising to an estimated 12 million in 2030 worldwide. Of all cancers, breast cancer is the most common in women, with an estimated 1.15 million new cases worldwide annually and also the leading cause of cancer mortality in women (Parkin, Bray et al. 2005). Locally, the breast cancer incidence and mortality rates reflect these global trends as well (Singapore Cancer Registry Report, 2008). Despite their high prevalence and mortality rates, current treatment regimens for breast cancer remain unsatisfactory. The relapse rate for breast cancer patients is 85% (Bernard-Marty, Cardoso et al. 2004). This highlights the

need for the continued research to develop and improve treatment regimens against breast cancer.

1.3 Treatment regimens against breast cancer

Surgery and radiation are often used to treat early stage localized breast cancer. Besides surgery and radiation, additional treatment modalities include endocrine and biological therapy. Endocrine therapy with tamoxifen or aromatase inhibitors such as letrozole, anastrozole and exemestane are used in tumors expressing either estrogen and/or progesterone receptors. In addition, biological therapy with trastuzumab is used in tumors overexpressing human epidermal growth factor receptor 2 (HER2). With the advert of endocrine and biological therapy, tumors expressing estrogen, progesterone and HER2 receptors have better prognosis as compared to breast cancer subtypes that do not express these receptors (Dizdar and Altundag 2010; Keshtgar, Davidson et al. 2010).

Chemotherapy is the cornerstone therapy for advanced breast cancer, especially for breast cancers that do not express estrogen, progesterone and HER2 receptors. In addition, chemotherapy is not only given for the treatment of systemic disease, it can also be given before surgery to reduce tumor size (neoadjuvant chemotherapy) or after surgery or radiation (adjuvant treatment). It is also often combined with either

endocrine or biological therapy to reduce the chance of relapse and to improve overall survival. Despite the principal role of chemotherapy in cancer treatment, current treatment regimes remain suboptimal due to the narrow chemotherapeutic index of the anti-cancer agents, which limits the dose that can be given. Hence, there is great interest in investigating ways to reduce the toxicity and increase the efficacy of chemotherapeutic agents.

1.4 Quercetin overview

Quercetin (Figure 1) is the most common flavonoid present in many fruits and vegetables (Casagrande, Georgetti et al. 2006). It is non-toxic and has been administered with oral doses of 4g without side effects (Lamson and Brignall 2000). It has a wide range of biological actions, such as antioxidant (Saija, Scalese et al. 1995; Ratnam, Ankola et al. 2006), anti-inflammatory (Gonzalez-Gallego, Sanchez-Campos et al. 2007) and antiviral activities (Cushnie and Lamb 2005). In addition, recent epidemiological studies have described the beneficial effects of dietary flavonoids in the reduction of cancer risk (Ramos 2007), leading to great interest in the use of flavonoids for both chemoprevention and chemotherapy.

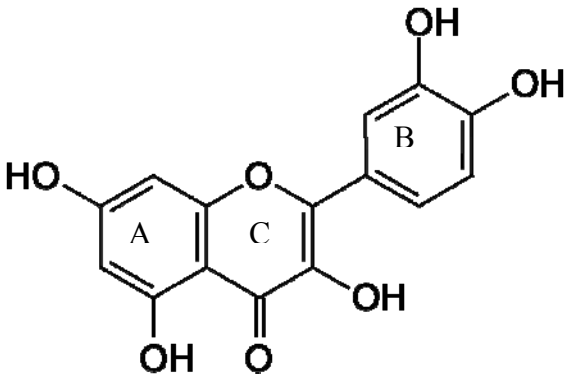

Figure 1 Structure of quercetin.

Recent *in vitro* studies have shown that quercetin exhibits antiproliferative activities in a wide range of cancers such as colon cancer (van der Woude, Gliszczynska-Swiglo et al. 2003), breast cancer (Hakimuddin, Paliyath et al. 2004), ovarian cancer (Ferry, Smith et al. 1996), prostate cancer (Chowdhury, Kishino et al. 2005) and lung cancer (Hung 2007). Quercetin exerts its antiproliferative effects through the inhibition of the PI3K-AKT/PKB pathway (Gulati, Laudet et al. 2006), downregulation of the expression of oncogenes and anti-oncogenes (Ranelletti, Maggiano et al. 2000), upregulation of cell cycle control proteins (Casagrande and Darbon 2001), inhibition of heat shock proteins (Sliutz, Karlseder et al. 1996), inhibition of tyrosine protein kinases such as epidermal growth factor receptor (EGFR) (Lee, Huang et al. 2002) and HER2 (Jeong, An et al. 2008) and through its interaction with Type II estrogen binding site (Scambia, Ranelletti et al. 1990). In addition, quercetin has been found to exhibit selective cytotoxic activity towards cancer cells

without affecting normal cells (Chowdhury, Kishino et al. 2005). As a consequence, there has been great interest in combining quercetin with conventional chemotherapeutic agents to enhance their therapeutic activities.

1.5 Methods to determine synergy

Combinations of chemotherapeutic agents can act in a synergistic, additive or antagonistic manner. Synergism occurs when the combined activities of the drugs are greater than predicted from the individual contribution of the individual drugs and antagonism occurs when the effect of combination is less than the sum of activities of the individual agents. Therefore, there is a need to evaluate whether the combination is synergistic, additive or antagonistic. In this Section, three of the most commonly used methods to determine synergy will be discussed. These methods are the isobologram (Loewe 1957; Steel and Peckham 1979), surface response analysis (Bliss 1939) and the median-effect principle (Chou and Talalay 1977).

In classical isobologram (Figure 2a), the concentrations of each drug, when used alone to attain a specific effect are plotted on the *x* and *y* axes on a graph (Loewe 1957). A line, called the line of additivity, is used to connect these two points. Subsequently, the concentrations of the drugs used in combination for the same effect is plotted in the same plot.

Synergy, additivity, or antagonism occurs when this point is located below, on, or above the line respectively.

The advantages of the classical isobologram method are that the isobologram is easy to plot and synergy, additivity or antagonism can be easily visualized from the graph. However, the disadvantages of this method are that it requires many experiments to attain the data needed to plot the isobologram, can only be used for fixed ratio drug combinations and fails to quantify the extent of synergism or antagonism.

In view of the disadvantages, Steel and Peckham further refined the classical isobologram method by developing an envelope of additivity which is enclosed within the boundaries of mode I and II curves in the isobologram (Figure 2b). The mode I curve is created by plotting a given dose of drug A against the dose of drug B needed to produce an effect equal to the difference between the chosen cytotoxic effect and the effect of the current dose of drug B. The mode II curve is generated by plotting the dose of drug A against the dose of drug B needed to increase the effect of drug B to the chosen effect level. For both modes, doses of drugs are varied to obtain a curve. Finally, the combination data obtained from experiments are plotted on the graph. Combinations of drugs that produce additive effects lay within the boundaries of Mode I and II, while combinations which produce effects displaced to the left are synergistic and combinations displaced to the right are antagonistic. The

advantage of this method is that the envelope of addivity helps to gauge whether the difference in addivity is large enough to warrant further investigation. Despite this, this method shares the other disadvantages of the classical isobologram, which are the large amount of data necessary to plot the graph and can only be used for fixed ratio drug combinations.

Another commonly used method is surface response analysis (Bliss 1939). In this method, the doses are plotted on the x and y axes and the effect are plotted on the z axis. Many different doses and effects are plotted on the 3 dimensional graph and a smooth surface representing the additivity of the combination is plotted (Figure 2c). A combination with values that are above the surface indicates a synergistic effect and an effect below this indicates antagonism. When a fixed ratio of drug combination is being used,

$$A = a + r_a b,$$

where A is the additive effect, a and b are the doses of Drug A and B used in combination and r_a is the ratio of drug A: B.

Subsequently,

$$\alpha = O/A$$

Where α represents the interaction index, O represents the dose of drug A to attain the observed effect obtained from the surface response graph. If α is less than one, there is synergism and if α is more than one there is antagonism.

The advantages of this method are that it gives a quantitative response which can be used to gauge and compare the extent of synergism of different drug combinations and doses. However, this method requires a complicated experimental design to obtain the large number of data points necessary and it is difficult to visualize the data points on the three dimensional graph.

The last method discussed here is the median-effect principle. In the median-effect principle, the dose of drug is correlated with cytotoxicity by the median-effect equation:

$$f_a / f_u = (D/D_m)^m \text{ or its alternative form,}$$

$$D = D_m[f_a / (1 - f_a)]^{1/m}$$

This equation is linearized,

$$\log (f_a / f_u) = m \log (D) - m \log D_m$$

and plotted as the median-effect plot,

where f_a refers the fraction affected by the dose, f_u is the fraction unaffected ($f_u = 1 - f_a$), D is the dose of the drug, D_m is the median-effect dose signifying the potency which is determined from the x-intercept of the median-effect plot. The value m is an exponent that signifies the sigmoidicity of the dose-effect curve, which is determined by the slope of the median-effect plot. In addition, the linear correlation coefficient r of the median-effect plot indicates the goodness of fit of the data to the equation.

For two drugs in which the effects of both drugs are mutually exclusive (with parallel median-effect plots for the

drugs and their drug combinations) and for drugs whose effects are mutually nonexclusive (non parallel median-effect plots for the drugs and their combinations), the general equation is:

$$[(f_a)_{1,2} / (f_u)_{1,2}]^{1/m}$$

$$= [(f_a)_1 / (f_u)_1]^{1/m} + [(f_a)_2 / (f_u)_2]^{1/m} + [(f_a)_1(f_a)_2 / (f_u)_1(f_u)_2]^{1/m}$$

$$= (D)_1 / (D_m)_1 + (D)_2 / (D_m)_2 + (D)_1(D)_2 / (D_m)_1(D_m)_2$$

Therefore, for mutually exclusive drug combinations,

$$CI = (D)_1 /(D_x)_1 + (D)_2 /(D_x)_2$$

And for mutually non exclusive drug combinations,

$$CI = (D)_1 /(D_x)_1 + (D)_2 /(D_x)_2 + (D)_1(D)_2/(D_x)_1(D_x)_2$$

where CI refers to the combination index, D_x which is the dose of a drug that inhibits "x" percent of cells.

In this equation, synergism is defined as a greater-than-the-expected-additive effect, and antagonism is defined as less than-the-expected-additive effect. Thus, CI = 1 indicates an additive effect, CI < 1 indicates a synergistic effect, and CI > 1 indicates antagonism. The precise significance of various degrees of synergism or antagonism has been proposed that to be interpreted as follows:

Table 1 Interpretation of combination index values generated by the median-effect equation.

<0.1	very strong synergism
0.1–0.3	strong synergism
0.3–0.7	synergism
0.7–0.9	moderate to slight synergism
0.9–1.1	nearly additive
1.1–1.45	slight to moderate antagonism
1.45–3.3	antagonism
>3.3	strong to very strong antagonism

In this work, median-effect equation is used to evaluate synergy as it is a flexible method which can be used to determine synergy when the drug combination is in a fixed ratio or when the drug combination is in a non-fixed ratio, where the dose of one drug is fixed and the other is varied. Most importantly, this method has biological relevance and the *in vitro* results have been shown to correlate whether the combination would work in a synergistic or antagonistic manner *in vivo* (Abraham, McKenzie et al. 2004).

(a)

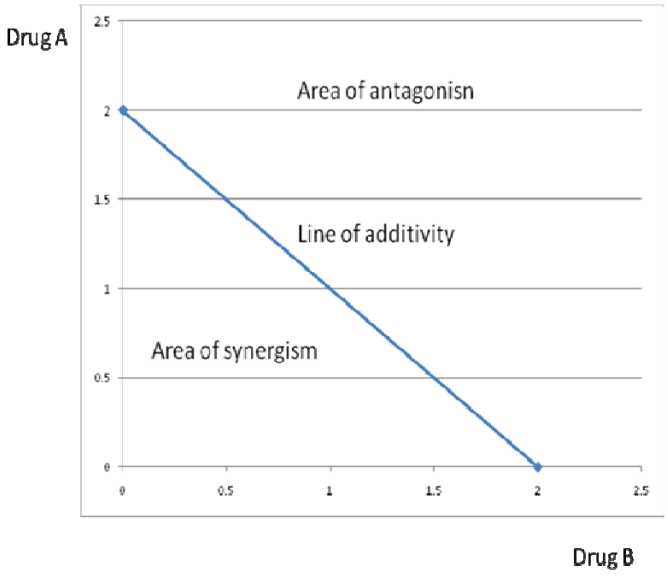

(b)

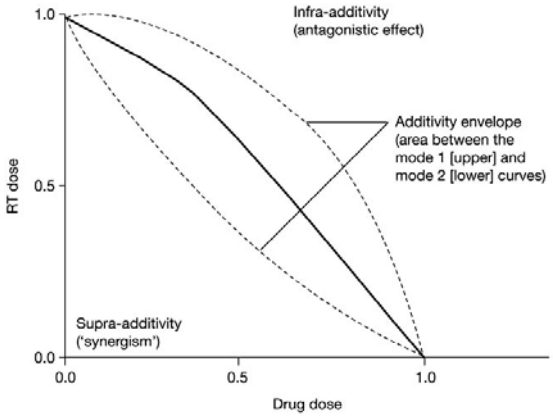

(c)

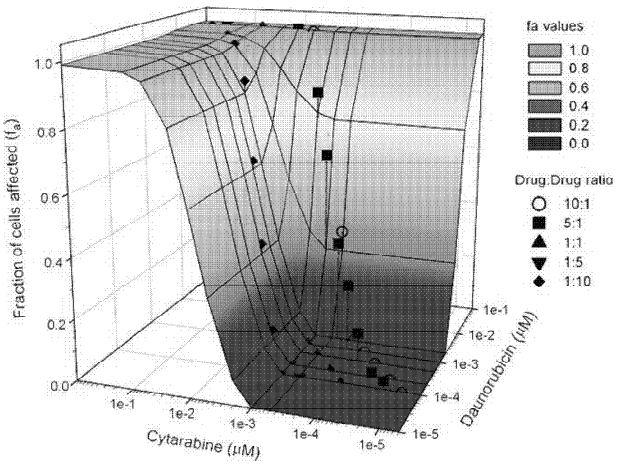

Figure 2 Representative plots illustrating (a) classical isobologram, (b) Steel and Peckham isobologram, reprinted with permission from Macmillan Publishers Ltd, Nature reviews "The

concurrent chemoradiation paradigm general principles" by Seiwert et al., 1969 and (c) surface response analysis. Reprinted with permission from Elsevier Limited, Leukemia Research "*In vivo* maintenance of synergistic cytarabine:daunorubicin ratios greatly enhances therapeutic efficacy", Tardi et al., 2009.

1.6 Synergism of quercetin with conventional chemotherapeutic drugs

Synergism can occur when the compounds act on different pathways which interact and lead to synergy (Shah and Schwartz 2001) or from the direct interaction of the compounds on different stages of the same pathway (Dancey and Chen 2006). Besides the mechanism of action, the efficacy of the anti-cancer activity of chemotherapeutic agents is also drug ratio dependent, exhibiting synergism at certain ratios but additivity or antagonism at other ratios (Mayer, Harasym et al. 2006; Harasym, Liboiron et al. 2009; Tardi, Johnstone et al. 2009). However, this effect has not been extensively researched because when drugs are administered, the synergistic ratio may not be maintained due to the variations in the different pharmacokinetic profiles of the individual drugs. Table 2 summarizes the synergism of quercetin with several chemotherapeutic agents and the mechanism of synergy.

Table 2 Summary of the synergism of quercetin with chemotherapeutic agents.

Drug class	Drug	Cell line tested	Mechanism of synergy
Alkylating agents	Carboplatin	Human Hepatoma cell line Hep 3B and Hep G2	Quercetin potentiates the action of carboplatin by inhibiting heat shock proteins (Sharma, Upadhyay et al. 2009).
	Cisplatin	Human ovarian cancer OVCA 433 cells	Quercetin synergized with cisplatin by acting through an interaction with Type II estrogen binding site (Scambia, Ranelletti et al. 1990).
		Human ovarian cancer CAOV3 and SKOV3 cells	Addition of quercetin increased sensitivity of the cells to cisplatin through the inhibition of interleukin 6 (Chan, Fong et al. 2003).
		Human laryngeal cancer Hep 2 cells	The combination of quercetin and cisplatin acted on complementary pathways, increasing the percentage of cells undergoing apoptosis. Quercetin inhibited Akt/PKB phosphorylation while cisplatin induced JNK activity and increased caspase 9 (Sharma, Sen et al. 2005).

Table 2: Continued

Camptothecin derivatives	Topotecan	Murine fibrosarcoma cell lines	Quercetin inactivated hsp 70, thereby sensitizing the cells to topotecan (Sliutz, Karlseder et al. 1996).
		Human breast cancer cells MCF-7 & MDA-MB-231	Quercetin enhanced the effects of topotecan by inhibiting the activities of tyrosine-specific protein kinases (Akbas, Timur et al. 2005).
	Irinotecan	Human and rat liver microsomes	Quercetin inhibited the metabolic inactivation of irinotecan (Iyer, Furimsky et al. 2006).
Plant alkaloids	Vincristine	Human cervical cancer cells MRP1-transfected HeLa T5	Quercetin inhibited the ATPase activity of MRP1 (Multidrug Resistance Protein 1), thereby increasing vincristine levels in the cells (Leslie, Mao et al. 2001).
Pyrimidine analogs	5 fluorouracil	Human colon cancer cells DLD-1 colon cancer cells	Co-administration of quercetin and 5 fluorouracil markedly inhibited thymidylate synthase and survivin expression as compared to the individual administration of each single agent (Nakayama, Sakamoto et al. 2000).

Table 2: Continued

Other agents	Carboxytriazole	Human breast cancer cell MDA-MB 435	Quercetin depressed IP3 levels that decreased the cytosolic calcium concentration while carboxytriazole inhibits calcium influx into cells (Yeh, Herenyiova et al. 1995).

1.7 Barriers to the adoption of quercetin in the clinical setting

Although quercetin has been shown to have antiproliferative effects *in vitro*, the median effective concentration is around 80 μM (van der Woude, Gliszczynska-Swiglo et al. 2003; Goniotaki, Hatziantoniou et al. 2004). In contrast, the peak plasma quercetin concentration that can be attained, after quercetin supplementation triple that of the average daily intake, is only 0.5 μM (Hollman, Gaag et al. 1996). This represents around 100-fold difference from the median effective dose needed for anti-cancer activity. The low plasma quercetin concentrations could be attributed to its low water solubility of 80 μM (van der Woude, Gliszczynska-Swiglo et al. 2003), which limits absorption (Hollman, Gaag et al. 1996). Hence, the concentrations used for *in vitro* studies cannot be attained by ingestion of quercetin alone (Hollman, Gaag et al. 1996). In addition, quercetin has been shown to be chemically unstable in physiological pH (van der Woude, Gliszczynska-Swiglo et al. 2003). Therefore, the development of an appropriate carrier for quercetin can facilitate its clinical use.

1.8 Pros and cons of current approaches to solubilize quercetin

Parenteral administration of chemotherapy is the most common route in the treatment of disseminated cancers as the

administered drug could go to almost anywhere in the body through the bloodstream (Brunton and Lazo 2005). However, due to the low solubility of quercetin, it has to be solubilized to prevent precipitation and emboli formation after intravenous administration (Joseph 1911). Therefore, many approaches have been attempted to improve quercetin solubility.

One of the approaches to improve quercetin solubility is through the synthesis of water soluble prodrugs of quercetin. A glycine carbamate prodrug of quercetin (QC12) has been synthesized by Mulholland et al. Despite improved water solubility, QC12 was not bioavailable when it was administered orally and had a short half life of 0.31 h when administered intravenously (Mulholland, Ferry et al. 2001). Besides QC12, water soluble sodium sulfonic derivatives of quercetin have also been synthesized (Krol, Dworniczak et al. 2002). Although these derivatives improved solubility, they were less potent than quercetin, suggesting that the cytotoxic activity of quercetin could be related to its lipophilicity. Therefore, despite improvements in water solubility, there has been limited success with the prodrug approach in terms of half life prolongation and maintenance of the potency of quercetin.

Besides chemical modification, drug carriers can also be used for the intravenous delivery of quercetin. Properties of an ideal drug carrier for parenteral administration include biocompatibility, non-toxicity, aqueous solubility, ability to

solubilize a considerable amount of drug, and the , ability to release drug at a controlled rate and to prevent or slow down drug degradation (Leung, Robinson et al. 1987). In addition, since it is of interest to co-encapsulate quercetin with conventional chemotherapeutic drugs, the drug delivery system should be able to co-encapsulate both hydrophobic and hydrophilic drugs in the same carrier. Another property that a drug carrier should possess is to be able to co-ordinate the release of quercetin with conventional chemotherapeutic agents in the optimal synergistic ratio to enhance anti-cancer activity, as only drug that is released from the carrier is active.

Microemulsions, which are dispersions comprising of an oil phase, a water phase and surfactants have been developed for the solubilization and intravenous administration of quercetin (Gupta, Moulik et al. 2005). Although a quercetin microemulsion comprising of clove oil/Tween 20/water has been developed for intravenous administration of quercetin, improving its solubility by seven fold, the excipients used were found to be hepatotoxic and nephrotoxic following intravenous administration. Similarly, other microemulsions developed to solubilize quercetin were mainly preparations for topical (Kitagawa, Tanaka et al. 2009), oral (Gao, Wang et al. 2009) or inhalation use (Rogerio, Dora et al. 2010), which cannot be adapted directly for intravenous administration due to the toxicity of the excipients (Date and Nagarsenker 2008). Given the toxicity of the excipients used in

the formulation of microemulsions, this formulation may not be appropriate for intravenous formulation of quercetin.

Besides microemulsions, the solubilization of quercetin with β-cyclodextrins has also been attempted (Zheng, Haworth et al. 2005). β-cyclodextrins are cyclic (α-1,4)-linked oligosaccharides composed of seven α-D-glucopyranose units, which together form a rigid cone shaped structure. Although quercetin was stabilized and solubilized around 200 fold, β-cyclodextrins have been associated with a risk of nephrotoxicity (Frijlink, Eissens et al. 1991) and have low aqueous solubility (Szejtli 1991). These two factors hamper their use for parenteral drug delivery.

Nanoparticulate delivery systems are solid colloidal particles, ranging in size from 1 to 500 nm, consisting of various polymeric matrices in which therapeutic moiety can be adsorbed, entrapped, or covalently attached (Uchegbu 1999). Quercetin nanoparticles comprising of polyvinyl alcohol & Eudragit® have been formulated. Although quercetin was efficiently encapsulated (up to 99%), *in vitro* studies showed that more than 95% of quercetin was released within 20 minutes (Wu, Yen et al. 2008). In addition, quercetin has also been incorporated in poly (D,L-lactideco-glycolide) nanoparticles together with vincristine. However, the encapsulation efficiency was suboptimal at 32.6% and rapid release of quercetin was also observed, with 70% of quercetin released over 3 hours (Song, Zhao et al. 2008). This rapid release from the carrier could

potentially prevent the accumulation of the anti-cancer drugs in tumor site via the enhanced permeability and retention (EPR) effect (Matsumura and Maeda 1986). Under the EPR effect, macromolecules with molecular weights larger than 40kDa (such as liposomes and other nanoparticulate systems) accumulate preferentially in the tumor tissue due to the abnormal architecture of the tumor blood vessels, which allow the escape of the macromolecules from the bloodstream and their accumulation in the tumor interstitium. When the drug is rapidly released from the carrier, it is unable to accumulate in the tumor interstitium through the EPR effect as the drug of low molecular weight leaks out from the tumor interstitium back to the blood circulation quickly (Maeda 2002). Therefore, more optimization is needed to slow down the release of quercetin and to incorporate quercetin more efficiently in polymeric nanoparticles for parenteral use. Besides polymeric nanoparticles, quercetin has been solubilized in solid lipid nanoparticles (Li, Zhao et al. 2009). Although solid lipid nanoparticles are biocompatible and could also protect quercetin from degradation, solid lipid nanoparticles are limited by their inefficient encapsulation of hydrophilic and amphipathic drugs (Cai, Wang et al. 2010), hence they are not suitable for co-encapsulation of quercetin with hydrophilic or amphipathic chemotherapeutic agents.

Liposomes, which are small spherical vesicles formed by a lipid bilayer enclosing an aqueous compartment (Bangham,

Standish et al. 1965), have been developed and their encapsulation efficiencies were close to 100% (Goniotaki, Hatziantoniou et al. 2004; Yuan, Chen et al. 2006; Priprem, Watanatorn et al. 2008). Due to their similarity with endogeneous substances in the body, liposomes are also biocompatible and non-toxic (Bonte, Hsu et al. 1987). In addition, as compared to the other delivery systems, liposomes are the most successful in terms of translating into clinical trials and approval, with four products available on the market for cancer treatment (Table 3) and many liposomal formulations are currently undergoing clinical trials (Table 4).

.

Table 3 Marketed liposomal products for cancer treatment.

Product name	Component	Indication
Doxil	Liposomal doxorubicin (PEGylated)	Ovarian cancer Multiple myeloma
Myocet	Liposomal doxorubicin	Metastatic breast cancer
DepoCyt	Liposomal cytarabine	Lymphomatous meningitis
Daunoxome	Liposomal daunorubicin	AIDS- related Kaposi's sarcoma

Table 4 Novel liposomal formulations under clinical trials for cancer.

Component	Indication	Phase of clinical trial
Liposomal BLP25 (peptide derived from mucin 1)	Non small cell lung cancer	Phase II
Liposomal CPX-351 (Cytarabine:Daunorubicin)	Advanced Hematologic cancer	Phase I
Liposomal cytarabine (intrathecal)	Solid tumor neoplastic meningitis	Phase I
Liposomal doxorubicin (heat activated)	Primary or metastatic liver tumor	Phase I
	Locally recurring breast cancer	Phase I
Liposomal irinotecan	Advanced solid tumor	Phase I
Liposomal irinotecan: floxuridine	Advanced colorectal cancer	Phase II
Liposomal mitoxantrone	Advanced cancer	Phase I
Liposomal pacilitaxel	Advanced gastric carcinoma	Phase I
Liposomal 7-ethyl-10-Hydroxycamptothecin (SN-38)	Small cell lung cancer	Phase I
	Metastatic colorectal cancer	Phase II
Liposomal topotecan	Small cell lung cancer	Phase I
	Ovarian cancer	
Liposomal vincristine	Relapsed acute lymphoblastic leukemia	Phase II
Liposomal vinorelbine	Advanced solid tumors, non-Hodgkin's lymphoma or Hodgkin's disease	Phase I
Liposomal camptothecin (aerosolized)	Metastatic or recurrent cancer of the endometrium or the lung	Phase 1
Liposomal cisplatin	Recurrent ovarian cancer	Phase II

Table 4 continued

Liposomal daunorubicin	HIV-Related Kaposi's Sarcoma	Phase III
Liposomal lurtotecan	Metastatic or locally recurrent head and neck cancer	Phase II
	Recurrent small cell lung cancer	

Reference: clinicaltrials.gov assessed on 1st June 2010

In addition, liposomes are also versatile drug delivery systems which can encapsulate hydrophobic, hydrophilic and amphiphilic compounds simultaneously. Furthermore, an appropriately optimized liposomal formulation can also release the encapsulated drug in a controlled manner (Dos Santos, Waterhouse et al. 2005), prolong the circulation time of the drug (Papahadjopoulos, Allen et al. 1991) and also accumulate preferentially in the tumor tissue through the EPR effect (Matsumura and Maeda 1986) so as to improve their therapeutic efficacy and reduce their toxicity profile. Finally, a liposome formulation has been shown to coordinate drug release and maintain the synergistic molar ratio of the two drugs for optimal anti-cancer activity (Harasym, Tardi et al. 2007). This is illustrated by the combination of irinotecan and floxuridine and that of cytarabine and daunorubicin, which are currently in clinical trials (Table 4). In view of these advantages, liposomes will be the drug delivery system explored in this thesis.

1.9 Classification of liposomes

Liposomes can be classified according to the number of lipid bilayers and size. Multilamellar vesicles (MLVs) are large "onion-like" structures formed when the lipids are hydrated in aqueous solutions. They have diameters of around 1 μm. Small unilamellar vesicles (SUV) have a single bilayer surrounding an aqueous core. They are prepared from MLVs by sonication and have diameters between 15-30 nm. However, due to the high degree of curvature of the membrane, SUVs will spontaneously fuse to form larger vesicles upon storage. Like SUVs, large unilamellar vesicles (LUV) also have a single bilayer surrounding an aqueous core. The size of LUVs ranges from 100-200 nm. LUVs can be prepared from MLVs by a variety of methods including extrusion and reverse phase evaporation (Szoka and Papahadjopoulos 1978). Extrusion, which is the process of passing vesicles through a series of filters under low pressure between 100-800 lb/in^2, (where 1 lb/in^2 = 6895 Pa) will be used in this project because it allows for rapid and reproducible production of narrow, monodisperse vesicle populations with diameters close to the chosen pore size of the filter into liposomes (Mui and Hope 2007).

1.10 Various generations of liposomes

The first generation of liposomes are conventional liposomes with "naked" phospholipid surfaces, without glycolipids, hydrophilic polymers or other surface grafted components (Allen and Stuart 1999). Initially liposomes were produced from unsaturated lipids such as egg phosphatidylcholine but these were found to be rapidly cleared from the bloodstream due to opsonization by plasma proteins and accumulation in the reticuloendothelial system (RES) (Scherphof, Dijkstra et al. 1985; Senior 1987). The use of small liposomes (around 100 nm) containing saturated fatty acyl chains and cholesterol has extended blood circulation time (Kirby, Clarke et al. 1980; Senior and Gregoriadis 1982; Senior, Crawley et al. 1985). Currently, three of the four marketed products for cancer treatment, namely, Myocet (liposomal doxorubicin), Daunoxome (liposomal daunorubicin) and DepoCyt (liposomal cytarabine) belong to the first generation of liposomes.

The second generation of liposomes consists of sterically stabilized liposomes where surface grafted hydrophilic polymers such as poly(ethylene glycol) are incorporated. The polymers reduce the recognition of the liposomes by the RES and hence, these liposomes have longer circulation half lives, which increases the levels of drug accumulation in the site of tumor growth as compared to the first generation liposomes (Papahadjopoulos, Allen et al. 1991). In addition, it has been

found that sterically stabilized liposomes could also prevent liposome aggregation and fusion with biological membranes to increase circulation half life (Cattel, Ceruti et al. 2003). Doxil (liposomal doxorubicin) is an example of a second generation liposome preparation available in the market. The circulation half life of Doxil is three times (Gabizon, Catane et al. 1994) that of Myocet (Cowens, Creaven et al. 1993), a first generation liposomal doxorubicin preparation.

The third generation of liposomes involves the attachment of ligands against cell surface antigens expressed selectively on tumor cells on the liposomes so as to increase the therapeutic efficacy of drugs encapsulated in them. These include the folate receptor (Andrew and Philip 2005), transferrin receptor (Singh 1999), antibodies (Sofou and Sgouros 2008) and peptides (Torchilin 2006). At the present moment, peptide-targeting with mucin 1 is being tested in Phase II clinical trials (Table 4).

The fourth generation of liposomes is designed to release drug at the target site in response to external stimuli. Currently, researchers have used external stimuli such as heat (Sandstroem, Ickenstein et al. 2005; Woo, Chiu et al. 2008), magnetism (Viroonchatapan, Sato et al. 1996; Kubo, Sugita et al. 2001; Dandamudi and Campbell 2007) and ultrasound (Huang 2010; Negishi, Omata et al. 2010; Suzuki and Maruyama 2010; Suzuki, Namai et al. 2010). Of these approaches, the use of temperature is the most advanced, where thermosensitive doxorubicin

liposomes are being tested in Phase I clinical trials (clinicaltrials.gov). This approach is suitable for locally occurring cancers that can be readily assessed by the application of external stimuli, such as melanomas.

Based on the developments in the field, future liposomal delivery systems will become increasingly sophisticated and multifunctional liposomes, such as liposomes with targeting and local release functions may be developed in the future as an armamentarium against cancer.

1.11 Lipids used for liposome making

1.11.1 Phospholipids

Phospholipids provide the structural framework and a major component of the cell membrane. All phospholipid molecules have a polar head group, a phosphate group and hydrophobic fatty acid chains connected by a glycerol backbone (Figure 3). At physiological pH, the phosphate group of the phospholipid molecule is negatively charged. The negative charge can be neutralized by the presence of positively charged headgroups, such as choline or ethanolamine. In contrast, when the headgroup is neutral, as in the cases of phosphatidylserine, phosphatidylglycerol, the phospholipid has an overall negative charge. Charged lipids can be used to reduce flocculation over

the shelf life of the product, influence drug retention and loading and direct liposomes to biological targets (Maurer-Spurej, Wong et al. 1999; Tardi, Gallagher et al. 2007). Besides alterations in the headgroup, alterations in acyl chain length can also affect stability, permeability and phase behavior of the liposomes (Anderson and Omri 2004). The most common acyl chain lengths used for drug delivery are myristic (C14), palmitic (C16) and stearic (C18).

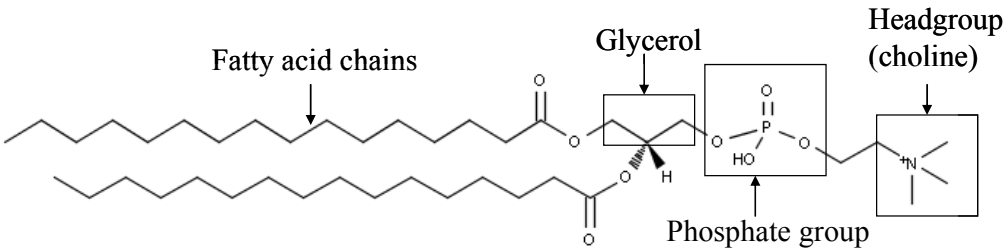

Figure 3 Structure of Phosphatidylcholines.

The most common phospholipids used in liposome making are the phosphatidylcholines (PC). PCs can be extracted from natural sources such as eggs, soy, brain and the liver. However, these natural extracts are a mixture of different lipids, including saturated and unsaturated PCs of different acyl chain lengths and sphingolipids and the lipid composition may vary from batch to batch. Besides natural sources, PCs can also be chemically synthesized. The advantage of chemically synthesized PCs is that they are chemically pure, and most current liposome work involves the use of chemically synthesized lipids.

Sphingolipids are another class of phospholipids commonly used in liposome making. They also occur naturally and are important components of the brain and nerve tissue. Sphingolipids have a sphingosine backbone. This backbone has one more hydroxyl and one more amino group as compared to the glycerol backbone of the phosphatidylcholines (Figure 4). Sphingolipids can be incorporated to reduce the permeability of lipid membranes through the formation of hydrogen bonds (Torchilin and Weissig 2003).

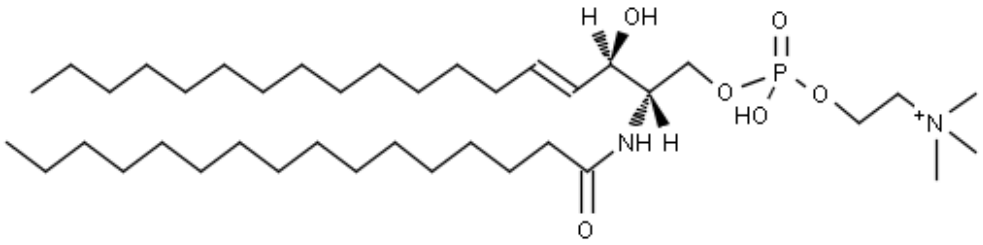

Figure 4 Structure of sphingomyelin.

1.11.2 Poly(ethylene glycol) conjugated lipids

Poly(ethylene glycol) (PEG) is a non-toxic, non-antigenic polymer that is commonly conjugated to phospholipids. Poly(ethylene glycol) conjugated lipids are incorporated into liposomes to impart steric stabilization and prolong *in vivo* circulation time of the liposomes (Woodle and Lasic 1992). The optimal molecular weight of PEG for prolonging the *in vivo* circulation time is 2,000 (de Gennes 1987; Woodle and Lasic

1992; Dos Santos, Allen et al. 2007). Due to the negative charge on the phosphate moiety, the poly(ethylene glycol) conjugated lipid is negatively charged when it is conjugated to lipids with a neutral headgroup such as distearoylphosphatidylethanolamine (DSPE) (Figure 5). In most cases, DSPE-PEG_{2000} is being used (Papahadjopoulos, Allen et al. 1991; Zamboni 2005) but the negative charge may increase drug leakage, necessitating the use of the neutral PEG-ceramide lipid (Figure 6) (Webb, Saxon et al. 1998).

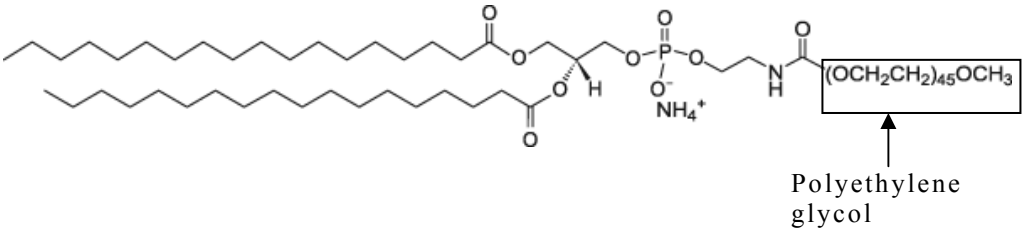

Figure 5 Diagram of 1,2-distearoyl-*sn*-glycero-3-phosphoethanolamine-N-[amino(polyethylene glycol)-2000] (DSPE-PEG_{2000}).

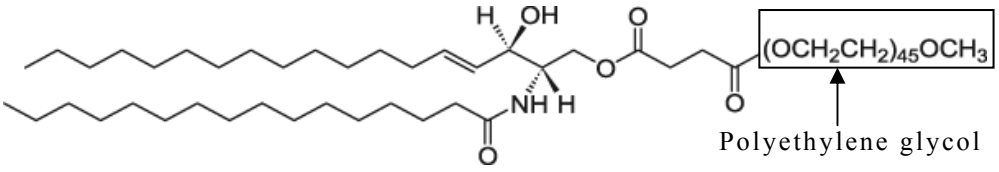

Figure 6 Diagram of N-palmitoyl-sphingosine-1-{succinyl[methoxy(polyethylene glycol)} (PEG-ceramide).

In a phospholipid bilayer, the lipid anchor partitions within the lipid bilayer while the PEG moiety extends from the liposome surface (Papahadjopoulos, Allen et al. 1991). Depending on the grafting density of PEG lipids on the bilayer, the PEG component can form either "mushroom" (less than 5 mol% of DSPE-PEG_{2000}), "brush" conformation (between 5 to 10 mol% of DSPE-PEG_{2000}). Mixed micelles are formed when the PEG component exceeds 10 mol% (de Gennes 1987). These conformations are illustrated in Figure 7. In the "mushroom" conformation, PEG can move freely from a fixed point that encompasses a half-sphere which exhibits a defined radius called Flory radius (R_f). This conformation occurs at low grafting densities ($D>R_f$), where polymer-polymer interactions are minimal. At high PEG concentrations ($D<R_f$), polymer-polymer interactions occur and the PEG polymers extend out from the lipid bilayer (brush regime). These are illustrated on Figure 8. At even higher PEG concentrations, mixed micelles are formed to reduce the interactions between the PEG chains (Hristova and Needham 1994). Since poly(ethylene glycol) conjugated lipids are incorporated into liposomes to impart steric stabilization, the concentration of PEG lipids is usually between 5 – 10 mol%, when the PEG-lipid is in brush regime.

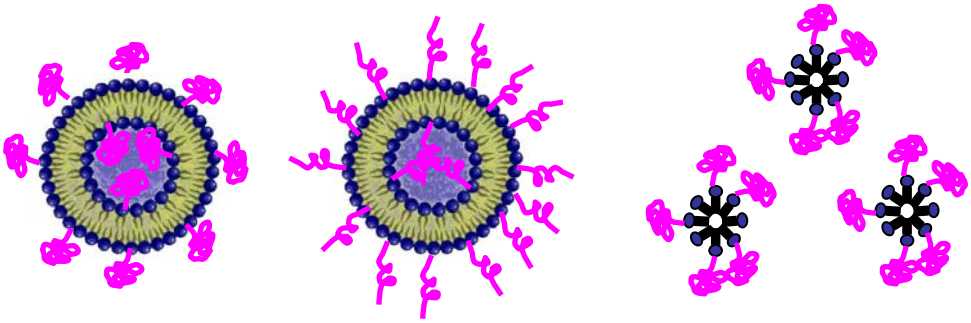

"Mushroom" regime: DSPE-PEG$_{2000}$ <5 mol%

"Brush" regime: DSPE-PEG$_{2000}$: 5-10 mol%

Micelle formation: DSPE-PEG$_{2000}$ >10 mol%

Figure 7 Diagram illustrating the different structures that can be adopted by DSPE-PEG$_{2000}$.

"Mushroom" Regime
D >> R_f

"Brush" Regime D < R_f

Figure 8 The conformation adopted by PEG is dependent on the grafting distance between the polymers (D) and the Flory radius (R_f) of the polymer.

1.11.3 Cholesterol

Cholesterol has a 4-membered sterol ring with a hydrocarbon chain and a hydrophilic hydroxyl group (Figure 9). Currently, most liposomal formulations contain a high percentage of cholesterol (around 50%) so as to confer biological stability *in vivo* as cholesterol reduces interaction with plasma

proteins which destabilize the liposomes (Kirby, Clarke et al. 1980; Senior and Gregoriadis 1982; Senior 1987; Gabizon, Catane et al. 1994). However, recent research has shown that the presence of DSPE-PEG_{2000} could also reduce the interaction of liposomes with plasma proteins (Bartucci, Pantusa et al. 2002), hence cholesterol may not be needed to reduce plasma protein interaction in the presence of PEG-conjugated lipids.

In addition, although it was thought that the inclusion of cholesterol would enhance the retention of entrapped hydrophilic drugs in the liposome carrier (Demel and De Kruyff 1976), recent studies have shown otherwise. In fact, the liposomal retention of some chemotherapeutic drugs was dramatically enhanced by the removal of cholesterol (Dos Santos, Waterhouse et al. 2005; Tardi, Gallagher et al. 2007). Lastly, cholesterol has an impact on the gel to liquid phase transition temperatures and this will be discussed in Section 1.11.4.

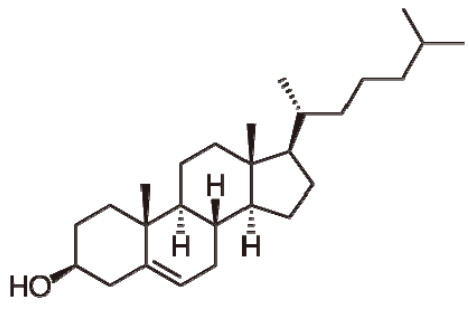

Figure 9 Structure of cholesterol.

1.11.4 Gel-to-liquid crystalline phase transition

Lipids undergo a gel-to-liquid crystalline phase transition beyond a critical temperature, called the transition temperature (T_c) (de Kruyff, Demel et al. 1972). This is the temperature needed to change the lipid from an ordered gel phase, where the hydrocarbon chains are fully extended and closely packed, to the disordered liquid crystalline phase, where the hydrocarbon chains are randomly oriented and fluid. A higher transition temperature is observed with an increased length of hydrocarbon chains, increasing degree of hydrocarbon saturation and a reduction in headgroup size.

The effect of cholesterol on phase transition temperatures of lipids has been elucidated with differential scanning calorimetery (DSC) (de Kruyff, Demel et al. 1972). In fluid membranes (above T_c), cholesterol increases order and packing density in the lipid membrane. In gel membranes (below T_c), cholesterol reduces order and packing density in the lipid membrane. At high cholesterol concentrations more than 30 mol%, the measured phase transition is eliminated, and hence, the membrane is in the liquid-ordered phase (Demel and De Kruyff 1976).

1.12 Methods of drug loading into liposomes

1.12.1 Passive loading

Both hydrophobic and hydrophilic drugs can be passively entrapped in the liposomes. Hydrophobic drugs can be efficiently incorporated with the lipid bilayers by mixing the drug with lipids dissolved in organic solvent, with encapsulation efficiencies of close to 100% (Allen and Stuart 1999). In contrast, passive loading of water soluble drugs during the hydration stage is usually inefficient (< 10%) (Mayer, Cullis et al. 1994; Torchilin and Weissig 2003).

1.12.2 Remote loading with acidic liposome interior

Remote loading of hydrophilic drugs can be applied when the drugs have protonation sites and exist in equilibrium between protonated and unprotonated states between pH values of around pH 4 and pH 9 (Mayer, Bally et al. 1986; Haran, Cohen et al. 1993; Mayer, Cullis et al. 1994). In this technique, drugs are loaded into preformed liposomes. The drugs are first incubated at neutral pH in the liposomes with an acidic interior. The uncharged form of the drug will diffuse down this concentration gradient into the liposomes. Under acidic conditions, the drug becomes protonated and trapped in the liposome as the charged form of the drug is membrane impermeable. The diffusion of the

neutral drug will continue as long as the pH gradient is maintained between the interior and exterior of the liposome or until all the drugs have been taken up. (Mayer, Bally et al. 1986; Mayer, Cullis et al. 1994; Fenske and Cullis 2007). High encapsulation efficiencies of up to 100% can be attained with this method.

1.12.3 Ionophore mediated generation of pH gradients via transmembrane ion gradients

Another method of generating a pH gradient can be through the use of ionophores and ion gradients (Fenske, Wong et al. 1998). Liposomes are formed by extrusion in either manganese, magnesium or potassium sulphate salts. These liposomes are passed down a column equilibrated in a sucrose-containing buffer. The drug is subsequently added. For liposomes with potassium salts, the ionophore nigericin is added. For the liposomes with either Mn^{2+} or Mg^{2+}, the ionophore A23187 and ethylenediaminetetraacetic acid (EDTA) are used. A23187 couples the outward flow of a single divalent cation to the inward flow of a pair of protons, while EDTA is used as a chelating agent for manganese or magnesium as they are transported out of the vesicles. In both cases, ionophore-mediated ion transport is electrically neutral and results in acidification of the vesicle interior, thereby creating a pH gradient that drives drug uptake.

1.13 Chapter Summary

This Chapter has provided background information on cancer, inadequacies of current treatment cancer regimens, highlighted the problems preventing clinical use of quercetin, pros and cons of drug delivery systems delivering quercetin and background information on liposome technology. The following Chapter will focus on the hypothesis and objectives of the project.

Chapter 2

HYPOTHESIS AND OBJECTIVES

2.1 Thesis rationale and hypothesis

Metastatic breast cancer has high relapse rates, highlighting the need to develop new treatment modalities against them. Quercetin is a flavonoid which is active against breast cancer and synergizes with many chemotherapeutic agents *in vitro*, but its clinical use is limited by its low water solubility. Since liposomes have been shown to (i) solubilize hydrophobic drugs, (ii) co-encapsulate multiple agents in the same liposome and (iii) release chemotherapeutic agents in a controlled and co-ordinated manner, it was hypothesized that an appropriately designed liposome system can efficiently solubilize quercetin and co-encapsulate it with conventional amphipathic chemotherapeutic agents with co-ordinated drug release, thereby maintaining the most synergistic molar ratio of the two drugs *in vitro* and *in vivo* so as to increase the therapeutic efficacy as compared to the free drug combination. This would represent a

or breast cancer.

2.2 Objectives

The objectives of this project are to develop a liposomal formulation to solubilize quercetin so as to facilitate intravenous administration of quercetin. Secondly, chemotherapeutic drugs that synergize with quercetin in breast cancer cells will be identified by *in vitro* studies by the median-effect equation. Thirdly, the quercetin/drug combinations showing synergism will be co-encapsulated into liposomes. Finally, the co-encapsulated formulation will be evaluated *in vitro* and *in vivo* and compared with the free drug combination.

Chapter 3

MATERIALS AND METHODS

3.1 Materials

All lipids were obtained from Avanti Polar Lipids (USA). MDA-MB-231 cells were obtained from the American Type Culture Collection and JIMT-1 cells were obtained from Deutsche Sammlung von Mikroorganismen und Zellkulturen GmbH (Germany). 3-(4,5-dimethylthiazolyl-2)-2,5-diphenyltetrazolium bromide (MTT), dimethyl sulfoxide (DMSO), chloroform were purchased from MP Biomedicals, Inc (Singapore). Balb/c mice were purchased from the Centre for Animal Resources, National University of Singapore (Singapore) while SCID mice were purchased from the Biological Resource Centre, Biopolis (Singapore). All other materials were purchased from Sigma-Aldrich (USA).

3.2 *In vitro* cytotoxicity studies

In vitro cytotoxicity was assessed by the 3-(4,5-diethylthiazoyl-2-yl)-2,5-diphenyltetrazolium bromide (MTT) colorimetric cytotoxicity assay (Mosmann 1983). MDA-MB-231 or JIMT-1 human breast cancer cells were grown in DMEM/F-12 media supplemented with 10% fetal bovine serum and seeded at 4000 cells/well in 96-well cell culture plates. They were

incubated at 37 ^{o}C with 5% CO_2 for 24 h for cell adherence to the cell culture plates. Cells were subsequently treated with serial dilutions of either single drugs (quercetin, vincristine), or drug combinations (quercetin and vincristine at molar ratios of 4:1, 2:1, 1:1 and 1:2) for 72 h. Subsequently, 50 µL of 1 mg/mL MTT reagent was added to each well. This was incubated with the cells for 4 h and aspirated. 150 µL of dimethyl sulfoxide (DMSO) was added to each well and the 96-well plates were shaken for 20 minutes to solubilize the cells. The plates were read on a microplate absorbance meter (Tecan Sunrise^{TM}, Männedorf, Switzerland,) set at 570 nm. Cell survival at the end of treatment was calculated from the optical density readings as a percentage of the control. All assays were performed in triplicate.

3.3 Median-effect analysis

CalcuSyn® (United Kingdom), a software program based on the median-effect principle described by Chou and Talalay (Chou and Talalay 1977) was used for the drug combination interaction analysis. For studies on the combined effects of quercetin with vincristine, fixed ratios of quercetin and vincristine (4:1, 2:1, 1:1 and 1:2) were used. The Calcu-Syn® program determines if the combined agents act in an additive, synergistic or antagonistic manner by using the mean cell survival percentages from the MTT assay as a function of drug

concentrations to generate a combination index (CI) value, which has been defined as being synergistic (CI < 0.9), additive (CI = 0.9-1.1) or antagonistic (CI > 1.1).

3.4 Liposome preparation

Liposomes were prepared by the thin film hydration method (Mayer, Tai et al. 1990). Briefly, the lipids were dissolved in chloroform while quercetin was dissolved in ethanol and mixed by vortexing. The preparation was subsequently dried under a stream of nitrogen gas, and the resulting lipid film was placed under vacuum to remove organic solvent. The dried lipid films were hydrated with 300 mmol/L manganese sulfate (pH3.4) for 1 h at 60 ^{o}C. The resulting preparation was extruded 15 times at 60 ^{o}C through one stacked 0.1 μm pore size polycarbonate filter (Northern Lipids Inc., Vancouver, BC, Canada) with an extruder apparatus (Northern Lipids Inc., Vancouver, BC, Canada). The resulting mean diameter of the liposomes was determined by quasi-elastic light scattering (QELS) using the Zetasizer 3000HS operating at 633 nm and had diameters around 130 nm.

3.5 pH gradient loading of irinotecan and vincristine

Irinotecan or vincristine (drug-to-lipid molar ratio of 0.1:1) were actively loaded into the liposomes using an ionophore-mediated proton gradient (Fenske, Wong et al. 1998).

The divalent cation ionophore A23187 (0.5 μg per 1 mg lipid) was incorporated into the liposomal bilayer after incubation at 37°C or 10°C above the phase transition temperature of the lipid for 10 minutes. Subsequently, the efficiency of irinotecan encapsulation by liposomes (drug-to-lipid molar ratio of 0.1:1) was determined at incubation temperatures of 37°C or 10°C above the phase transition temperature of the lipid as a function of time. Encapsulated drug was separated from free drug using a Sephadex G-50 mini spin column. Irinotecan was quantified by measuring its fluorescence intensity with at an excitation wavelength at 385 nm and emission wavelength at 535 nm following the solubilization of the liposomal formulation. Quercetin was quantified by measuring its absorbance at 376nm after solubilization of the liposomes (Goniotaki, Hatziantoniou et al. 2004) in ethanol. Vincristine was quantified by measuring its absorbance at 297nm (Waterhouse, Madden et al. 2005) after solubilization of the liposomes in n-Octyl -D-glucopyranoside.

3.6 Evaluation of quercetin stability

The stability of encapsulated quercetin was compared with unencapsulated quercetin with the 2,2-diphenyl-1-picrylhydrazyl ($DPPH^{\bullet}$) assay, which is a stable free radical used to measure the stability of quercetin (Casagrande, Georgetti et al. 2007). The free quercetin and liposomal formulations of quercetin were stored at 37 ^{o}C for 2 weeks. $DPPH^{\bullet}$ was incubated with the

samples containing 1µg/ml of quercetin for 10 minutes and its absorbance determined at 517 nm (Dinis, Maderia et al. 1994).

3.7 Drug release studies

The drug release characteristics of this formulation were assessed by dialyzing (3500 molecular weight cut off, Pierce, USA) the liposomes against 2 liters of 0.9% w/v sodium chloride for 72 hours at 37°C. At 4, 6, 24, 48 hours, 3 x 50 µL aliquots were removed from the dialyzer and analyzed for encapsulated quercetin, irinotecan or vincristine concentrations with the same methods outlined in the previous Section.

3.8 Animal studies

All the mice used were female and between 20-22 g. They were housed in micro-isolator cages and given free access to food and water. They were quarantined for 7 days before the study was initiated. The studies were conducted according to the procedures approved by the National University of Singapore Institutional Animal Care and Use Committee.

3.9 Pharmacokinetic studies

Both free drugs and drug loaded liposomes (2:1 molar ratio of vincristine: quercetin; corresponding to 1.33 mg/kg vincristine and 0.24 mg/kg of quercetin) were injected intravenously into the

lateral tail vein of female Balb/c mice. At 10 minutes, 30 minutes, 1 hours, 2 hours, 4 hours and 24 hours after intravenous drug administration, the animals were euthanized with carbon dioxide asphyxiation and the blood collected by cardiac puncture (4 mice per time point). Blood samples were centrifuged for 10 minutes at 1000 g to isolate the plasma and stored at -20 ºC until analysis of quercetin and vincristine concentrations by UPLC. The liver and spleen were snap frozen in liquid nitrogen and stored at -80 ^{o}C until analysis.

3.10 *In vivo* efficacy study

Tumors were established in SCID mice by a single subcutaneous injection of 5 x 10^6 JIMT-1 cells in the upper back area. Tumor progression was monitored by caliper measurements of the tumors along the length and width thrice a week. Tumor volumes were calculated by the following formula: Tumor volume = (length x width^2)/2. When the tumor size reached 200-300 mm^3, mice were randomized into 5 groups of 5 animals each. The mice were either treated with (i) sucrose HEPEs buffer (vehicle) control (ii) free quercetin (iii) free vincristine (iv) quercetin and vincristine (v) liposomal quercetin and vincristine. The doses of vincristine administered was 1.33 mg/kg (2/3 of the maximum tolerated dose in SCID mice (Waterhouse, Madden et al. 2005) and quercetin administered was 0.24 mg/kg. At these values, the molar ratio of vincristine: quercetin was 2:1. Tumor

size and body weight of the mice was monitored thrice weekly until day 60. Animals whose tumor size reached 1000 mm^3, developed ulcerations, displayed a weight loss of more than 5% were euthanized.

3.11 UPLC method development and analysis

A Waters AcQuity Ultra Performance Liquid Chromatography (UPLC) system (USA) was used to quantify quercetin and vincristine for the pharmacokinetic study. A Waters AcQuity UPLC BEH C18 2.1 x 50 mm, 1.7 µM column protected by a guard column was used. The assay was performed at 25 ºC with 0.1% formic acid as weak solvent and acetonitrile with 0.1% formic acid as strong solvent**.** The initial phase composition comprised of 75% 0.1% formic acid (weak solvent) and 25% acetonitrile with 0.1% formic acid (strong solvent) and the final phase comprised of 5% 0.1% formic acid and 95% acetonitrile with 0.1% formic acid at 3.8 min at a flow rate 0.5 ml/min and the detection wavelength of quercetin was 376 nm and that of vincristine was 297 nm.

The procedure for extraction of quercetin and vincristine from plasma and organs were modified from previously reported methods (Yang, Hsiu et al. 2005; Park, de Oca et al. 2009). Briefly, the organs were weighed and 0.1 g of the organ was homogenized in 2 volumes of 0.2 M sodium acetate buffer (pH5) in a Retsch Mixer Mill MM 200 (Germany). Either 100 µL of

plasma or organ tissue homogenate was mixed with 50 µL of β-glucuronidase, sulfatase and 25 µL of ascorbic acid and incubated at 37 ºC for 1 hour in a capped amber HPLC vial purged with nitrogen gas. The plasma or homogenate was acidified with 10 µL of 0.1 N HCl with apigenin as the internal standard and extracted four times with 100 µL of ethyl acetate. The ethyl acetate layer was collected and evaporated under nitrogen gas to dryness and reconstituted with acetonitrile with 0.1% formic acid for UPLC analysis. 1 µl of the supernatant was injected into the UPLC system. The concentration of quercetin and vincristine in the sample was determined by comparing the peak area ratios of the samples versus a calibration curve obtained by spiking known amounts of quercetin and vincristine into pooled mice plasma or the respective tissue organs. Pharmacokinetic analyses were performed using non-compartmental analysis with WinNonlin software standard Version 1.0 (Scientific Consulting Inc., USA).

3.12 Statistics

Statistical analysis was performed using the NCSS 2004 statistical analysis software (USA). All experimental data were expressed as mean ± SEM. T-test, one way ANOVA and the post hoc Tukey test were used. Kaplan-Meier survival curves were compared with the log-rank test. P values of less than 0.05 were considered to be statistically significant.

Chapter 4

QUERCETIN INCORPORATION INTO LIPOSOMES

4.1 Introduction

As highlighted in Section 1.7, quercetin has low water solubility with log P value of around 3, hampering its clinical use. Liposomal incorporation of quercetin could be a potential means to solubilize quercetin to facilitate its intravenous administration. Therefore, this Chapter aims to (1) determine the optimal conditions for quercetin incorporation in liposomes, (2) evaluate whether liposomal incorporation of quercetin would solubilize quercetin, (3) determine the *in vitro* drug release profile of liposomal quercetin and (4) compare the *in vitro* cytotoxicity between free and liposomal quercetin.

4.2 Results

4.2.1 Effect of cholesterol on quercetin incorporation

Both quercetin and cholesterol intercalate between the phospholipids in biological membranes (Hendrich 2006). Therefore, the presence of cholesterol could influence the incorporation of quercetin. As a consequence, the effect of cholesterol on quercetin incorporation was investigated by varying the cholesterol content while keeping the drug:lipid (D:L) molar ratio constant at 5:95. Table 5 shows that the

presence of cholesterol reduced quercetin incorporation. The percentage of quercetin incorporation was 100.4%, 89.0%, 30.3% and 5.4%, with standard error of mean (SEM) values of 9.6%, 8.5%, 6.7% and 1.3% in the presence of 0.0%, 10.0%, 20.0%, 40.0% of cholesterol, respectively. In addition, the extent of solubilization of quercetin was also determined by dividing the quercetin concentration in the liposomes with the concentration of quercetin in water (80 μM). As shown in Table 5, all liposomal formulations solubilized quercetin and the extent of solubilization was highest at 0.0 mol% cholesterol.

Table 5 Effect of cholesterol on the percentage incorporation of quercetin, quercetin concentration and extent of solubilization in DPPC liposomes.

	Cholesterol concentration (mol%)			
	0.0	10.0	20.0	40.0
% incorporation of quercetin (SEM)	100.4 (9.6)	89.0 (8.5)	30.3 (6.7)	5.4 (1.3)
Quercetin Concentration[a] (μM) (SEM)	880.5 (5.4)	794.9 (5.8)	280.7 (5.4)	84.6 (4.4)
Extent of solubilization	11.0	9.9	3.5	1.1

[a] The concentration of quercetin in water is 80 μM.
DPPC/quercetin/cholesterol molar ratios were 95:5:0, 85:5:10, 75:5:20 and 55:5:40 and the D:L ratio was kept at 5:95. Results shown are the average values ± SEM obtained from three independent experiments.

4.2.2 Effect of incorporation of 5 mol% of DSPE-PEG_{2000} on the incorporation of quercetin

DSPE-PEG_{2000} was added to the formulation of the liposomes to confer stability in the biological milieu and to prevent aggregation of liposomes during storage (Dos Santos,

Waterhouse et al. 2005). As shown in Table 6, the incorporation of quercetin into the liposomes was similar for the formulations with and without 5 mol% of DSPE-PEG_{2000}. Hence, the incorporation of 5 mol% of DSPE-PEG_{2000} did not affect quercetin incorporation.

Table 6 Comparison of the percentage incorporation of quercetin in DPPC liposomes with or without 5 mol% of DSPE-PEG_{2000}.

	% of DSPE-PEG_{2000}	
	0.0	5.0
% incorporation of quercetin (SEM)	100.4 (9.6)	100.7 (1.3)
Quercetin Concentration[a] (μM) (SEM)	880.5 (5.4)	883.1 (3.2)
Extent of solubilization	11.0	11.0

[a] The concentration of quercetin in water is 80 μM. DPPC/quercetin/DSPE-PEG_{2000} molar ratios were 95:5:0 and 90:5:5. All formulations were formulated at D:L ratio of 5:95. Results shown are the average values ± S.E.M obtained from three independent experiments.

4.2.3 Influence of different lipids on quercetin incorporation

Besides cholesterol, changes in the type of lipid used can also influence quercetin incorporation in the liposomal membrane. Firstly, the effect of headgroups on the quercetin incorporation was assessed by comparing quercetin incorporation in 1,2-Dipalmitoyl-sn-Glycero-3-Phosphocholine (DPPC) with egg sphingomyelin (ESM), both containing 16 carbons in the acyl chain, with ESM comprising one more hydroxyl and amino group

at the headgroup. There was no significant difference in terms of quercetin incorporation ($p > 0.05$).

Subsequently, the effect of varying acyl chain length of the lipids was assessed. Phosphocholines comprising of 14 carbon atoms 1,2-Dimyristoyl-sn-Glycero-3-Phosphocholine (DMPC), 16 carbon atoms 1,2-Dipalmitoyl-sn-Glycero-3-Phosphocholine (DPPC), and 18 carbon atoms 1,2-Distearoyl-sn-Glycero-3-Phosphocholine (DSPC) were used.

Table 7 shows the effect of different lipids on quercetin incorporation. There was no significant difference in terms of quercetin incorporation among the DMPC, DPPC and ESM groups ($p > 0.05$). However, there was statistical difference for the DSPC group ($p < 0.05$) as compared to the DMPC, DPPC and ESM groups.

Table 7 Effect of different lipids on quercetin incorporation.

	Type of lipid			
	DMPC	DPPC	DSPC	ESM
% incorporation of quercetin (SEM)	99.4 (6.8)	100.4 (9.6)	17.0* (0.3)	101.8 (2.1)
Quercetin concentration [a] (μM) (SEM)	900.6 (8.4)	880.5 (5.4)	152.4* (4.6)	884.6 (9.7)
Extent of solubilization	11.3	11.0	1.91*	11.1

[a] The concentration of quercetin in water is 80 μM.
For all the formulations, the D:L ratio was fixed at 5:95. Results shown are the average values ± SEM obtained from three independent experiments.
* $p < 0.05$.

4.2.4 Effect of pH on quercetin incorporation in liposomal membranes

There are a number of drug loading methods which can be used to load chemotherapeutic drugs into the aqueous core of the liposomes. This involves hydration of the lipids at different pH values. For example, drug loading with citrate buffer involves hydration at pH 4 (Mayer, Tai et al. 1990), the use of manganese sulphate involves hydration at pH 3.4 (Messerer, Ramsay et al. 2004), the use of magnesium sulphate involves hydration at pH 5.2 (Zhigaltsev, Maurer et al. 2005) while the passive encapsulation of drugs involves a pH of 7.5. pH has been shown to influence the incorporation of flavonoids in lipid membranes (Movileanu, Neagoe et al. 2000). Hence, the effect of pH on the incorporation of quercetin was studied to select an appropriate drug loading condition for the loading of chemotherapeutic drugs in the subsequent Chapters. The lipid formulation tested comprised of DPPC/DSPE-PEG_{2000}/Quercetin (90:5:5 molar ratio). Figure 10 shows that at acidic pH, quercetin incorporation was around 100 % but at pH 7.5, quercetin incorporation declined to 47.0 %. There was no significant difference in terms of quercetin incorporation at acidic pHs ($p>0.05$). However, there was statistical difference at pH 7.5 ($p < 0.05$) as compared to the other groups.

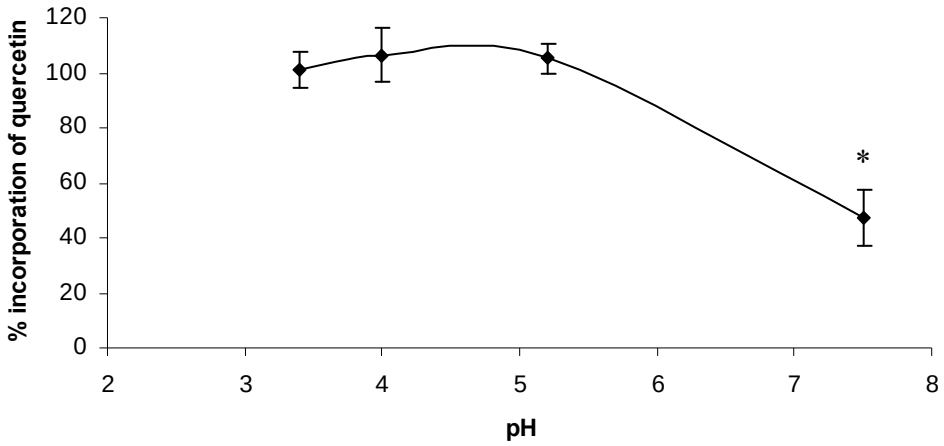

Figure 10 Effect of pH on the incorporation of quercetin in DPPC/DSPE-PEG_{2000}/Quercetin (90:5:5 molar ratio) liposomes. Results shown are the average values ± S.E.M obtained from three independent experiments, * $p<0.05$.

4.2.5 Physical stability of the liposomes

The three lipids with the best incorporation of quercetin were selected for studies on the physical stability of liposomes. DMPC/DSPE-PEG_{2000}/Quercetin (90:5:5 molar ratio), DPPC/DSPE-PEG_{2000}/Quercetin (90:5:5 molar ratio) and ESM/DSPE-PEG_{2000}/Quercetin (90:5:5 molar ratio) liposomes were sized at regular intervals to assess their diameters and polydispersities after storage at 4ºC for 16 weeks. There were no significant change in the either the diameters (Figure 11a) or polydispersity (Figure 11b) of the liposomes, indicating physical stability over 16 weeks.

(a)

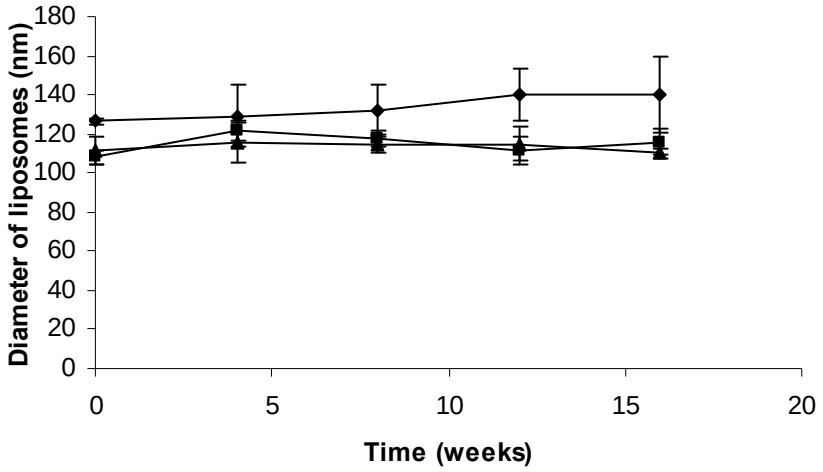

(b)

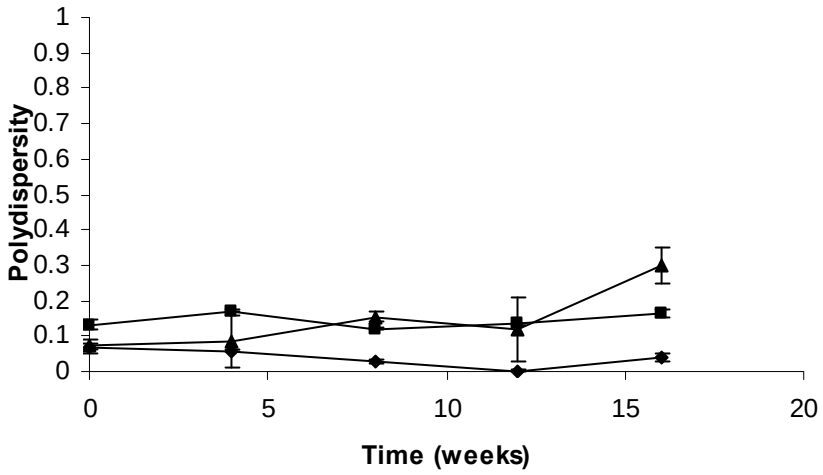

Figure 11 (a) Diameters and (b) polydispersities of DPPC/DSPE-PEG_{2000}/Quercetin (■), DMPC/DSPE-PEG_{2000}/Quercetin (▲) and ESM/DSPE-PEG_{2000}/Quercetin (♦) liposomes over 16 weeks after storage at 4°C. The D:L ratio was kept at 5:95 for all three liposomal formulations. Results shown are the average values ± S.E.M obtained from three independent experiments.

4.2.6 *In vitro* release profile of quercetin

Figure 12 shows the release profile of DPPC/DSPE-PEG_{2000}/Quercetin (90:5:5 molar ratio), DMPC/DSPE-PEG_{2000}/Quercetin (90:5:5 molar ratio), and ESM/DSPE-

PEG_{2000}/Quercetin (90:5:5 molar ratio) liposomes over 72 hours at 37ºC. There was no significant difference in the drug release profile among the three liposomal formulations ($p > 0.05$).

The quercetin release data were further analyzed by fitting the data to the three most common release kinetics patterns for drug delivery systems, including zero order, first order and square root of time release models. The coefficients of determination (r^2) for different models are shown in (Table 8). The best r^2 values were obtained for the square root of time release model with a r^2 values of 0.95 for DPPC/DSPE-PEG_{2000}/Quercetin liposomes, 0.85 for DMPC/DSPE-PEG_{2000}/Quercetin liposomes and 0.94 for ESM/DSPE-PEG_{2000}/Quercetin liposomes.

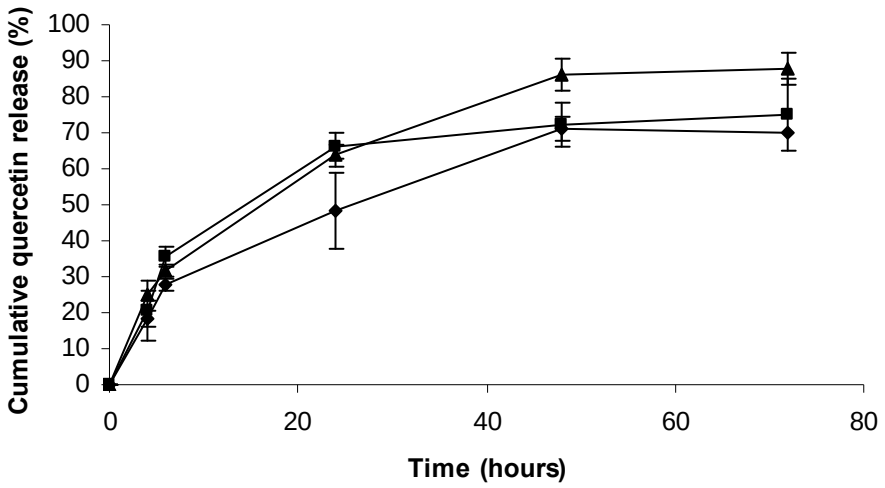

Figure 12 Release profile of quercetin at 37 ºC from different formulations of liposomes. DPPC/DSPE-PEG_{2000}/Quercetin is represented by ■, DMPC/DSPE-PEG_{2000}/Quercetin is represented by ▲ and ESM/DSPE-PEG_{2000}/Quercetin is represented by ♦. The D:L ratio was kept at 5:95 for all three liposomal formulations. Results shown are the average values ± S.E.M obtained from three independent experiments.

Table 8 r^2 values of zero order, first order and square root of time release models for the liposomes.

	Zero order drug release	First order drug release	Square root of time drug release
DPPC/DSPE-PEG_{2000}/Quercetin liposomes	0.73	0.66	0.95
DMPC/DSPE-PEG_{2000}/Quercetin liposomes	0.84	0.81	0.85
ESM/DSPE-PEG_{2000}/Quercetin liposomes	0.84	0.79	0.94

The D:L ratio was kept at 5:95 for all three liposomal formulations.

.

4.2.7 Stability studies with quercetin

$DPPH^{\bullet}$ is a stable free radical which can either accept an electron or hydrogen radical to form a stable, diamagnetic molecule. Due to the presence of the odd electron, it has a strong absorption band at 517 nm. When the electron becomes paired, the absorption at 517 nm decreases proportionally with respect to the number of electrons taken up. This change in absorbance can be used to test the ability of molecules to act as hydrogen donors.

Prior stability studies have established that the hydroxyl groups on quercetin are vulnerable to oxidation (Zenkevich, Eshchenko et al. 2007). When this occurs, the hydrogen donating ability of quercetin to $DPPH^{\bullet}$ is reduced, leading to a reduced change in absorbance of $DPPH^{\bullet}$. Hence, the stability of liposomal encapsulated quercetin was compared with that of

quercetin in 4-(2-hydroxyethyl)-1-piperazineethanesulfonic acid buffered saline (HBS) buffer. Figure 13 shows the percentage reduction in hydrogen donating ability of quercetin over 14 days. Among the four groups, ESM/DSPE-PEG_{2000}/Quercetin and DPPC/DSPE-PEG_{2000}/Quercetin liposomes displayed similar profiles in terms of percentage reduction in hydrogen donating activity. They also showed smaller percentages in the hydrogen donating activity as compared to the other groups, followed by DMPC/DSPE-PEG_{2000}/Quercetin liposomes. Un-encapsulated quercetin showed the greatest reduction in hydrogen donating ability of quercetin.

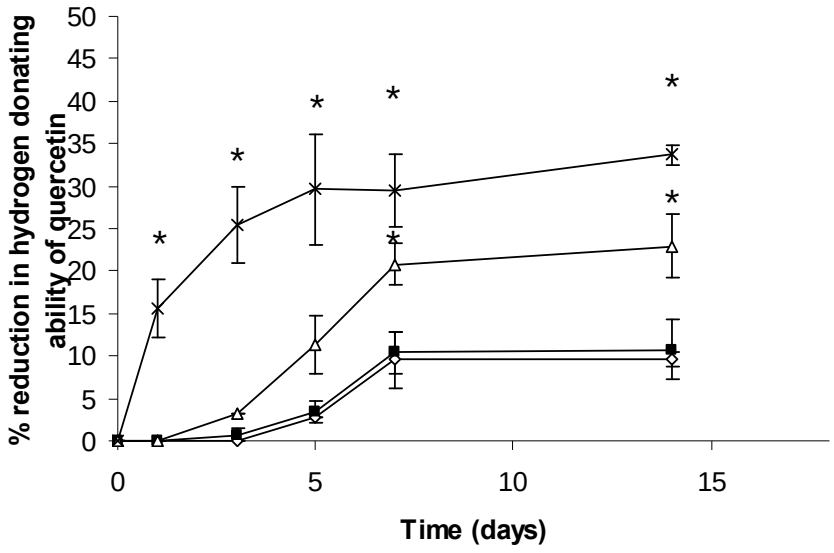

Figure 13 Comparison of un-encapsulated quercetin (x), ESM/DSPE-PEG_{2000}/Quercetin (90:5:5 molar ratio) (◊), DPPC/DSPE-PEG_{2000}/Quercetin (90:5:5 molar ratio) (■) and DMPC/DSPE-PEG_{2000}/Quercetin (90:5:5 molar ratio) (Δ) as assessed by the percentage reduction in hydrogen donating ability of quercetin. Results shown are the average values ± S.E.M obtained from three independent experiments. * $p < 0.05$.

4.2.8 *In vitro* cytotoxicity studies of liposomal quercetin

From Section 4.2.7, ESM/DSPE-PEG_{2000}/Quercetin and DPPC/DSPE-PEG_{2000}/Quercetin showed smaller percentages in the reduction in hydrogen donating ability of quercetin as compared to other groups, indicating that they conferred superior protection against quercetin degradation. Therefore, the cytotoxicity of these two formulations was assessed in two representative breast cancer cell lines, MDA-MB-231 and JIMT-1.

Before initiating the study on liposomes containing quercetin, *in vitro* cytotoxicity studies of the liposomes without quercetin were first conducted on MDA-MB-231 and JIMT-1 cells to determine if the liposome carrier itself contributed to the cytotoxicity of the cells. The concentration of lipid tested was matched to the amount of lipid used in the formulation. At the concentrations of lipids used, there was no effect on the cell kill (Figure 14 and Figure 15).

(a)

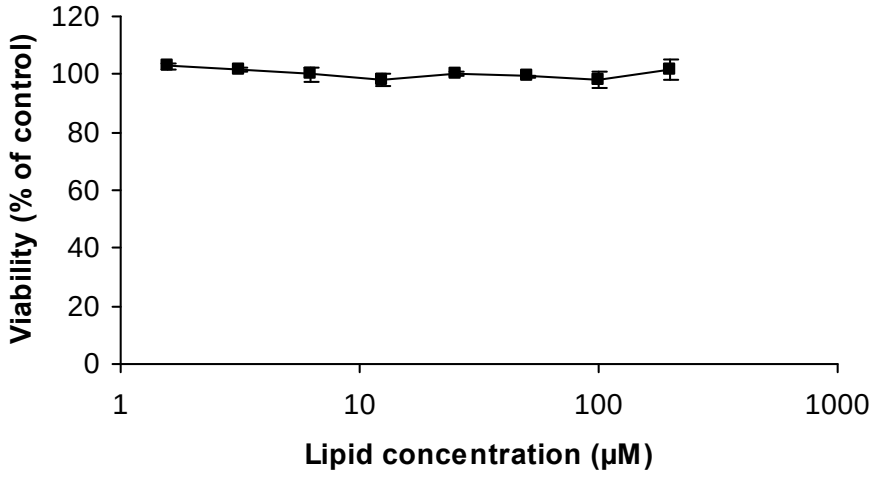

(b)

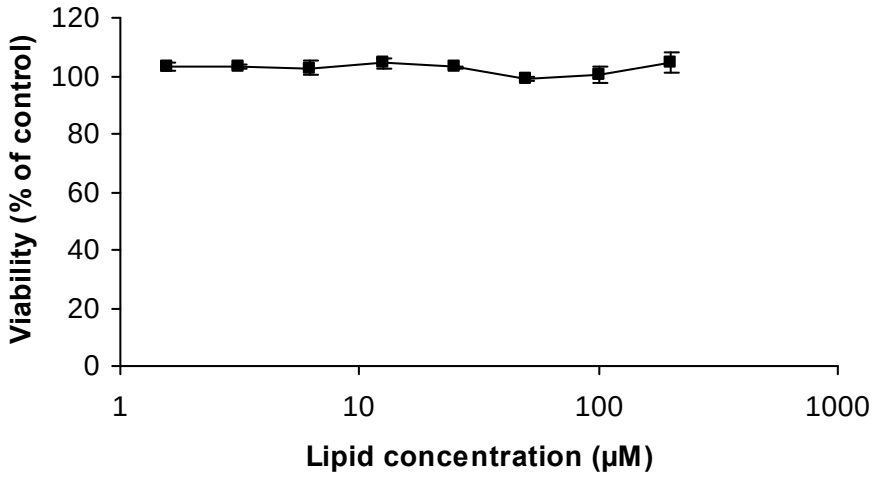

Figure 14 *In vitro* cytotoxicity of the liposome carrier (a) DPPC/DSPE-PEG_{2000} (b) ESM/DSPE-PEG_{2000} in MDA-MB-231 cells. Results shown are the average values ± S.E.M obtained from three independent experiments.

(a)

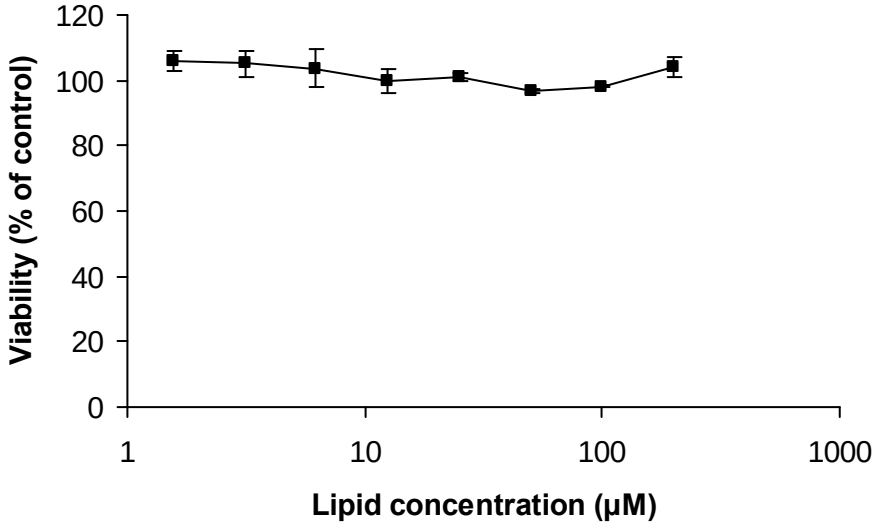

(b)

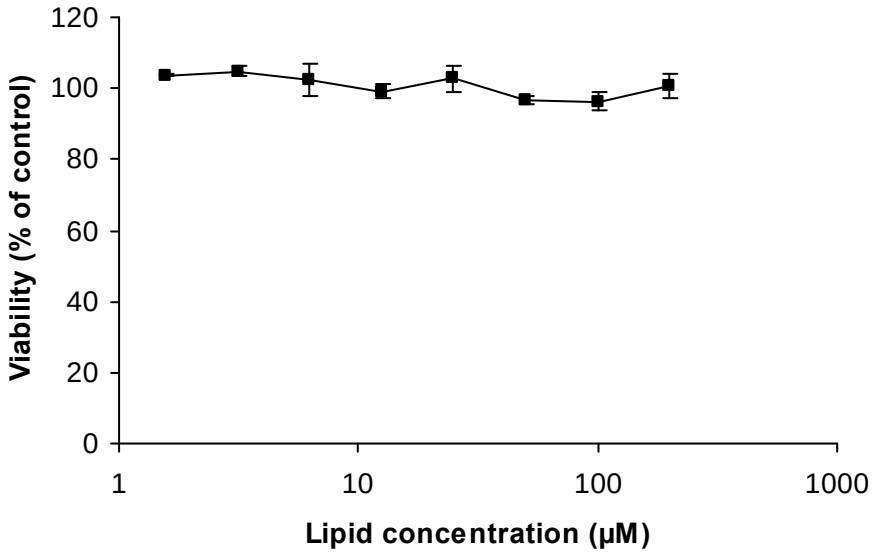

Figure 15 *In vitro* cytotoxicity of the liposome carrier (a) DPPC/DSPE-PEG_{2000} (b) ESM/DSPE-PEG_{2000} in JIMT-1 cells. Results shown are the average values ± S.E.M obtained from three independent experiments.

Although quercetin has a solubility of 80 μM in water, the solubility of free quercetin can be increased to 250 μM in the presence of 10% fetal bovine serum in cell culture media through its binding to serum proteins (van der Woude, Gliszczynska-Swiglo et al. 2003). Therefore, the highest concentration of free quercetin tested was 250 μM. Table 9 shows the median-effect concentrations (EC_{50}) and linear correlation coefficient (r) values of free, un-encapsulated quercetin, DPPC/DSPE-PEG_{2000}/Quercetin liposomes and ESM/DSPE-PEG_{2000}/Quercetin liposomes in both JIMT-1 and MDA-MB-231 breast cancer cell lines. EC_{50} is an indication of the potency of the drug, while r value indicates the goodness of fit for the data to the median-effect equation used to calculate EC_{50}. As shown in Table 9, the amount of quercetin needed to attain the EC_{50} was reduced approximately 10-fold for both liposomal formulations as compared to free quercetin in both breast cancer cell lines.

Table 9 *In vitro* cytotoxicity of quercetin in free and liposomal form.

	Free Quercetin		DPPC/DSPE-PEG_{2000}/ Quercetin		ESM/DSPE-PEG_{2000}/ Quercetin	
	EC_{50}[a]/ μM	r	EC_{50}[a]/ μM	r	EC_{50}[a]/ μM	r
JIMT-1	105.4	0.92	7.2	0.93	8.6	0.96
MDA-MB-231	109.2	0.93	6.2	0.95	7.5	0.94

[a] EC_{50} values were derived from 8 points.
Both ESM/DSPE-PEG_{2000}/Quercetin and DPPC/DSPE-PEG_{2000}/Quercetin liposomes were in 90:5:5 molar ratios, n=3

4.3 Discussion

This Chapter aims to determine the optimal conditions for quercetin incorporation in liposomes, evaluate the extent of quercetin solubilization, and determine the *in vitro* drug release and cytotoxicity profiles so as to select the optimal formulation for co-encapsulation with chemotherapeutic agents in the subsequent Chapters. The first parameter assessed was the effect of cholesterol on quercetin incorporation. Table 5 shows that the presence of cholesterol reduced quercetin incorporation. Two possible reasons could lead to this finding. Firstly, cholesterol competes with quercetin for the same space in the lipid bilayer (Zhang, Anyarambhatla et al. 2005). Therefore, an increase in the mole fraction of cholesterol would reduce the space available for quercetin in the lipid bilayer. Secondly, cholesterol incorporation in liposomes reduces the flexibility of the hydrocarbon chains of the lipids (Demel and De Kruyff 1976), hampering quercetin penetration into the lipid bilayer. The results obtained here were similar to those obtained for paclitaxel, another hydrophobic compound, where an increase in the cholesterol content in liposomes decreased the loading efficiency of paclitaxel (Zhang, Anyarambhatla et al. 2005). The extent of solubilization of quercetin after liposomal incorporation was also determined. All liposomal formulations solubilized quercetin (Table 5). This could be due to the incorporation of quercetin into the liposomal bilayer (Goniotaki,

Hatziantoniou et al. 2004), protecting it from unfavorable interactions with water.

As mentioned in Section 1.11.3, cholesterol increases the biological stability of the liposomes by reducing the interaction of the liposomes with plasma proteins which destabilize them (Kirby, Clarke et al. 1980; Senior and Gregoriadis 1982; Senior 1987; Gabizon, Catane et al. 1994). However, recent research has shown that this could also be accomplished by DSPE-PEG_{2000} (Bartucci, Pantusa et al. 2002). Therefore, after it has been established that quercetin incorporation was the most optimal with 0% cholesterol, 5 mol% of DSPE-PEG_{2000} was added to the formulation to stabilize the liposomes. There was no statistical difference in quercetin incorporation after adding 5 mol% of DSPE-PEG_{2000}.

Besides DSPE-PEG_{2000}, the type of lipid used for liposome making can also influence quercetin incorporation. There was no significant difference in terms of quercetin incorporation between DPPC and ESM ($p>0.05$), suggesting that the presence of additional hydroxyl and amino groups on ESM did not have a significant impact on the incorporation of quercetin. This could be attributed to quercetin interacting primarily with the acyl chain of the phospholipids rather than the headgroup (Goniotaki, Hatziantoniou et al. 2004). Subsequently, the effect of acyl chain length on quercetin incorporation was explored. Quercetin incorporation was lowest in liposomes with DSPC. This could be

due to the formation of a more rigid lipid bilayer by DSPC (Anderson and Omri 2004) as compared to DMPC and DPPC, which can limit quercetin incorporation in the liposomes.

As shown in Figure 10, the incorporation of quercetin at acidic pH was close to 100%. This is because at acidic pHs, quercetin is neutral and completely soluble in lipids (Movileanu, Neagoe et al. 2000). Therefore, the incorporation of quercetin into the lipid bilayer is high due to the favorable interactions with both the acyl group and the headgroup of the phospholipid. In contrast, at alkaline pH, the incorporation of quercetin decreased to 47%. This could be due to the deprotonation of the hydroxyl-pyrone of quercetin (Figure 1), which leads to the formation of a negatively charged molecule. The percentage incorporation of quercetin could be reduced since the intercalation of a charged quercetin molecule in the hydrophobic space between the phospholipids is less unfavorable. In summary, the incorporation of quercetin is close to 100% at acidic pH, the citrate, manganese and magnesium sulphate gradients can be used in the loading of chemotherapeutic drugs without adversely affecting the incorporation of quercetin.

Subsequently, the size and polydispersity of the three formulations with the best quercetin incorporation, namely DMPC/DSPE-PEG_{2000}/Quercetin (90:5:5 molar ratio), DPPC/DSPE-PEG_{2000}/Quercetin (90:5:5 molar ratio) and ESM/DSPE-PEG_{2000}/Quercetin (90:5:5 molar ratio) were

monitored to assess their stability. In this Chapter, the size and stability of the liposomes were assessed for 16 weeks so that further studies on *in vitro* drug release and cytotoxicity on the liposomes with good physical stability can proceed in a timely manner. A longer study period of 360 days will be conducted for formulations that are chosen for co-encapsulation of conventional chemotherapeutic agents (Sections 6.2.5 and 7.2.6). Nevertheless, the absence of significant changes in either the diameters (Figure 11a) or polydispersity (Figure 11b) indicates physical stability, due to the presence of DSPE-PEG_{2000}, preventing aggregation after 16 weeks of storage (Dos Santos, Allen et al. 2007).

After the stability studies, the three liposomal formulations were subjected to *in vitro* quercetin release studies. The quercetin release data were further analyzed by fitting the data to the three most common release kinetics patterns for drug delivery systems. The best fit was obtained for the square root of time release model for the three liposome formulations. This model suggests that quercetin incorporated in the liposome has to diffuse through the lipid bilayer to be released (Nounou, El-Khordagui et al. 2006). The results obtained were consistent with that of another hydrophobic drug dibucaine, which was loaded in cholesterol free liposomes in a similar manner as quercetin. Dibucaine also had the best correlation for the square root of

time release as compared to the other models (Nounou, El-Khordagui et al. 2006).

Subsequently, the DPPH$^{\bullet}$ study was used to assess the extent of quercetin degradation. All liposomal formulations showed less reduction in hydrogen donating activity of quercetin as compared to free quercetin. This suggests that quercetin degradation was reduced in liposomal formulations, preserving the ability to reduce DPPH$^{\bullet}$. However, the DMPC/DSPE-PEG_{2000}/Quercetin formulation showed a greater percentage reduction in DPPH$^{\bullet}$ as compared to either ESM/DSPE-PEG_{2000}/Quercetin or DPPC/DSPE-PEG_{2000}/Quercetin. This could be attributed to the quercetin molecule interacting primarily with the acyl chain of the phospholipids (Goniotaki, Hatziantoniou et al. 2004). Since DMPC has only 14 carbon atoms, and thereby a shorter acyl chain, hence it conferred less protection from degradation compared with either ESM or DPPC, both with 16 carbon atoms.

Finally, the *in vitro* cytotoxicity of quercetin liposomes was assessed in JIMT-1 and MDA-MB-231 breast cancer cells. The concentration needed to attain ED_{50} was reduced by approximately 10-fold in both cell lines after liposomal incorporation, which can be explained by the results from the DPPH$^{\bullet}$ study. Encapsulated quercetin showed less reduction in the hydrogen donating activity compared with free quercetin (Figure 13). This could be due to the protective effect of

liposome incorporation, whereby the hydroxyl groups of quercetin are protected from oxidation which are necessary for the cytotoxicity of quercetin (Lopez-Lazaro 2002). It should be highlighted that this effect was not reported in the previous work with EPC/Quercetin liposomes (Goniotaki, Hatziantoniou et al. 2004). This could be because saturated DPPC/DSPE-PEG_{2000} based liposomes are less likely to undergo lipid peroxidation (Ioku, Tsushida et al. 1995) compared to unsaturated egg phosphatidylcholine (EPC), where free radicals produced from lipid peroxidation could degrade quercetin to its less cytotoxic form (Lopez-Lazaro 2002).

Overall, the formulations of DPPC/DSPE-PEG_{2000}/Quercetin (90:5:5 molar ratio) and ESM/DSPE-PEG_{2000}/Quercetin (90:5:5 molar ratio) had high percentage incorporation of quercetin, good *in vitro* stability, protected quercetin from degradation and improved the cytotoxcity of quercetin. Therefore, they will be used in the subsequent Chapters to co-encapsulate chemotherapeutic agents.

Chapter 5

EVALUATION OF VARIOUS COMBINATIONS OF QUERCETIN WITH CONVENTIONAL CHEMOTHERAPEUTIC AGENTS

5.1 Introduction

Cancer cells are heterogeneous as they acquire different genetic abnormalities (Hanahan and Weinberg 2000). Hence, the use of a single drug is unlikely to achieve significant cancer cell kill, and could even lead to the development of drug resistance due to insufficient cancer cell inhibition (Shah and Schwartz 2001). Therefore, combination chemotherapy is the mainstay of cancer treatment (Devita, Serpick et al. 1970; Schwartz and Smith 1976; Keppen 2010). However, not all drug combinations are beneficial. Drugs may counteract each other, so that the treatment effect of combination is less than the sum activities of the individual agents (Drewinko, Loo et al. 1976; Abraham, McKenzie et al. 2004). In contrast, when the drugs interact synergistically, the combined activities of the drugs are greater than that predicted from the contributions of the individual drugs (Paterson and Moriwaki 1969; Krainer 2003). Such synergism could produce equivalent efficacy at a fraction of doses of the individual drugs, thereby reducing dose-dependent side effects and improve patient response clinically (Shah and Schwartz 2001). Therefore, there is a need to determine whether the combination is synergistic, antagonistic or additive before

clinical use. In this Chapter, the synergy of quercetin with conventional chemotherapy drugs will be analyzed with the Chou and Talalay median-effect principle through the CalcuSyn® software.

As summarized in Section 1.6, quercetin exhibited synergism with camptothecin derivatives, plant alkaloids, alkylating agents and pyrimidine analogs in different types of human and animal cancer cell lines (Scambia, Ranelletti et al. 1990; Sliutz, Karlseder et al. 1996; Nakayama, Sakamoto et al. 2000; Leslie, Mao et al. 2001; Akbas, Timur et al. 2005). In addition, irinotecan, vincristine, carboplatin and 5-fluorouracil have been shown to be effective against metastatic breast cancer refractory to first line treatment (Ries and Dicato 1991; Chu, Sutton et al. 1996; Perez, Hillman et al. 2004; Chan, Yeo et al. 2009). Hence, these drugs were selected and analyzed for synergy with quercetin in two representative breast cancer cell lines, JIMT-1 and MDA-MB-231. These cell lines were selected on the basis that they are hormone receptor negative and non responsive to trastuzumab treatment. The aim of this Chapter is to determine whether irinotecan, vincristine, carboplatin and 5-fluorouracil exhibit synergy with quercetin in the breast cancer cell lines, JIMT-1 and MDA-MB-231.

5.2 Results

5.2.1 *In vitro* activities of quercetin, irinotecan, vincristine, carboplatin and 5-fluorouracil monotherapy in JIMT-1 and MDA-MB-231 breast cancer cell lines

JIMT-1 and MDA-MB-231 breast cancer cell lines were treated with various concentrations of quercetin, irinotecan, vincristine, carboplatin and 5-fluorouracil monotherapy for 72 hours. CalcuSyn® was used to determine the median-effect concentration (ED_{50}) and linear correlation coefficient (r). The ED_{50} values indicate the potency of the drug while the r values show the goodness of fit for the data to the median-effect equation used to calculate ED_{50}.

Table 10 EC_{50} and r values of quercetin, irinotecan, vincristine, carboplatin and 5-fluorouracil in JIMT-1 and MDA-MB-231 breast cancer cells.

	JIMT-1		MDA-MB-231	
	EC_{50}[a]/ μM	r	EC_{50}[a]/ μM	r
Quercetin	105.4	0.92	109.2	0.91
Irinotecan	53.4	0.94	56.1	0.95
Vincristine	15.9	0.98	8.4	0.94
Carboplatin	118.4	0.90	92.4	0.96
5-fluorouracil	142.1	0.95	98.3	0.98

[a]EC_{50} values were derived from 8 points, n=3.

5.2.2 Drug combination studies

Drug combination studies designed to assess the concurrent administration of quercetin and (i) irinotecan, (ii) vincristine, (iii) carboplatin (iv) 5-fluorouracil were performed

and evaluated after 72 hours of drug exposure. Serial dilutions of irinotecan, vincristine, carboplatin and 5-fluorouracil were used while the concentrations of quercetin were fixed at the ED_{50} (100 μM), ED_{20} (50 μM) and ED_{10} (25 μM) values of quercetin monotherapy. These levels of quercetin have been selected as they have been shown to have no significant effect on the growth of normal cells (Chowdhury, Kishino et al. 2005).

Figure 16 and Figure 17 illustrate the combination index (CI) values at different concentrations of quercetin and irinotecan for JIMT-1 and MDA-MB-231 breast cancer cells, respectively. The combination of quercetin and irinotecan was either synergistic or additive over a wide range of concentrations. For the two breast cancer cell lines, the combination of irinotecan and quercetin showed either synergism or addition for concentrations below 250 μM and antagonism at the highest concentration tested at 500 μM.

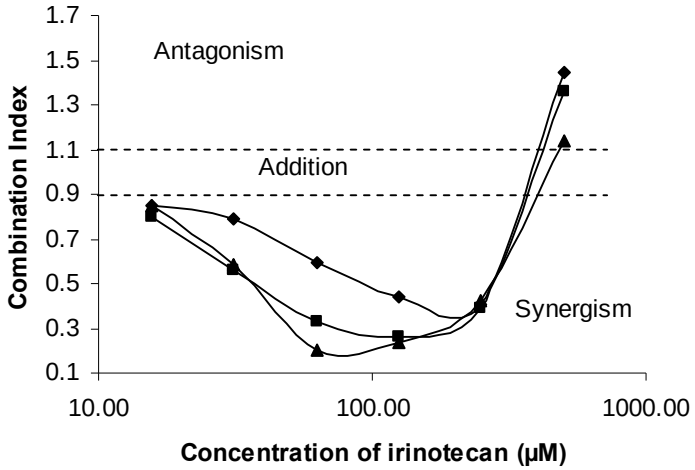

Figure 16 Combination index values as a function of irinotecan concentration exposed to JIMT-1 breast cancer cells at 25 µM (♦), 50 µM (■) and 100 µM (▲) of quercetin.

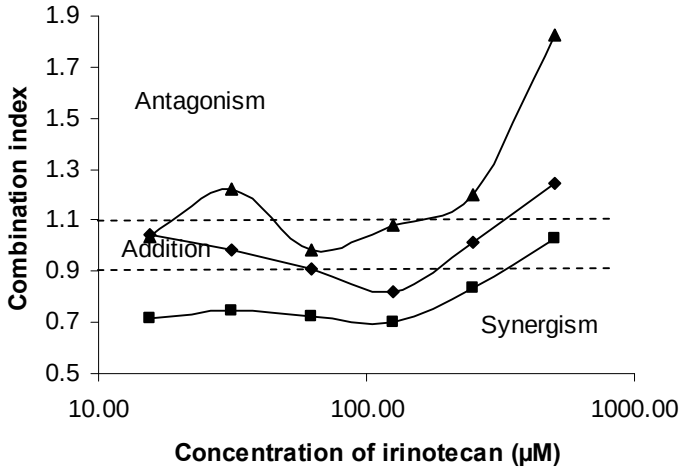

Figure 17 Combination index values as a function of irinotecan concentration exposed to MDA-MB-231 breast cancer cells at 25 µM (♦), 50 µM (■) and 100 µM (▲) of quercetin.

Figure 18 and Figure 19 show the CI values plotted against concentration for quercetin and vincristine. For JIMT-1 and MDA-MB-231 cells, combining either 25 μM or 50 μM of quercetin with varying concentrations of vincristine were found to be either synergistic or additive.

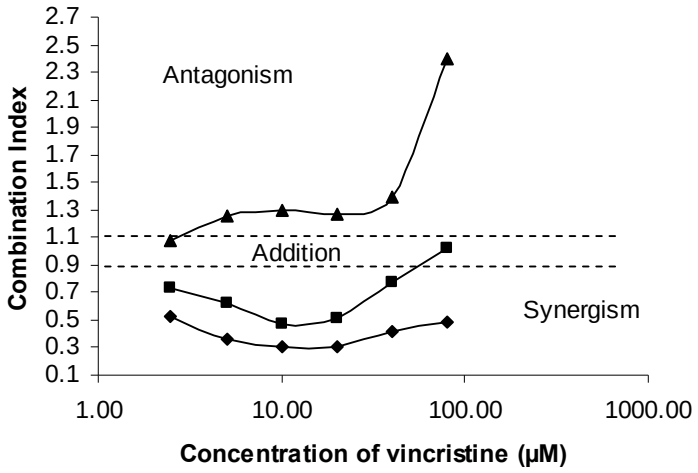

Figure 18 Combination index values as a function of vincristine concentration exposed to JIMT-1 breast cancer cells at 25 μM (♦), 50 μM (■) and 100 μM (▲) of quercetin.

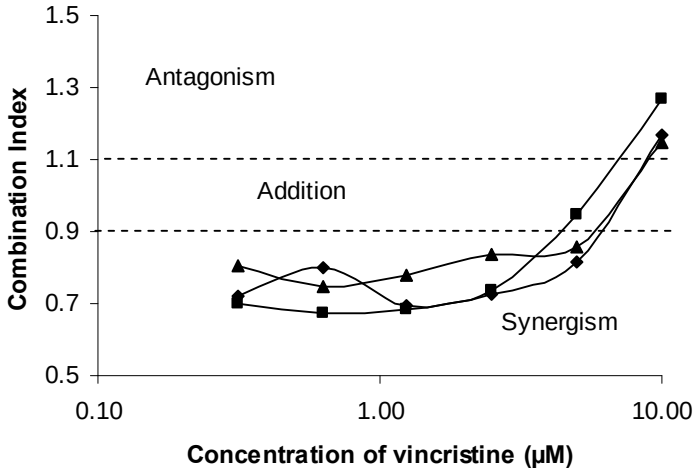

Figure 19 Combination index values as a function of vincristine concentration exposed to MDA-MB-231 breast cancer cells at 25 μM (♦), 50 μM (■) and 100 μM (▲) of quercetin.

Figure 20 and Figure 21 show the CI values at varying concentrations of carboplatin and quercetin for JIMT-1 and MDA-MB-231 breast cancer cells respectively. The best synergy was observed with the combination of carboplatin and 100 µM of quercetin while the other concentrations where either antagonistic or additive.

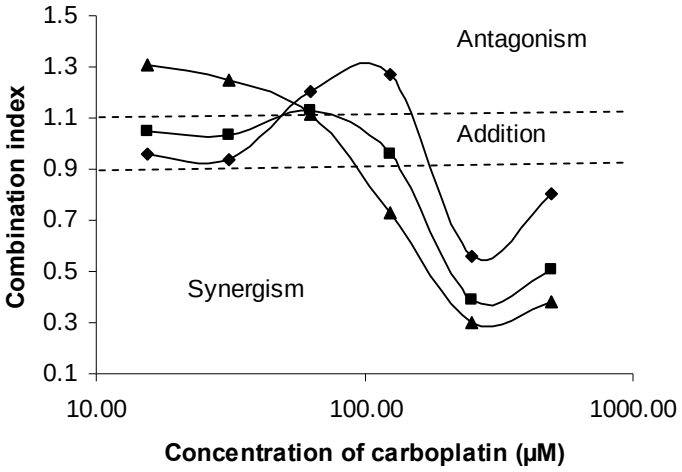

Figure 20 Combination index values as a function of carboplatin concentration exposed to JIMT-1 breast cancer cells at 25 µM (♦), 50 µM (■) and 100 µM (▲) of quercetin.

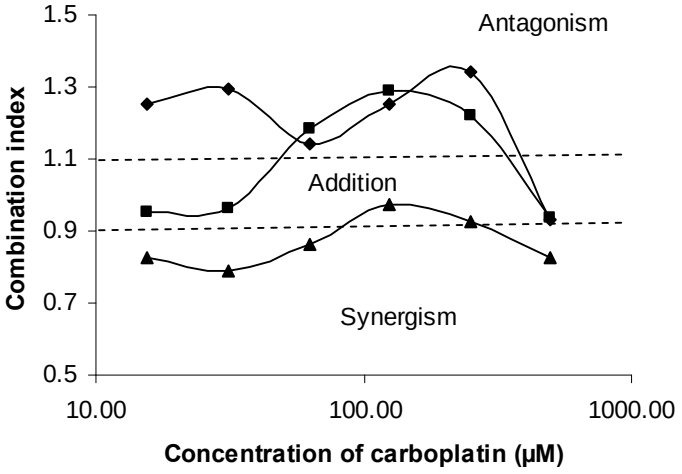

Figure 21 Combination index values as a function of carboplatin concentration exposed to MDA-MB-231 breast cancer cells at 25 µM (♦), 50 µM (■) and 100 µM (▲) of quercetin.

Lastly, Figure 22 and Figure 23 show the CI values at varying concentrations of 5-fluorouracil and quercetin for JIMT-1 and MDA-MB-231 cells, respectively. In both cell lines, synergistic or additive effect was observed at lower concentrations of 5-fluorouracil.

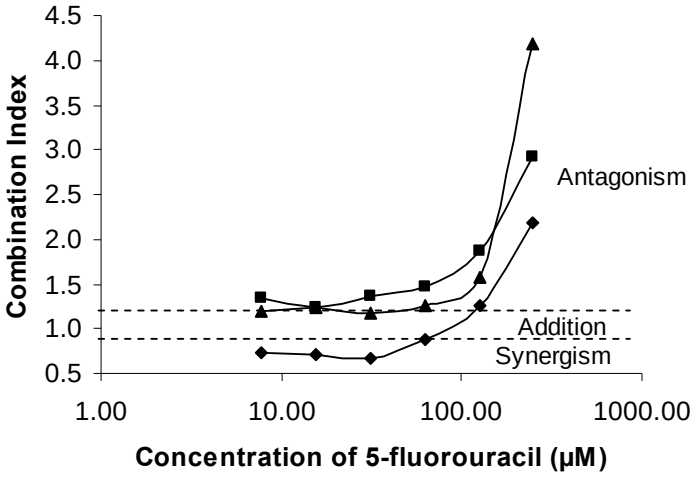

Figure 22 Combination index values as a function of 5-fluorouracil concentration exposed to JIMT-1 breast cancer cells at 25 µM (♦), 50 µM (■) and 100 µM (▲) of quercetin.

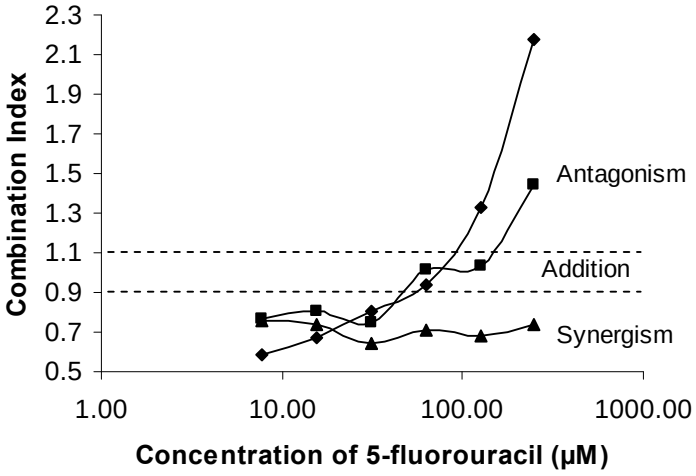

Figure 23 Combination index values as a function of 5-fluorouracil concentration exposed to MDA-MB-231 breast cancer cells at 25 µM (♦), 50 µM (■) and 100 µM (▲) of quercetin.

5.3 Discussion

The anti-cancer activity of chemotherapeutic drugs is drug ratio dependent, exhibiting synergism at some ratios but additivity or antagonism at other ratios (Mayer, Harasym et al. 2006; Harasym, Liboiron et al. 2009; Tardi, Johnstone et al. 2009). In order to screen for a wider range of drug ratios with a smaller number of experiments, the concentration of the chemotherapeutic agents were varied while the concentration of the quercetin was kept constant at 25 μM, 50 μM and 100 μM, which were selected as they have been shown to have no significant effect on the growth of normal cells (Chowdhury, Kishino et al. 2005). Table 10 shows that the r values of all the drugs tested were above 0.90. Hence, the data had good conformity with the median-effect equation, and the EC_{50} values obtained reflect the potency of the drugs (Chou and Talalay 1977). This in turn confirmed the reliability of the CI values, which were derived from the EC_{50} values (Chou 2008).

In this Chapter, combination studies of quercetin and irinotecan showed that there was synergy between these two drugs over a wide range of concentrations (Figure 16 and Figure 17). The results are consistent with previous work by Akbas et al., which had also demonstrated synergy between quercetin and camptothecin derivatives in the MDA-MB-231 breast cancer cell line through the inhibition of tyrosine specific protein kinase by

quercetin (Akbas, Timur et al. 2005). Another possible mechanism for synergy could be the effect of quercetin on heat shock proteins, a protein which confers resistance of cancer cells to certain anti-cancer drugs. Quercetin downregulated Hsp70 expression in fibrosarcoma WEHI-S cells and reduced the concentration of camptothecin derivatives needed to exert cytotoxic activity (Sliutz, Karlseder et al. 1996), which could also be a possible mechanism leading to synergy between quercetin and irinotecan in the breast cancer cell lines.

As shown in Figure 18 and Figure 19, quercetin and vincristine displayed synergy over a wide range of concentrations in breast cancer cells. A possible mechanism could be extrapolated from LY294002 (Figure 24), which was developed based on quercetin as the lead compound (Vlahos, Matter et al. 1994). LY294002 has been shown to enhance the induction of apoptosis by vincristine through the activation of glycogen synthase kinase-3β, which phosphorylates microtubule-associated protein tau (MAPT) and thereby reduces their ability to bind and stabilize microtubules. This increased the sensitivity of cancer cells to vincristine, especially at low concentrations of vincristine that alone do not lead to the disruption of cytoplasmic microtubules (Fujiwara, Hosokawa et al. 2007). Given the structural similarities between quercetin and LY294002, the synergism with vincristine could be due to similar pathways as well.

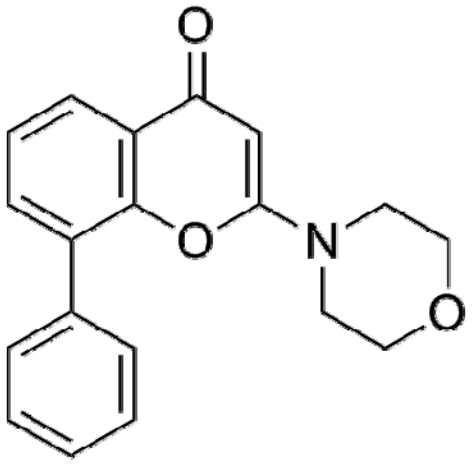

Figure 24 Structure of LY294002.

For carboplatin, antagonism was observed at low quercetin concentrations and synergism at high concentrations across all the cell lines (Figure 20 and Figure 21). This could be due to the dependency of alkylating agents such as carboplatin on the generation of reactive oxygen species for its cytotoxicity (Godbout, Pesavento et al. 2002). At quercetin concentrations less than 100 µM, quercetin acts as an antioxidant (Lee, Kim et al. 2003), thereby antagonizing the effects of carboplatin. In contrast, at higher concentrations of 100 µM, quercetin acts as a prooxidant (Laughton, Halliwell et al. 1989), synergizing with carboplatin in cancer cell kill.

Finally, antagonism was observed for 5-fluorouracil and quercetin at most of the concentrations tested in all cell lines (Figure 22 and Figure 23). This could be attributed to quercetin arresting cancer cells in the late G1 phase of the cell cycle

(Yoshida, Yamamoto et al. 1992), thereby preventing the cells from entering the S phase in which 5-fluorouracil acts.

Taking the data together, the combinations of quercetin with either irinotecan or vincristine were more synergistic as compared to that of carboplatin and 5-fluorouracil. Based on the results obtained, the co-enencapsulation of quercetin with (i) irinotecan and (ii) vincristine in liposomes will be attempted in the subsequent Chapters.

Chapter 6

CO-ENCAPSULATION OF QUERCETIN AND IRINOTECAN INTO LIPOSOMES

6.1 Introduction

In Chapter 5, quercetin was shown to synergize with irinotecan in breast cancer cell lines over a wide range of concentrations. Irinotecan is a water-soluble analogue of camptothecin which acts during the S-phase of DNA replication by stabilizing the complex formed between topoisomerase I and DNA (Kawato, Aonuma et al. 1991). It is active against ovarian, colorectal and small-cell cancer lung cancers (Rosen 1998). In addition, irinotecan is currently undergoing clinical trials for metastatic breast cancer refractory to anthracyclines, taxanes or both (Perez, Hillman et al. 2004). Despite its promising anti-cancer activity, irinotecan is hydrolyzed from the active lactone to the inactive carboxylate form at physiological pH (Chollet, Goumaz et al. 1998). This is illustrated on Figure 25. Therefore, encapsulation of irinotecan in a drug carrier can protect irinotecan from hydrolysis to its inactive carboxyl group, thereby increasing therapeutic efficacy.

Irinotecan has been entrapped in DSPC/Cholesterol (55:45 mol%) liposomes with an Mn^{2+}/A23187-mediated proton gradient. The A23187 ionophore generates a stable transmembrane gradient by transferring two protons for each

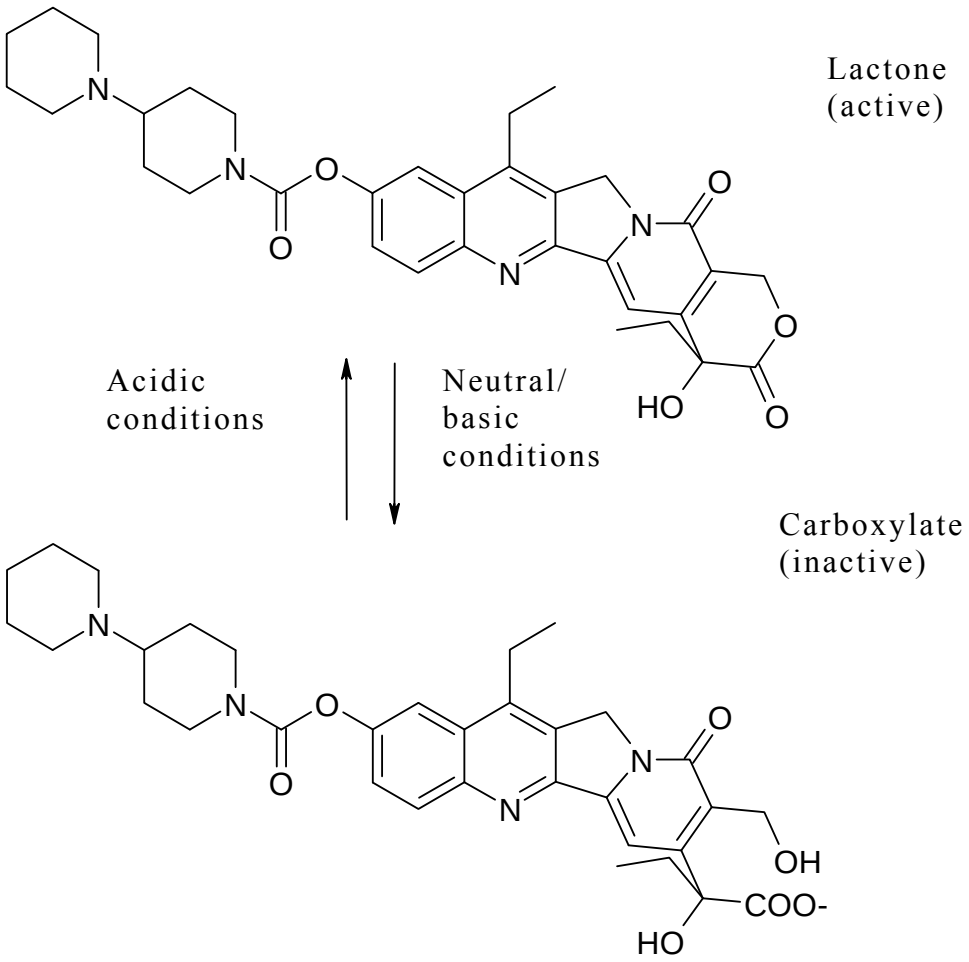

Figure 25 Inactivation of irinotecan under basic conditions.

Mn^{2+} ion transported out from the inner core of the liposomes for protons in the external buffer (Fenske, Wong et al. 1998). This creates an acidic inner core which can maintain irinotecan in its active lactone form. In addition, this formulation has been shown to increase the circulation longevity of irinotecan as compared with free irinotecan and has also been shown to be more effective in the treatment of two models of colorectal cancer (Messerer, Ramsay et al. 2004).

However, in Chapter 4 it was found that the presence of cholesterol and DSPC led to low quercetin incorporation. In contrast, the liposomal formulation of DPPC/DSPE-PEG_{2000}/Quercetin (90:5:5 molar ratio) showed 100% quercetin incorporation. In addition, due to the structural similarilty of DPPC and DSPC, which had been previously used to load irinotecan, this formulation was selected instead of the ESM/DSPE-PEG_{2000}/Quercetin (90:5:5 molar ratio). Therefore, irinotecan will be loaded into DPPC/DSPE-PEG_{2000}/Quercetin (90:5:5 molar ratio) liposomes with the Mn^{2+}/A23187-mediated proton gradient. Despite the advantages of irinotecan encapsulation in liposomes, irinotecan loading in cholesterol free liposomes has not been attempted previously. Therefore, the objectives of this Chapter are to (1) determine the optimal molar ratio to co-encapsulate irinotecan and quercetin, (2) develop a physically stable liposomal formulation that can co-encapsulate quercetin and irinotecan efficiently, (3) determine the release profile of quercetin and irinotecan and (4) evaluate the *in vitro* cytotoxicity of the liposomal formulation.

6.2 Results

6.2.1 *In vitro* activities of quercetin and irinotecan

Recently, it was found that the efficacy of chemotherapeutic drugs can be enhanced by administering them

in their synergistic ratio (Mayer, Harasym et al. 2006). In Chapter 5, a wide range of ratios of quercetin and chemotherapeutic drug were tested by fixing the concentration of quercetin at 25 μM, 50 μM and 100 μM while changing the concentration of the chemotherapeutic drug. Irinotecan and quercetin were found to synergize over wide concentration ranges. Therefore, in this Section, the optimal molar ratio to encapsulate quercetin and irinotecan in the liposomes was assessed from the combination index values at the fixed irinotecan/quercetin molar ratios of 4:1, 2:1, 1:1, and 1:2 in two representative breast cancer cell lines MDA-MB-231 and JIMT-1. These ratios were selected based on the expectation that the two drugs could be successfully encapsulated in liposomes. The optimal ratio will be used for liposome encapsulation.

Figure 26 shows the CI values at the four molar ratios of quercetin/irinotecan at ED_{75}, the dose needed to attain 75% cell kill. CI values at ED_{75} are shown because the aim of cancer treatment is to eradicate cancer cells, hence high cell kill values are more clinically relevant as compared to low cell kill values (Harasym, Tardi et al. 2007). The CI values of irinotecan/quercetin at molar ratios of 4:1, 2:1, 1:1 and 1:2 were 0.189, 0.0180, 0.0252 and 0.0408 for JIMT-1 cells and 0.0409, 0.0125, 0.0147 and 0.0499 for MDA-MB-231 cells. Therefore, the most optimal irinotecan/quercetin molar ratio was 2:1. Since the quercetin/lipid molar ratio was 0.05, the irinotecan/lipid

molar ratio to be encapsulated will be 0.1, so as to achieve the 2:1 irinotecan/quercetin drug molar ratios.

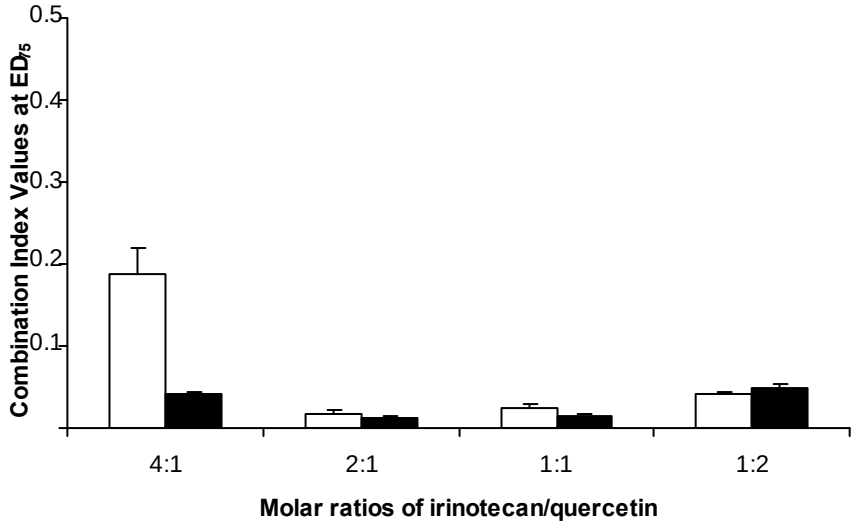

Figure 26 Combination index (CI) values at ED_{75} for irinotecan/quercetin exposed to JIMT-1 (white bars) and MDA-MB-231 (black bars) breast cancer cells at molar ratios of irinotecan/quercetin of 4:1, 2:1, 1:1 and 1:2. Each value represents the mean ± SEM from three independent experiments. CI values of 0.9-1.1 indicate additive activity, CI values < 0.9 indicate drug synergy and values > 1.1 indicate antagonism.

6.2.2 Effect of ionophore on irinotecan loading

Firstly, the role of ionophore A23187 in irinotecan loading into cholesterol free liposomes was determined. Figure 27 shows that a maximum of 27.3 % of irinotecan could be loaded at 55 ºC in the absence of ionophore; whilst a maximum of 15.0 % irinotecan could be loaded at 37 ºC (Figure 28). This percentage of drug loading was similar with cholesterol containing liposomes (Fenske, Wong et al. 1998).

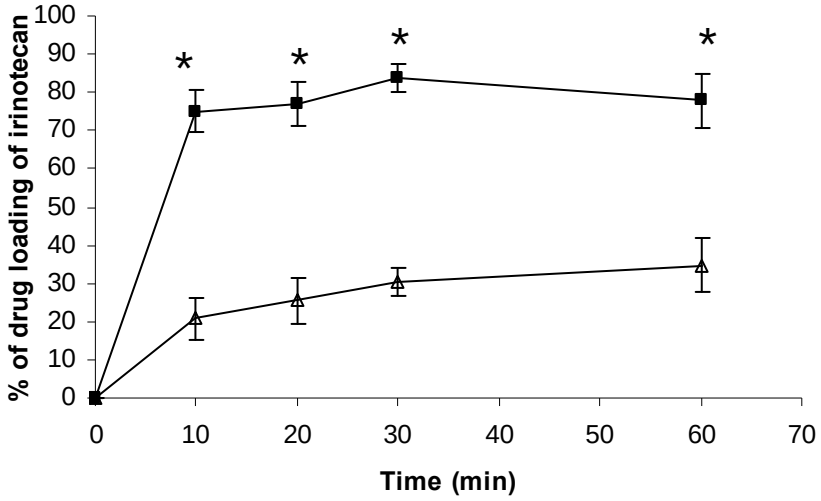

Figure 27 Irinotecan loading into DPPC/DSPE-PEG_{2000}/Quercetin liposomes (90:5:5 molar ratio) in the absence (Δ) and presence of ionophore (■) at 55 ºC. Results shown are the average values ± SEM obtained from three independent experiments. *$p<0.05$.

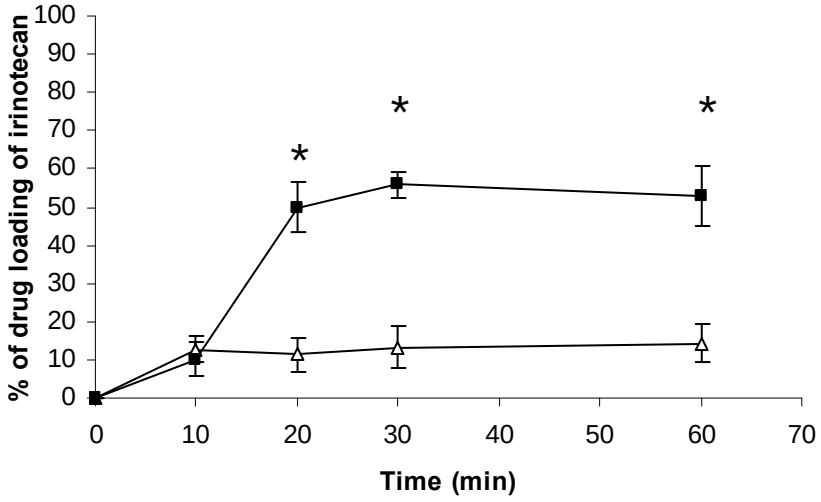

Figure 28 Irinotecan loading into DPPC/DSPE-PEG_{2000}/Quercetin liposomes (90:5:5 molar ratio) in the absence (Δ) and presence of ionophore (■) at 37 ºC. Results shown are the average values ± SEM obtained from three independent experiments. * $p<0.05$.

6.2.3 Effect of quercetin incorporation on irinotecan loading

Since quercetin is incorporated in the lipid bilayer (Goniotaki, Hatziantoniou et al. 2004), the presence of quercetin could influence the permeability of the liposomes, thereby affecting irinotecan loading. Hence, the effect of quercetin incorporation on irinotecan loading with the Mn^{2+}/A23187-mediated proton gradient was explored at 37 ºC and 55 ºC. As shown in Figure 29 and Figure 30**,** there was no statistical difference in irinotecan loading at 37 ºC and 55 ºC.

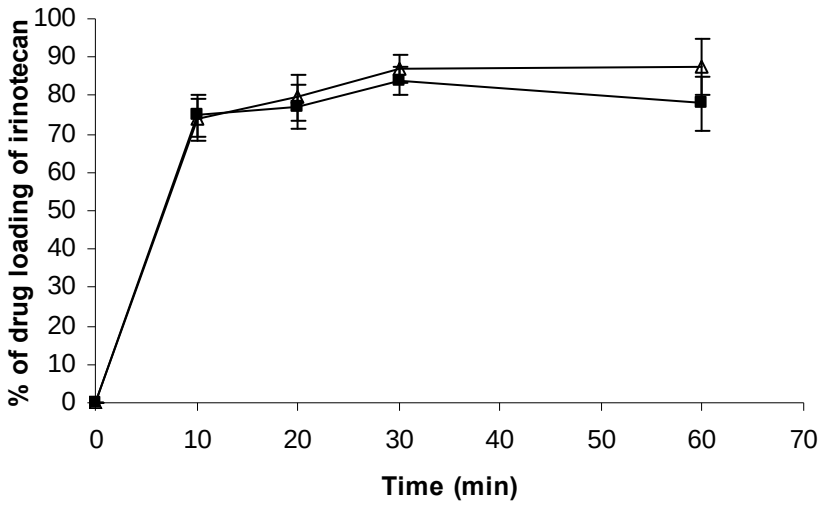

Figure 29 Comparison of irinotecan loading in DPPC liposomes in the presence and absence of quercetin at 55 ºC in the presence of ionophore. DPPC/DSPE-PEG_{2000} (95:5 molar ratio) liposomes are represented by (Δ) and DPPC/DSPE-PEG_{2000}/Quercetin (90:5:5 molar ratio) liposomes are represented by (■). Results shown are the average values ± SEM obtained from three independent experiments. * $p<0.05$.

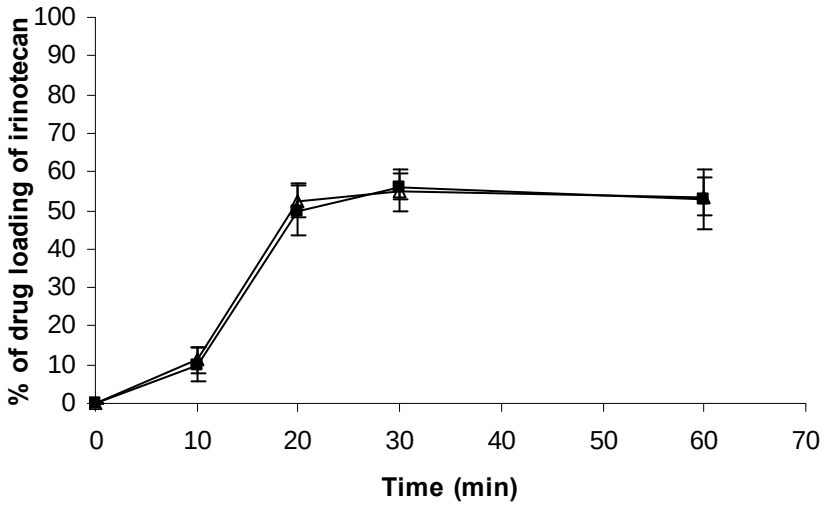

Figure 30 Comparison of irinotecan loading in DPPC liposomes in the presence and absence of quercetin at 37 ºC. DPPC/DSPE-PEG_{2000} (95:5 molar ratio) liposomes are represented by (Δ) and DPPC/DSPE-PEG_{2000}/Quercetin (90:5:5 molar ratio) liposomes are represented by (■). Results shown are the average values ± SEM obtained from three independent experiments. * $p<0.05$.

6.2.4 Effect of temperature on the loading of irinotecan into DPPC/DSPE-PEG_{2000}/Quercetin (90:5:5 molar ratio) liposomes

After determining the role of quercetin on irinotecan loading, the role of temperature on irinotecan loading with the Mn^{2+}/A23187-mediated proton gradient was assessed. As shown in Figure 31, 75.5% of irinotecan was loaded by 10 minutes and the maximal loading efficiency of irinotecan was 83.7% at 55 ºC. In contrast, only 9.8% of irinotecan was loaded by 10 minutes and the maximum percentage of irinotecan loaded was 55.3 % at 37 ºC. Hence, irinotecan loading was faster and more efficient at 55 ºC compared with 37 ºC. Quercetin levels were reassessed after irinotecan loading and was shown to be similar to the levels prior to quercetin loading.

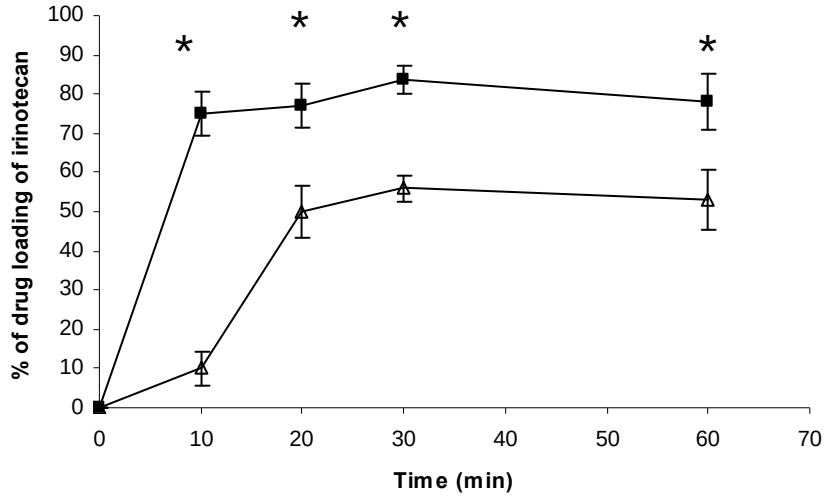

Figure 31 Effect of temperature on irinotecan loading in DPPC/DSPE-PEG_{2000}/Quercetin (90:5:5 molar ratio) liposomes at 37 ºC (Δ) and 55 ºC (■).Results shown are the average values ± SEM obtained from three independent experiments. * $p<0.05$.

6.2.5 Physical stability of the liposomes

Size and polydispersity of the DPPC/DSPE-PEG2000/Quercetin liposomes loaded with irinotecan were studied for 360 days at the storage temperature of 4 ºC. As shown in Figure 32 and Figure 33, there was no significant change in size and polydispersity over the entire monitoring period.

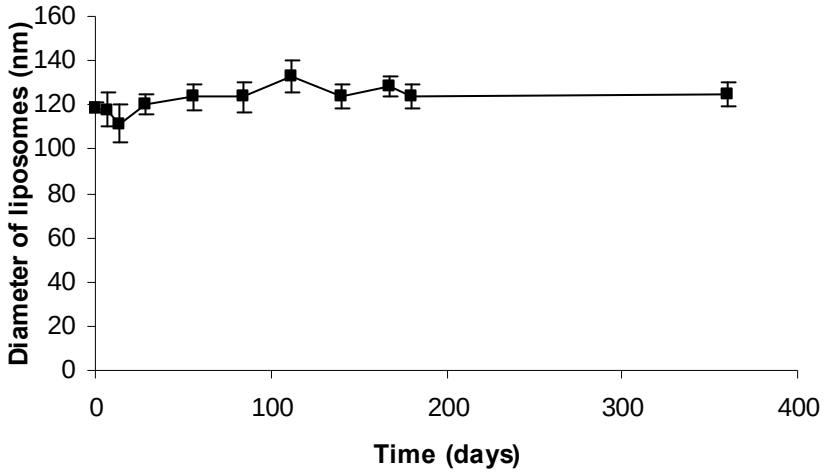

Figure 32 Diameters of DPPC/DSPE-PEG_{2000}/Quercetin liposomes (90:5:5 molar ratio) over 360 days. Results shown are the average values ± SEM obtained from three independent experiments.

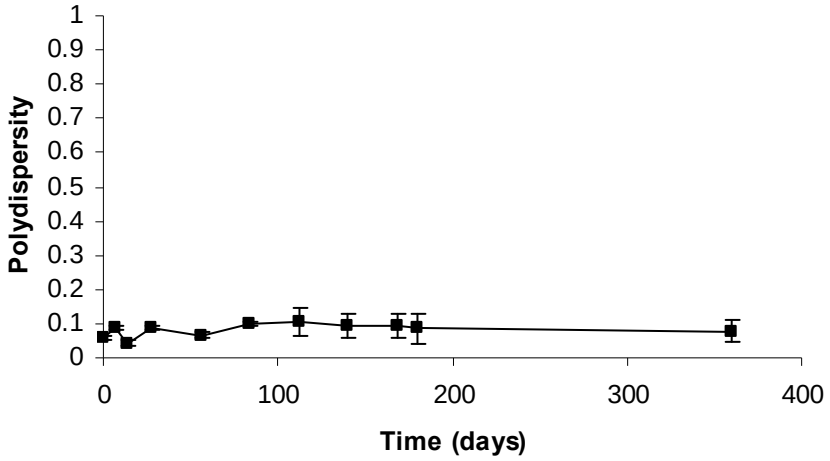

Figure 33 Polydispersities of DPPC/DSPE-PEG_{2000}/Quercetin liposomes (90:5:5 molar ratio) over 360 days. Results shown are the average values ± SEM obtained from three independent experiments.

6.2.6 *In vitro* drug release of irinotecan

From Section 4.2.2, the incorporation efficiency of quercetin in DPPC/DSPE-PEG_{2000}/Quercetin (90:5:5 molar ratio) liposomes was 100.7% at 0.05 drug-to-lipid molar ratio and from Section 6.2.4, the irinotecan loading efficiency was 83.7% at 0.1 drug-to-lipid molar ratio in DPPC/DSPE-PEG_{2000}/Quercetin liposomes. Hence the ratio of irinotecan/quercetin ratio in liposomes is 1.7. This value was obtained by (83.7 x 0.1)/(100.7/100*0.05). This is close to the initial irinotecan/quercetin ratio of 2 and the co-encapsulated liposomes will be used for *in vitro* drug release studies (Section 6.2.6) and *in vitro* cytotoxicity studies (Section 6.2.7).

The *in vitro* release profile of irinotecan and quercetin from DPPC/DSPE-PEG_{2000}/Quercetin liposomes was assessed by

dialysis at 37ºC, and the results are shown in Figure 34 and Figure 35. The release profiles of the two drugs were unaffected by the presence of the other ($p > 0.05$). The release data were further analyzed by fitting into the three most common release kinetics patterns for drug delivery systems. They are zero order, first order and square root of time release models (Table 11 and Table 12). The best coefficient of determination (r^2) were obtained for the square root of time release model with r^2 values of 0.98 for quercetin release in liposomes co-encapsulating quercetin and irinotecan, 0.95 for quercetin release in liposomes containing quercetin only, 0.97 for irinotecan release in liposomes containing quercetin and irinotecan and 0.96 for irinotecan release in liposomes without quercetin.

Figure 36 shows the molar ratio of irinotecan and quercetin over the duration of the release study. There was no statistical difference in the molar ratios of irinotecan/quercetin for the first 48 hours as compared to the initial ratio, however, the molar ratio of irinotecan/quercetin was statistically different from the initial irinotecan/quercetin molar ratio at 72 hours ($p<0.05$).

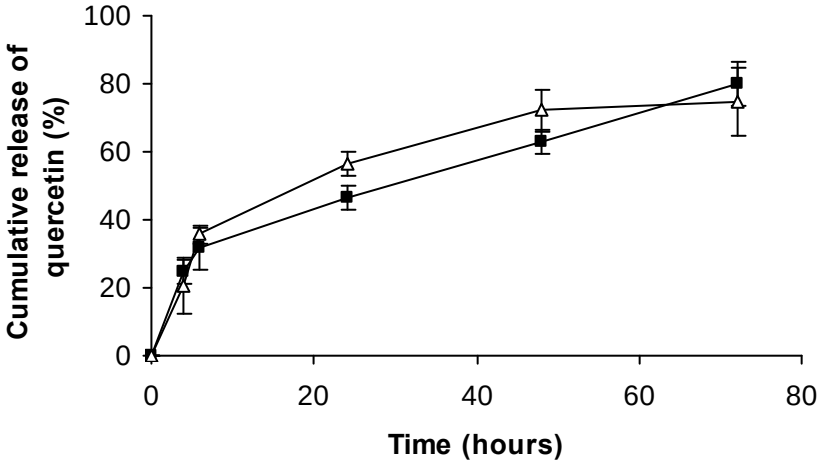

Figure 34 *In vitro* release profile of quercetin from liposomes loaded with quercetin only (Δ) and loaded with both irinotecan and quercetin (■) at 37°C in 0.9%w/v sodium chloride determined with dialysis membrane. The liposome composition consisted of DPPC/Quercetin/DSPE-PEG_{2000} (90:5:5 molar ratio). Each value represents the mean ± SEM from three independent experiments.

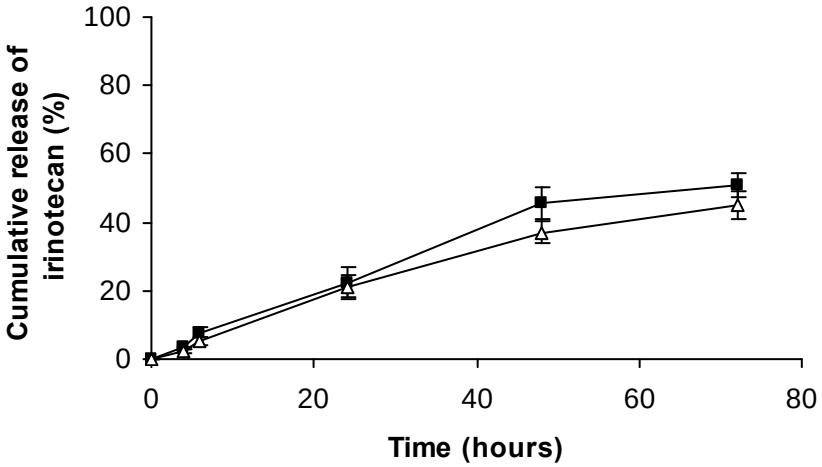

Figure 35 *In vitro* release profile of irinotecan from liposomes loaded with irinotecan only (Δ) and loaded with both irinotecan and quercetin (■) at 37°C in 0.9%w/v sodium chloride determined with dialysis membrane. The liposome composition consisted of DPPC/Quercetin/DSPE-PEG_{2000} (90:5:5 molar ratio). Each value represents the mean ± SEM from three independent experiments.

Table 11 r^2 values of zero order, first order and square root of time release models for quercetin.

	Zero order drug release	First order drug release	Square root of time drug release
No irinotecan[a]	0.80	0.94	0.95
Irinotecan[b]	0.88	0.74	0.98

[a]DPPC/DSPE-PEG_{2000}/Quercetin 90:5:5 molar ratio liposomes
[b]DPPC/DSPE-PEG_{2000}/Quercetin 90:5:5 molar ratio liposomes co-encapsulated with irinotecan

Table 12 r^2 values of zero order, first order and square root of time release models for irinotecan.

	Zero order drug release	First order drug release	Square root of time drug release
No quercetin[a]	0.95	0.82	0.96
Quercetin[b]	0.96	0.80	0.97

[a]DPPC/DSPE-PEG_{2000} 95:5 molar ratio liposomes encapsulated with irinotecan
[b]DPPC/DSPE-PEG_{2000}/Quercetin 90:5:5 molar ratio liposomes co-encapsulated with irinotecan

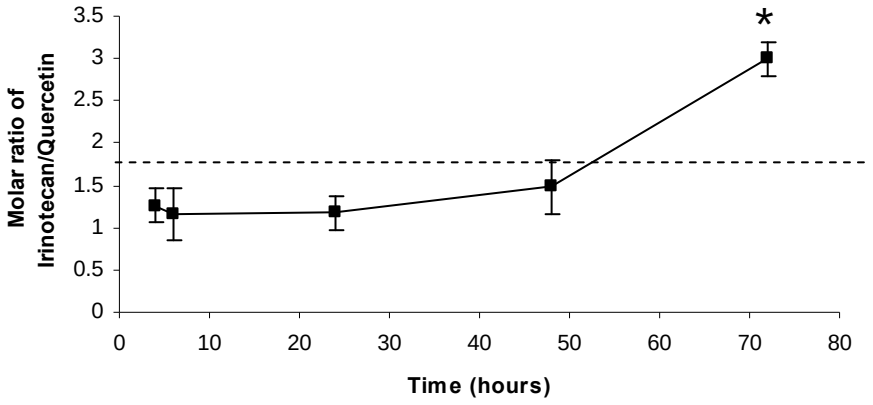

Figure 36 Ratio of irinotecan/quercetin released over 72h. The ratios were obtained by dividing the drug:lipid ratios of irinotecan by that of quercetin. The dotted line represents the initial ratio of irinotecan/quercetin in the liposomes (1.7). Each value represents the mean ± SEM from three independent experiments, * $p<0.05$, one way ANOVA with post hoc Tukey test.

6.2.7 *In vitro* cytotoxicity studies on the liposomal formulation

As mentioned in Section 4.2.8, empty liposomes comprising of DPPC/DSPE-PEG_{2000} (95:5) molar ratio had no significant effect on cell viability in MDA-MB-231 and JIMT-1 cells. Liposomes encapsulating quercetin or irinotecan alone or the drug combination were diluted serially and exposed to both JIMT-1 and MDA-MB-231 breast cancer cell lines for 72 hours. When irinotecan and quercetin were co-encapsulated, the concentrations of the two drugs required to attain 75% cell kill were reduced by approximately one log-fold as compared to monotherapy in JIMT-1 cells (Figure 37). In addition, the CI was 0.72 (synergistic) at ED_{75}. For the MDA-MB-231 cell line, the concentrations of irinotecan and quercetin required to attain 75% cell kill were reduced by approximately 2 log-fold as compared to monotherapy for quercetin and 1 log-fold for irinotecan (Figure 38). In addition, the CI was 0.49 (synergistic) at ED_{75}. Similar trends were observed at other ED values in both cell lines in terms of CIs. As explained in Section 6.2.7, ED_{75} values were reported here due to the clinical relevance of these values as compared to other ED values (Harasym, Tardi et al. 2007).

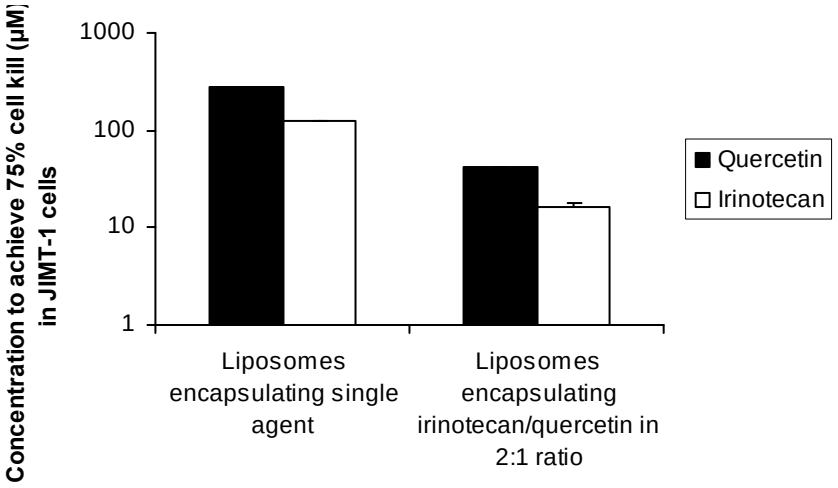

Figure 37 Plot of quercetin and irinotecan concentrations needed to achieve 75% cell kill in JIMT-1 cells after liposomal encapsulation. Data were obtained with the CalcuSyn® software which uses the median dose effect method developed by Chou and Talalay to determine the Combination index. Each value represents the mean ± SEM from three independent experiments.

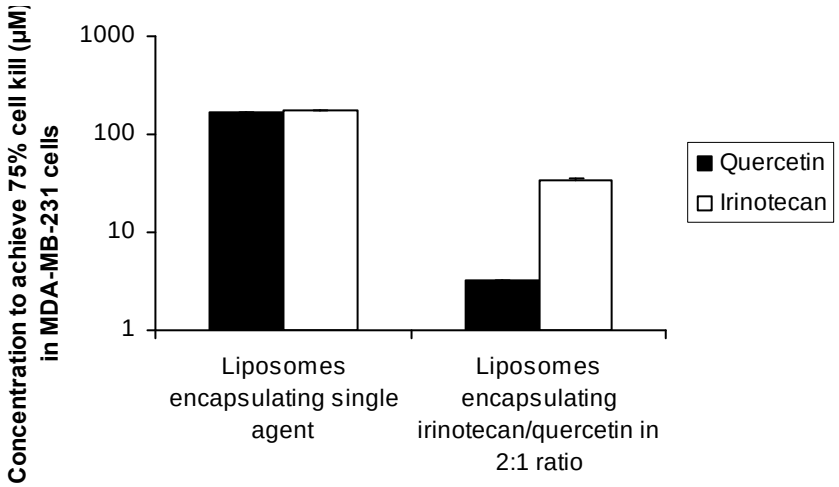

Figure 38 Plot of quercetin and irinotecan concentrations needed to achieve 75% cell kill in MDA-MB-231 cells after liposomal encapsulation. Data were obtained with the CalcuSyn® software which uses the median dose effect method developed by Chou and Talalay to determine the Combination index. Each value represents the mean ± SEM from three independent experiments.

6.3 Discussion

Although synergy between quercetin and irinotecan had been reported previously (highlighted in Section 1.6), this is the first known attempt to co-deliver quercetin and irinotecan in a single drug carrier. Besides being a novel combination in a drug carrier, this is also the first known attempt to load irinotecan in cholesterol free liposomes. Previous attempts by other groups to load irinotecan into liposomes used 45 mol% of cholesterol (Chou, Chen et al. 2003; Messerer, Ramsay et al. 2004; Drummond, Noble et al. 2006; Ramsay, Anantha et al. 2008). The drug loading efficiency and time needed for loading of irinotecan in DPPC/DSPE-PEG_{2000}/Quercetin liposomes was not significantly different from DSPC/Cholesterol liposomes. Hence, drug loading rate was not adversely affected by the absence of cholesterol or the substitution of cholesterol with DSPE-PEG-2000.

In addition, this is also the first successful attempt in the use of temperatures above the phase transition temperature (T_c) of the lipid for drug loading in cholesterol free liposomes. Previously, drug loading into cholesterol free liposomes have been limited to the use of temperatures below T_c. This was attributed to the collapse of the pH gradient at temperatures above T_c, as cholesterol-free liposomes were more permeable above T_c as compared to cholesterol containing liposomes (Dos Santos, Waterhouse et al. 2005). This had limited the utility of

cholesterol free liposomes due to the longer drug loading times and lower drug:lipid ratio achievable as compared to conventional cholesterol containing liposomes. The ability to load drugs at temperatures above Tc in this Chapter could be attributed to the presence of ionophore A23187, which maintains a stable transmembrane gradient through proton exchange between the interior and exterior of the liposomes (Fenske, Wong et al. 1998) to prevent the collapse of pH gradient crucial to drug loading.

The importance of the ionophore A23187 in irinotecan loading was further exemplified by Figure 27 and Figure 28. In the absence of the ionophore, loading efficiency of irinotecan was only 27.3% as compared to 83.7% in the presence of the ionophore at 55 ºC. Similarly at 37 ºC, the loading efficiency of irinotecan was also lower in the absence of the ionophore (15.0 %) versus 55.3% in the presence of ionophore. Some irinotecan could still be loaded at both temperatures because the manganese sulphate solutions in the inner core of the liposomes are acidic (pH 3.4), generating a pH gradient with the buffer surrounding the liposomes (pH 7.5). In addition, irinotecan can also partition into the lipid bilayer and could contribute to irinotecan loading (Burke, Mishra et al. 1993). Nevertheless, the low percentage of drug that could be loaded into the liposomes suggests that an ionophore is crucial in maintaining the transmembrane pH

gradient for higher drug loading in the Mn^{2+}/A23187-mediated proton gradient.

The effect of temperature on the loading efficiency of irinotecan was also explored. The higher loading efficiency of irinotecan at 55 ºC as compared to 37 ºC could be explained as follows: At 55 ºC (14 ºC above the phase transition temperature of DPPC), the lipids are fluid, facilitating the diffusion of irinotecan from the external buffer to the inner acidic aqueous core of the liposome. Once it is in the aqueous core, irinotecan becomes charged due to the low pH and is subsequently trapped as charged molecules cannot diffuse through the membrane. In contrast, below the phase transition temperature,at 37 ºC, the hydrocarbon chains of the lipids remain fully extended and closely packed. This configuration does not facilitate the diffusion of irinotecan through the membrane, leading to less efficient and slower irinotecan loading.

In addition, when the size and polydispersity of DPPC/Quercetin/DSPE-PEG_{2000} (90:5:5 molar ratio) liposomes was assessed over 360 days, there was no significant change in the size or polydispersity over the entire monitoring period, indicating the physical stability of the liposomes. This could be attributed to the sufficient steric hindrance conferred by 5 mol% of DSPE-PEG_{2000}, preventing the self aggregation of liposomes (Woodle and Lasic 1992).

Due to the different loading efficiencies of quercetin and irinotecan, the final irinotecan/quercetin ratio was 1.7, which is slightly different from the initial irinotecan/quercetin ratio of 2. However Figure 26 shows that significant synergism has been observed at the irinotecan/quercetin molar ratios of 2:1 and 1:1 in both the JIMT-1 and MDA-MB-231 breast cancer cell lines, this molar ratio is expected to be synergistic as well. *In vitro* release studies showed that the ratio of irinotecan/quercetin was maintained close to the initial irinotecan/quercetin ratio of 1.7 in the initial 48 hours, suggesting that the release of irinotecan and quercetin were co-ordinated; however by 72 hours the ratio of irinotecan/quercetin shifted to around 3. From the CI data in Figure 26**,** which show that the irinotecan/quercetin molar ratios of 4:1 and 2:1 were synergistic, so a molar ratio of 3:1 is likely to be synergistic too.

The release data indicates that the release of the two drugs were unaffected by the presence of the other (Figure 34 and Figure 35). Previous research has indicated that quercetin rigidifies lipid membranes through the formation of intermolecular hydrogen bonds (Tsuchiya, Nagayama et al. 2002). This could alter the drug release profile from the liposomes. However, this effect did not occur here due to the lack of hydrogen bonding of quercetin with DPPC lipids (Pawlikowska-Pawlega, Ignacy Gruszecki et al. 2007). In addition, the release data was fitted into the common models of

drug release, and the data conformed to the square root of time release model best. Hence, both quercetin and irinotecan had to diffuse through the lipid bilayer of the liposomes in order to be released (Nounou, El-Khordagui et al. 2006). This could be due to the lipid composition of liposomes. The data demonstrated that the liposomes co-ordinated and controlled the release of quercetin and irinotecan.

Finally, the liposomal formulation was tested on JIMT-1 and MDA-MB-231 breast cancer cells. The formulation displayed synergism in both cell lines (Section 6.2.7). Figure 37 and Figure 38 show that both irinotecan and quercetin levels were reduced when used in combination hence, both drugs enhanced the cell killing effect of one another and this observation was not simply a “one sided” enhancement of cell kill by one agent (Chou 2008).

In summary, a physically stable liposomal formulation that encapsulated both irinotecan and quercetin efficiently and co-ordinated their release over 48 hours has been developed. The liposomal formulation was also synergistic, as demonstrated by the CI values. Therefore, a similar anti-cancer effect could be attained by lower doses of irinotecan and quercetin in this novel drug carrier.

Chapter 7

CO-ENCAPSULATION OF QUERCETIN AND VINCRISTINE INTO LIPOSOMES

7.1 Introduction

In this Chapter, the co-encapsulation of quercetin and vincristine (Figure 39) in liposomes will be attempted in view of the significant synergism observed between quercetin and vincristine in Chapter 5. Vincristine is a vinca alkaloid derived from the Madagascan periwinkle. It inhibits microtubule formation in mitotic spindle, arresting the dividing cells at metaphase (Johnson, Armstrong et al. 1963). Although vincristine is currently used in cancer treatment, dose-dependent side effects such as bone marrow suppression or neuropathy require patients to stop treatment. These dose-dependent side effects can be reduced through the use of vincristine-based synergistic drug combinations, whereby the same antitumor effect can be achieved at lower doses of vincristine, such as the combination of quercetin and vincristine.

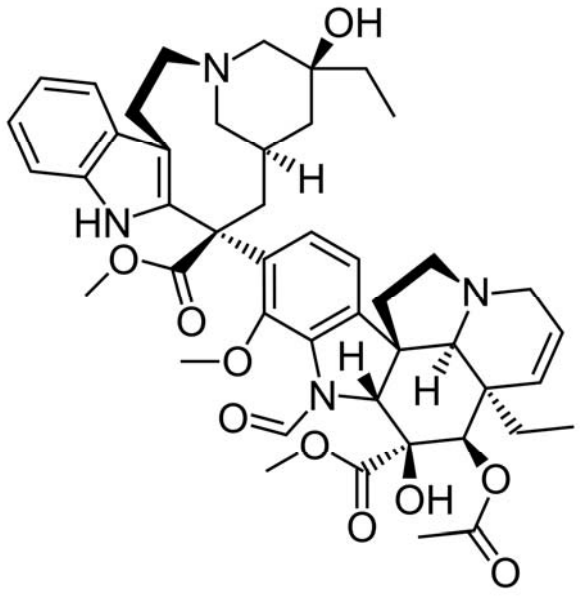

Figure 39 Structure of vincristine.

Previously, poly(D,L-lactide-co-glycolide) (PLGA) nanoparticles have been developed to co-encapsulate quercetin and vincristine (Song, Zhao et al. 2008). Although a high entrapment efficiency of 92.8% was achieved for vincristine, the entrapment efficiency of quercetin was suboptimally at 32.7% only (Song, Zhao et al. 2008). In addition, both quercetin and vincristine were released rapidly, with around 70% of both drugs released in 24 hours (Song, Zhao et al. 2008). This rapid release from the carrier could potentially undermine the benefit from enhanced permeability and retention (EPR) that allows the accumulation of anti-cancer drugs in tumor site (Matsumura and Maeda 1986). Finally, the release of quercetin and vincristine were not coordinated, with quercetin being released more slowly than vincristine (Song, Zhao et al. 2008). This could lead to non-

synergistic molar ratios of the two compounds being released, potentially hampering therapeutic efficacy. Therefore, a more appropriate drug carrier for the co-delivery of the vincristine/quercetin combination is necessary.

In this study, vincristine was encapsulated in the aqueous liposomal core by remote loading using manganese sulfate and the A23187 ionophore (Fenske, Wong et al. 1998; Waterhouse, Madden et al. 2005), while quercetin was intercalated within the hydrophobic region of the lipid bilayer and thus solubilized by the same liposome carrier (Goniotaki, Hatziantoniou et al. 2004). The overall aim of the current study is therefore to develop a physically stable liposome formulation which allows for the solubilization of quercetin, efficient co-encapsulation of quercetin and vincristine, and coordinated release of the two drugs such that synergism could be demonstrated using 2 human breast cancer cell lines, MDA-MB-231 and JIMT-1.

7.2 Results

7.2.1 *In vitro* activities of quercetin and vincristine

The optimal molar ratio to encapsulate quercetin and vincristine in the liposomes was determined by assessing the combined effects of quercetin and vincristine in the MDA-MB-231 and JIMT-1 breast cancer cell lines. The data was analyzed with the median-effect principle at fixed molar ratios of vincristine/quercetin of 4:1, 2:1, 1:1, and 1:2. These ratios were

selected based on the expectation that the two drugs could be successfully encapsulated in the liposomes. The optimal ratio will be used for liposome encapsulation. Figure 40 shows the Combination index (CI) values at the four molar ratios of vincristine/quercetin at ED_{75}. The CI values of vincristine/quercetin at molar ratios of 4:1, 2:1, 1:1 and 1:2 were 0.41, 0.0022, 2.50 and 1.17 for JIMT-1 cells and 12.60, 0.85, 1.09 and 1.48 for MDA-MB-231 cells. Therefore, the most optimal combination of vincristine/Quercetin was 2:1.

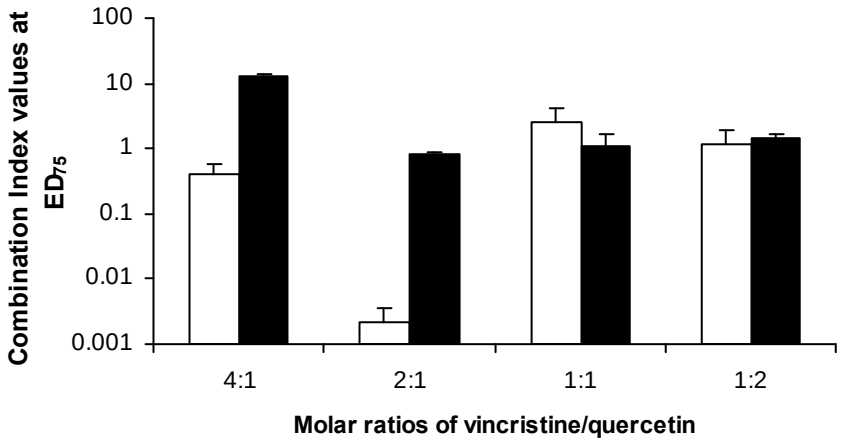

Figure 40 Combination index (CI) values at ED_{75} for vincristine/quercetin exposed to JIMT-1 (white bars) and MDA-MB-231 (black bars) breast cancer cells at molar ratios of vincristine/quercetin of 4:1, 2:1, 1:1 and 1:2. Each value represents the mean ± SEM from three independent experiments. CI values of 0.9-1.1 indicate additive activity, CI values < 0.9 indicate drug synergy and values > 1.1 indicate antagonism.

7.2.2 Quercetin incorporation into ESM liposomes and stability studies

Although quercetin has been efficiently encapsulated in egg phosphocholine (EPC) liposomes previously (Goniotaki,

Hatziantoniou et al. 2004), quercetin loading in egg sphingomyelin (ESM) liposomes was explored due to the superior *in vivo* circulation lifetime of vincristine encapsulated into ESM/Cholesterol liposomes (Krishna, Webb et al. 2001) as compared to EPC/Cholesterol liposomes (Boman, Mayer et al. 1993). The formulation comprising of ESM/Cholesterol/Quercetin (50:45:5 mole ratio) was initially used. However, due to the low encapsulation efficiency of quercetin (30.3%, Table 13) in the ESM/Cholesterol/Quercetin (50:45:5 mole ratio) liposomes, the proportions of ESM and quercetin was varied so as to obtain the optimal liposomal formulation for quercetin loading.

Table 13 shows the quercetin loading efficiency in the presence of 0.0 mol%, 10.0 mol%, 15.0 mol%, 17.5 mol%, 20.0 mol% and 45.0 mol% of cholesterol, respectively. Overall, quercetin incorporation in the liposomes decreased in the presence of cholesterol. The percentage of quercetin loaded in the liposomes was 101.8%, 93.6%, 88.4%, 81.5%, 62.9% and 30.3% in the presence of 0.0 mol%, 10.0 mol%, 15.0 mol%, 17.5 mol%, 20.0 mol% and 45.0 mol% of cholesterol, respectively. In addition, the extent of solubilization of quercetin by liposomes was calculated based on the concentration of quercetin in the liposomes divided by the solubility of quercetin in free buffer (80 μM). All liposomal formulations could improve quercetin solubilization, ranging from 3.3 to 11.2 times (Table 13).

In addition, the physical stability of these liposomes was monitored immediately after extrusion and storage for 7 days at 4 ºC following extrusion. Although the liposomes were of similar sizes after extrusion, the liposomes containing less than 45.0 mol% of cholesterol showed increases in sizes and polydispersities after storage at 4 ºC for 7 days (Table 14), suggesting liposome aggregation. Prior research has shown that the inclusion of PEG_{2000}-lipids would reduce liposome aggregation (Dos Santos, Allen et al. 2007). Although negatively charged DSPE-PEG_{2000} is normally used, it has been shown to increase *in vivo* leakage rates of vincristine (Webb, Saxon et al. 1998). Therefore, neutral PEG_{2000}-ceramide was used in the formulation. Quercetin incorporation was found to be not significantly different following PEG_{2000}-ceramide incorporation ($p>0.05$) (Table 13). In addition, the physical stability of these liposomes was monitored immediately after extrusion and 7 days following extrusion. There was no significant change in size and polydispersity of the liposomes (Table 15).

Table 13 Quercetin loading efficiency (%) expressed as a function of the mol% cholesterol in the liposomes in the presence and absence of 5 mol% PEG_{2000}-ceramide in ESM liposomes.

Mol% of cholesterol	In absence of 5 mol% PEG_{2000}-ceramide		In presence of 5 mol% PEG_{2000}-ceramide	
	% quercetin loading	Extent of solubilization	% quercetin loading	Extent of solubilization
0.0	101.8 ± 1.8	11.2	101.4 ± 2.1	11.1
10.0	93.6 ± 6.8	10.3	97.2 ± 3.2	10.6
15.0	88.4 ± 1.7	9.7	89.3 ± 2.4	9.8
17.5	81.5 ± 3.0	8.9	78.3 ± 1.9	8.6
20.0	62.9 ± 1.5	6.9	54.4 ± 10.7	6.0
45.0	30.3 ± 2.0	3.3	25.7 ± 2.2	2.8

For formulations without 5 mol% PEG_{2000}-ceramide, ESM/Quercetin/Cholesterol liposomes were in molar ratios of 95:5:0, 85:5:10, 80:5:15, 77.5:5:17.5, 75:5:20 and 50:5:45. For formulations with 5 mol% PEG_{2000}-ceramide, ESM/Quercetin/PEG_{2000}-ceramide/Cholesterol liposomes were in molar ratios of 90:5:5:0, 80:5:5:10, 75:5:5:15, 72.5:5:5:17.5, 70:5:5:20 and 45:5:5:45. All formulations were formulated at 5:95 drug-to-lipid molar ratios. Each value represents the mean ± SEM from three independent experiments.

Table 14 Physical stability of the ESM/Cholesterol/Quercetin liposomes immediately and 7 days after extrusion.

Mol% cholesterol	Immediately after extrusion		7 days after extrusion	
	Size (nm)	Polydispersity	Size (nm)	Polydispersity
0.0	135.9 ± 14.2	0.135 ± 0.082	1120.8 ± 116.4	1.000 ± 0.001
10.0	131.5 ± 13.8	0.137 ± 0.062	1320.4 ± 110.2	1.000 ± 0.001
15.0	158.0 ± 26.5	0.470 ± 0.043	1034.6 ± 123.4	0.434 ± 0.024
17.5	141.5 ± 17.8	0.424 ± 0.134	1043.6 ± 236.4	0.463 ± 0.045
20.0	200.0 ± 34.5	0.637 ± 0.073	201.3 ± 143.6	0.634 ± 0.056
45.0	145.6 ± 22.3	0.195 ± 0.023	143.5 ± 29.7	0.200 ± 0.034

ESM/Quercetin/Cholesterol liposomes were in molar ratios of 95:5:0, 85:5:10, 80:5:15, 77.5:5:17.5, 75:5:20 and 50:5:45. All formulations were formulated at 5:95 drug-to-lipid molar ratios. Each value represents the mean ± SEM from three independent experiments.

Table 15 Physical stability of the ESM/Quercetin/PEG_{2000}-ceramide/Cholesterol liposomes immediately and 7 days after extrusion.

Mol% cholesterol	Immediately after extrusion		7 days after extrusion	
	Size (nm)	Polydispersity	Size (nm)	Polydispersity
0.0	117.9 ± 12.3	0.123 ± 0.002	123.9 ± 12.3	0.132 ± 0.045
10.0	121.5 ± 16.4	0.100 ± 0.003	120.5 ± 13.2	0.181 ± 0.023
15.0	131.5 ± 14.6	0.153 ± 0.045	134.0 ± 15.6	0.112 ± 0.053
17.5	135.9 ± 12.0	0.161 ± 0.032	134.7 ± 13.2	0.143 ± 0.043
20.0	133.3 ± 13.5	0.137 ± 0.034	134.5 ± 14.5	0.146 ± 0.046
45.0	140.6 ± 12.6	0.172 ± 0.089	143.6 ± 16.8	0.187 ± 0.036

ESM/Quercetin/PEG_{2000}-ceramide/Cholesterol liposomes were in molar ratios of 90:5:5:0, 80:5:5:10, 75:5:5:15, 72.5:5:5:17.5, 70:5:5:20 and 45:5:5:45. All formulations were formulated at 5:95 drug-to-lipid molar ratios. Each value represents the mean ± SEM from three independent experiments.

7.2.3 Effect of cholesterol on vincristine loading

Previously, vincristine has been loaded in liposomes containing high concentration of cholesterol (45.0 mol%) (Waterhouse, Madden et al. 2005; Johnston, Semple et al. 2006). However, due to the low incorporation of quercetin in ESM/ PEG2000-ceramide liposomes containing 45.0 mol% cholesterol, the effect of vincristine loading with varying cholesterol levels was explored. Table 16 shows the effect of cholesterol on vincristine loading. The maximum percentage of vincristine loaded in the liposomes was 25.5%, 26.1%, 55.0%, 70.0%, 95.8% and 90.8% in the presence of 0.0 mol%, 10.0 mol%, 15.0 mol%, 17.5 mol%, 20.0 mol% and 45.0 mol% of cholesterol, respectively. Therefore, vincristine loading is increased with higher cholesterol levels. In addition, vincristine loading declined with time for liposomes with cholesterol levels of 0.0 mol%, 10.0 mol% and 15.0 mol%, but this was not observed for liposomes with higher cholesterol levels of 17.5 mol%, 20.0 mol% and 45.0 mol%.

Table 16 Vincristine loading efficiency (%) expressed as a function of the amount of cholesterol for liposomes comprising of ESM/PEG_{2000}-ceramide and varying ratios of cholesterol at 60°C.

Mol% of cholesterol	Time (min)			
	15	30	60	90
0.0	25.5 ± 5.5	7.2 ± 1.6	15.3 ± 3.0	8.9 ± 3.5
10.0	26.1 ± 3.4	11.4 ± 0.8	16.2 ± 3.6	14.8 ± 0.7
15.0	48.3 ± 4.2	55.0 ± 0.5	30.7 ± 5.4	36.1 ± 5.2
17.5	43.7 ± 1.8	65.0 ± 2.9	67.0 ±1.2	70.0 ± 1.4
20.0	68.7 ± 5.1	88.8 ± 5.1	90.8 ± 5.3	95.8 ± 2.4
45.0	86.5 ± 2.0	90.7 ± 5.4	90.8± 2.9	90.0 ± 2.6

ESM/PEG_{2000}-ceramide/Cholesterol were in molar ratios of 95:5:0, 85:5:10, 80:5:15, 77.5:5:17.5, 75:5:20 and 50:5:45. Each value represents the mean ± SEM from three independent experiments.

7.2.4 Effect of quercetin on vincristine loading

Besides the amount of cholesterol, the presence of quercetin could also influence vincristine loading. This is because quercetin is incorporated in the lipid bilayer (Goniotaki, Hatziantoniou et al. 2004) and could alter the permeability of the liposomes, thereby affecting vincristine loading. Hence, the effect of quercetin incorporation on vincristine loading was also explored by comparing the loading of vincristine in the presence and absence of quercetin (Figure 41). Quercetin incorporation had no effect on vincristine loading at 0.0 mol%, 10.0 mol%, 20.0 mol% and 45.0 mol% of cholesterol (Figure 41 a,b,e,f). However, quercetin incorporation affected the vincristine loading profile at 15 mol% and 17.5 mol% of cholesterol (Figure 41 c,d). In the absence of quercetin, vincristine loading peaked at 30 minutes at 59.3% but subsequently declined to 30.7% upon

longer incubation at 15 mol% of cholesterol (Figure 41 c). In contrast, this decline did not occur in the presence of quercetin. In addition, at 17.5 mol% of cholesterol, the amount of vincristine loaded was higher in liposomes containing quercetin as compared to those without quercetin for the time points of 15, 30 and 60 minutes (Figure 41 d).

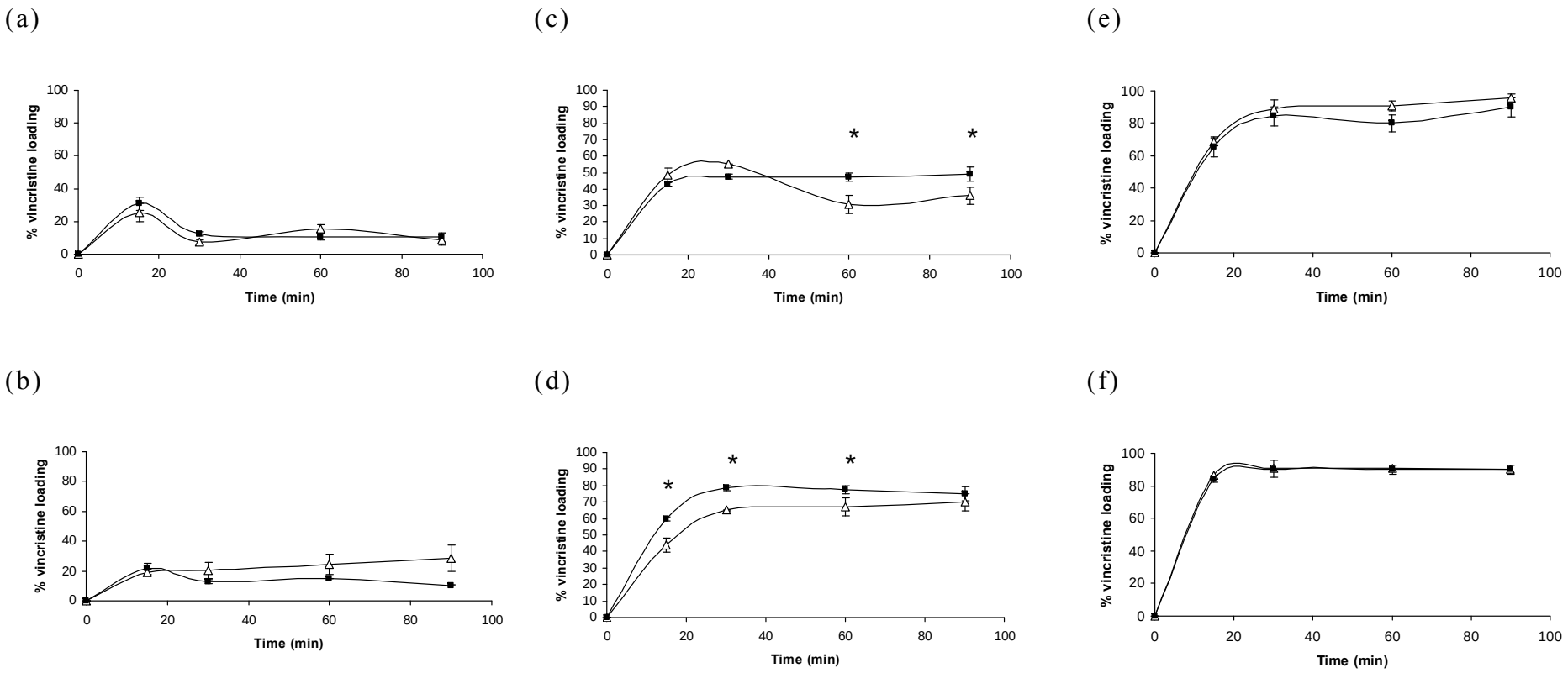

Figure 41 Comparison of vincristine loading efficiency (%) in the presence (■) and absence (Δ) of 5 mol%, quercetin at varying cholesterol levels: (a) 0.0 mol% cholesterol, (b) 10.0 mol% cholesterol, (c) 15.0 mol% cholesterol, (d) 17.5 mol% cholesterol, (e) 20.0 mol% cholesterol, (f) 45.0 mol% cholesterol. * $p < 0.05$

7.2.5 Effect of temperature on vincristine loading

Temperature is another factor that can influence the efficiency of vincristine loading. Hence, a comparison was done between vincristine loading at 60 ºC which is above the phase transition temperature of ESM, and 37 ºC which is below. Although vincristine loading at 37 ºC prevented the decrease in vincristine concentration over time for formulations containing low levels of cholesterol, the amount of vincristine loaded remained low, with the maximal loading around 30%. In addition, for liposomes with cholesterol levels of 20 mol% and 45 mol%, the maximal amount of vincristine loaded was approximately 40%, and this level of loading is much lower as compared to that at 60 ºC.

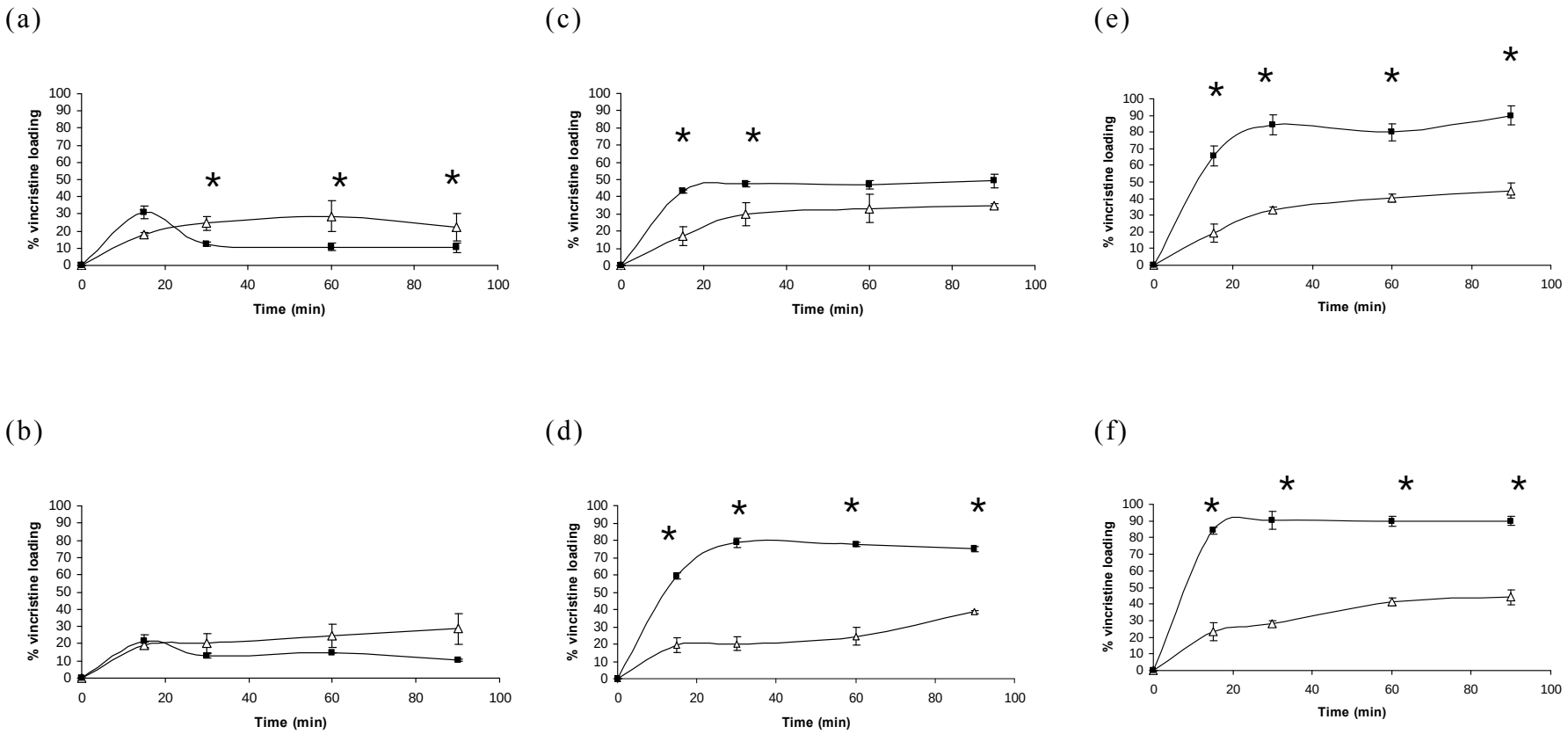

Figure 42 Comparison of vincristine loading efficiency (%) of ESM/PEG_{2000}-ceramide/Cholesterol/Quercetin liposomes at 60 ºC (■) and 37 ºC (Δ). (a) 0.0 mol% cholesterol, (b) 10.0 mol% cholesterol, (c) 15.0 mol% cholesterol, (d) 17.5 mol% cholesterol, (e) 20.0 mol% cholesterol (f) 45.0 mol% cholesterol, * $p < 0.05$.

7.2.6 Physical stability of the liposomes

Taking the quercetin incorporation and vincristine loading data together, the best formulation to co-encapsulate vincristine and quercetin was the ESM/Cholesterol/PEG_{2000}-ceramide/Quercetin formulation at 72.5:17.5:5:5 molar ratio. Hence, the physical stability of these liposomes was studied for 360 days at the storage temperature of 4 ºC. There was no significant change in the size (Figure 43) and polydispersity (Figure 44) of the liposomes over the entire monitoring period.

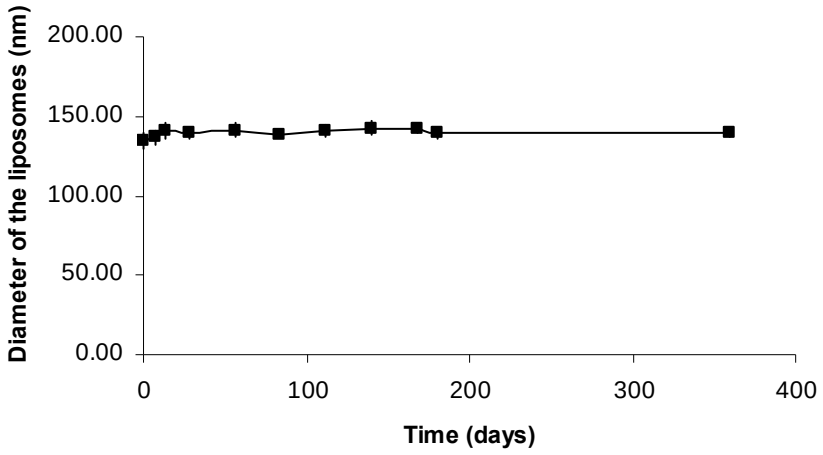

Figure 43 Diameters of the ESM/PEG ceramide/Quercetin/Cholesterol liposomes 72.5:5:5:17.5 molar ratio measured with quasi-elastic light scattering over 360 days. Each value represents the mean ± SEM from three independent experiments.

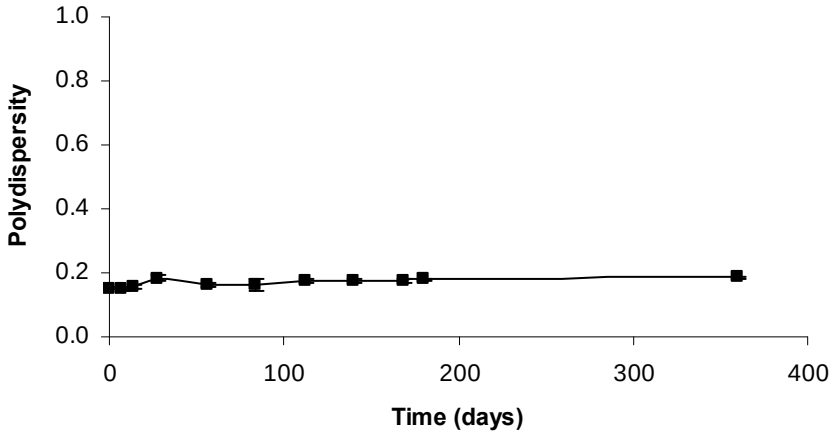

Figure 44 Polydispersity of the ESM/PEG ceramide/Quercetin/Cholesterol liposomes 72.5:5:5:17.5 molar ratio measured with quasi-elastic light scattering over 360 days. Each value represents the mean ± SEM from three independent experiments.

7.2.7 *In vitro* drug release of vincristine and quercetin

The *in vitro* drug release profiles of vincristine and quercetin were determined through membrane dialysis in 0.9%w/v sodium chloride. In order to determine if the release of vincristine and quercetin from the co-encapsulated liposomes would be altered by the presence of the other drug, the *in vitro* release profile of vincristine and quercetin in co-encapsulated liposomes were compared with liposomes comprising of vincristine and quercetin only. As shown in Figure 45, the release of quercetin was unchanged by the presence of vincristine ($p>0.05$). In contrast, the release of vincristine was altered by the presence of quercetin (Figure 46). In the presence of quercetin, vincristine release was slowed down to 57.7% and 65.9% in 48 and 72 hours as compared to 86.5% and 96.6% in the absence of quercetin, respectively ($p<0.05$). The data demonstrated sustained release of vincristine and quercetin over 72 hours and coordinated release of both drugs, with the optimal ratio for drug synergism of 2:1 maintained for the duration of the study (Figure 47).

Finally, the kinetics of drug release was determined by fitting the data into the most common models of drug release, namely, zero order, first order and square root of time release. For all the preparations, the best fit was observed for first order kinetics (Table 17 and Table 18). The r^2 values for quercetin release for liposomes containing quercetin only and the co-

encapsulated preparation were 0.89 and 0.83 respectively. The r^2 values for vincristine release for liposomes containing vincristine only and the co-encapsulated preparation were 0.85 and 0.87, respectively.

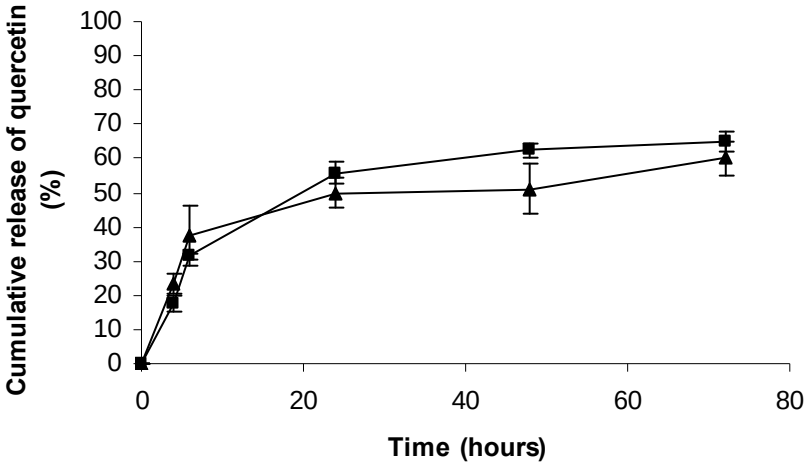

Figure 45 *In vitro* release profile of quercetin from liposomes loaded with quercetin only (Δ) and loaded with both vincristine and quercetin (■) at 37°C in 0.9%w/v sodium chloride determined with dialysis membrane. The liposome lipid composition consisted of ESM/Quercetin/PEG_{2000}-ceramide/Cholesterol (72.5:5:5:17.5 molar ratio). Each value represents the mean ± SEM from three independent experiments.

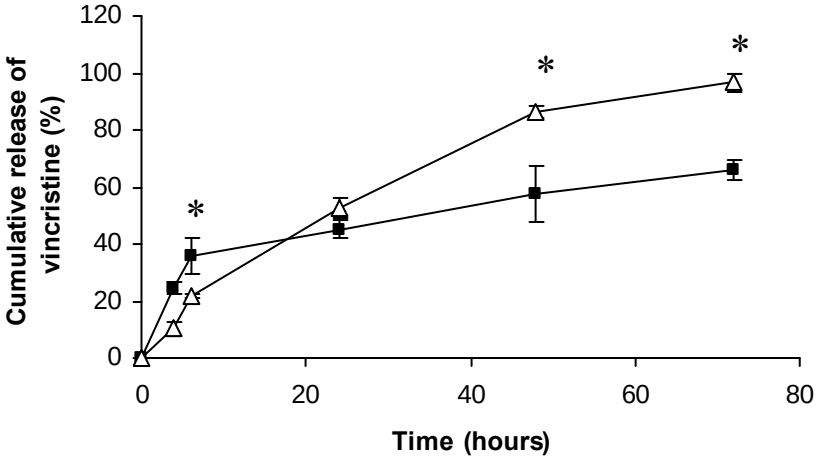

Figure 46 *In vitro* release profile of vincristine from liposomes loaded with vincristine only (Δ) and loaded with both vincristine and quercetin (■) at 37°C in 0.9%w/v sodium chloride determined with dialysis membrane. The liposome lipid composition consisted of ESM/Quercetin/PEG_{2000}-ceramide/Cholesterol (72.5:5:5:17.5 molar ratio). Each value represents the mean ± SEM from three independent experiments. * $p < 0.05$.

Table 17 r^2 values of zero order, first order and square root of time release models for quercetin from liposomes.

	Zero order drug release	First order drug release	Square root of time drug release
No vincristine[a]	0.75	0.89	0.78
Vincristine[b]	0.70	0.83	0.74

[a]ESM/Quercetin/PEG_{2000}-ceramide/Cholesterol 72.5:5:5:17.5 molar ratio liposomes.
[b]ESM/Quercetin/PEG_{2000}-ceramide/Cholesterol 72.5:5:5:17.5 molar ratio liposomes containing vincristine.

Table 18 r^2 values of zero order, first order and square root of time release models for vincristine from liposomes.

	Zero order drug release	First order drug release	Square root of time drug release
No quercetin[a]	0.72	0.85	0.79
Quercetin[b]	0.77	0.87	0.78

[a]ESM/PEG_{2000}-ceramide/Cholesterol 77.5:5:17.5 molar ratio liposomes.
[b]ESM/Quercetin/PEG_{2000}-ceramide/Cholesterol 72.5:5:5:17.5 molar ratio liposomes.

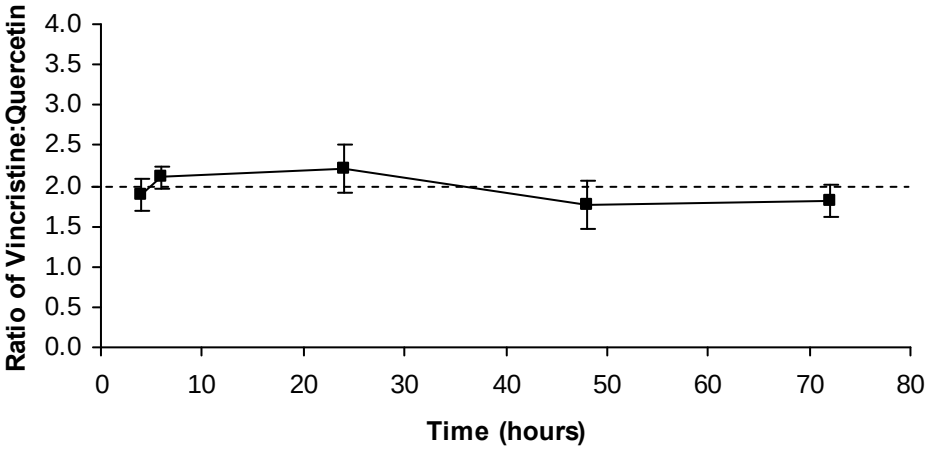

Figure 47 Ratio of vincristine/quercetin released over 72h. The ratio of drug released was close to the initial loading vincristine/quercetin ratio of 2:1. The ratios were obtained by dividing the drug-lipid-ratios of vincristine by that of quercetin. Each value represents the mean ± SEM from three independent experiments, $p>0.05$.

7.2.8 *In vitro* cytotoxicity studies

In order to determine if the liposome carrier comprising of ESM/PEG_{2000}-ceramide/Cholesterol (77.5:5:17.5 molar ratio) contributed to the cytotoxicity of the cells, *in vitro* cytotoxicity studies were conducted with these liposomes on the MDA-MB-231 and JIMT-1 cells. There was no significant effect on the cell kill by the lipids (Figure 48). Subsequently, liposomes encapsulating vincristine or quercetin alone or the drug combination were diluted serially and exposed to both the MDA-MB-231 and JIMT-1 breast cancer cell lines for 72 hours. The drugs were diluted by serial dilutions. When vincristine and quercetin were co-encapsulated, the concentrations of vincristine and quercetin required to attain 75% cell kill were reduced by approximately 2 log-fold as compared to monotherapy (Figure 49) in JIMT-1 cells. In addition, the CI was 0.12 (very synergistic) at ED_{75}. For the MDA-MB-231 cell line, the concentrations of vincristine and quercetin required to attain 75% cell kill were reduced approximately 1 log-fold as compared to monotherapy for quercetin and 2 folds for vincristine (Figure 50). In addition, the CI was 0.83 (synergistic) at ED_{75}. Similar trends were observed at other ED values in both cell lines in terms of CIs.

(a)

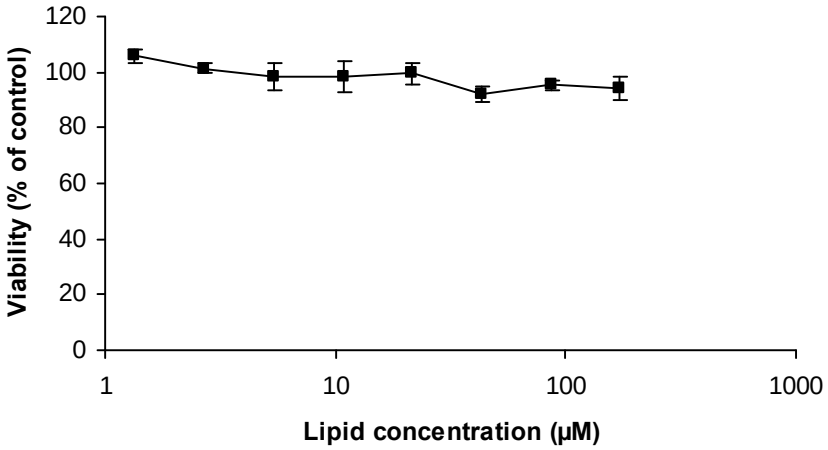

(b)

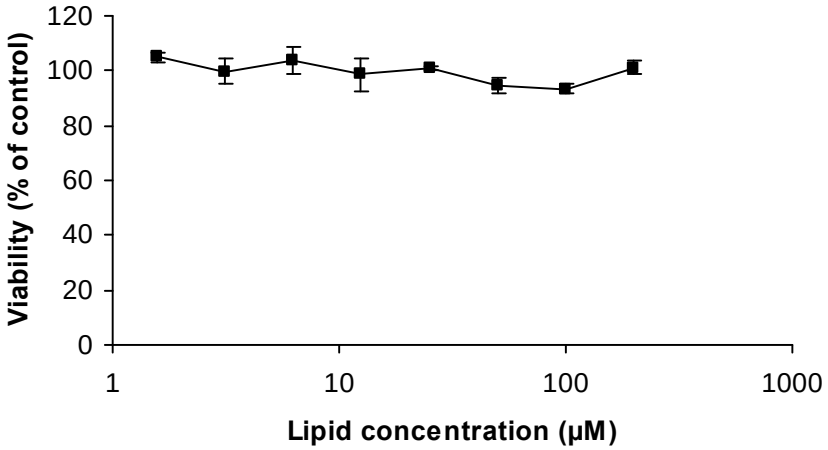

Figure 48 *In vitro* cytotoxicity of the liposome carrier in (a) MDA-MB-231 and (b) JIMT-1 cells.

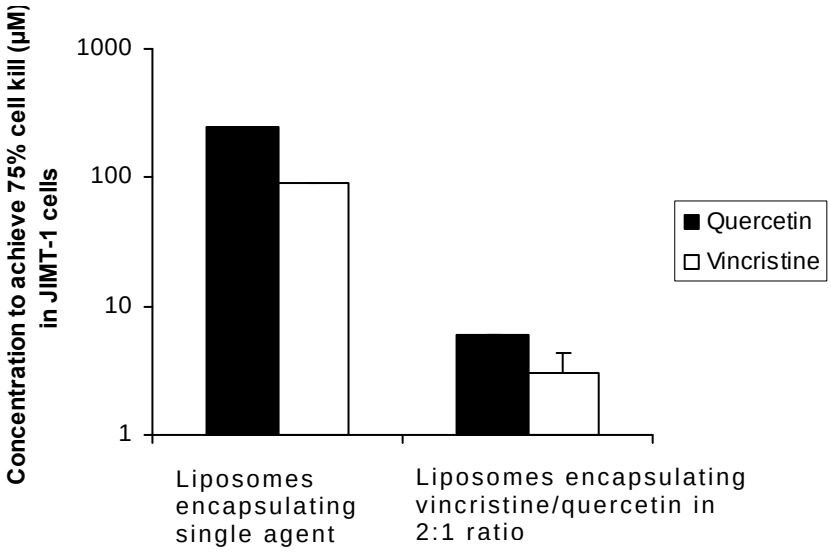

Figure 49 Plot of vincristine and quercetin concentrations needed to achieve 75% cell kill in JIMT-1 cells. Data were obtained with the CalcuSyn® software which uses the median dose effect method developed by Chou and Talalay to determine the Combination index. Each value represents the mean ± SEM from three independent experiments.

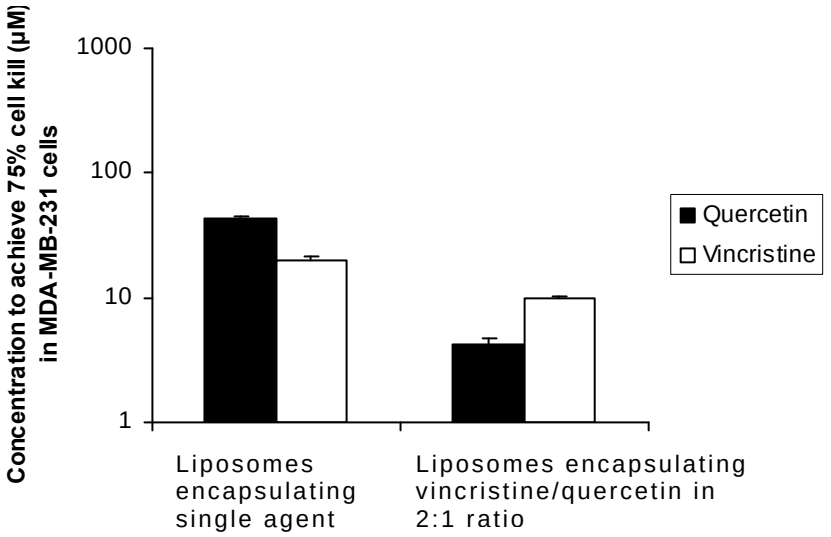

Figure 50 Plot of vincristine and quercetin concentrations needed to achieve 75% cell kill in MDA-MB-231 cells. Data were obtained with the CalcuSyn® software which uses the median dose effect method developed by Chou and Talalay to determine the Combination index. Each value represents the mean ± SEM from three independent experiments.

7.3 Discussion

An appropriately designed drug delivery system can be used to coordinate the release of drugs in their synergistic ratios, allowing for the drug combination to achieve its maximal therapeutic efficacy. Liposomes were selected as the drug delivery system to co-encapsulate vincristine and quercetin due to the presence of a hydrophilic liposome core and a hydrophobic lipid bilayer, which makes it suitable for the co-encapsulation of amphipathic and hydrophobic drugs simultaneously.

A physically stable combination liposomal formulation that solubilized quercetin, efficiently co-encapsulated vincristine and quercetin and also coordinated the release of the two drugs such that synergism was demonstrated *in vitro* has been developed. A drug delivery system that coordinates the release of vincristine and quercetin is crucial, as illustrated by Figure 40**,** where a slight change in the vincristine/quercetin molar ratio from 2:1 to 1:1 shifted the combination effect of the two drugs from synergism to antagonism. Therefore, the previous formulation of PLGA nanoparticles, which failed to coordinate the release of vincristine and quercetin (Song, Zhao et al. 2008) may not exert its full antitumor potential due to the narrow range in which synergism occurs.

The liposomal formulation developed maintained the synergistic ratio of vincristine/quercetin 2:1 throughout the entire duration of the *in vitro* study. This ratio was maintained

for a sufficiently long period for synergism to be exerted, as shown by the CI value of 0.12 for JIMT-1 cells and 0.83 for MDA-MB-231 cells. This means that the doses needed to achieve the same cell kill was reduced. This could reduce the incidence of dose-dependent side effects associated with vincristine such as neurotoxicity and potentially allow for the same therapeutic effect to be attained with fewer side effects as compared to monotherapy.

The development of a liposomal formulation which coordinates the release of both vincristine and quercetin is challenging due to the hydrophobic nature of quercetin and the amphipathic nature of vincristine, which requires the optimization of formulation variables to co-encapsulate the two drugs efficiently together. For example, quercetin incorporation and solubilization was found to be most efficient either in the absence or at low levels of cholesterol, possibly due to the competition of cholesterol and quercetin for the same hydrophobic space in the lipid bilayer (Goniotaki, Hatziantoniou et al. 2004). Quercetin penetration into the lipid bilayer would also be interfered by the reduced flexibility of the hydrocarbon chains of the lipids after cholesterol addition (Demel and De Kruyff 1976). In contrast, efficient and stable vincristine loading required at least 17.5 mol% of cholesterol. This could be due to the higher permeability of liposomes with low cholesterol levels as compared to liposomes with higher cholesterol levels, leading

to the leakage of manganese sulfate from the core of the liposomes and the elimination of the transmembrane pH gradient driving vincristine into the liposomes (Dos Santos, Waterhouse et al. 2005).

However, with 17.5 mol% of cholesterol, the liposomes were physically unstable and increased in size and polydispersity, although this was not observed at higher cholesterol levels of 45.0 mol%. This could be due to the ability of high levels of cholesterol to decrease the attractive van der Waals forces while increasing the net repulsive forces, thereby reducing the tendency for liposomal aggregation and fusion as compared to lower cholesterol concentrations (Souza and Teschke 2003). Although the inclusion of cholesterol could increase the physical stability of liposomes, high cholesterol levels reduced quercetin loading and had also been shown to reduce the retention of some other drugs such as floxuridine (Tardi, Gallagher et al. 2007). This warrants alternative methods for increasing liposome physical stability. Therefore, PEG_{2000}-conjugated lipids, which confer physical stability through steric stabilization, were added to the formulation (Dos Santos, Allen et al. 2007). Although negatively charged DSPE-PEG_{2000} lipid is conventionally used, it has been shown to increase vincristine release from liposomes (Webb, Saxon et al. 1998). Therefore, the neutral PEG_{2000}-ceramide lipid was used instead. Besides preventing liposome aggregation, the inclusion of PEG_{2000}-

ceramide had no adverse effect on quercetin loading. In addition, there was no significant change in size and polydispersity of the liposomes over 360 days. Therefore, PEG_{2000}-ceramide lipids could be used in place of cholesterol to stabilize liposomes from physical aggregation without affecting the incorporation of hydrophobic drugs in the lipid bilayer.

The effect of temperature on vincristine loading was also explored as a possible avenue to improve vincristine loading. At 37 ºC, slightly below the phase transition temperature of ESM, the amount of vincristine loaded was low (maximal loading was around 40%). The low amount of vincristine loaded could be attributed to the impedance of vincristine diffusion due to the tightly packed and fully extended configuration of the hydrocarbon chains of the lipids below the phase transition temperature.

In addition, it was shown for the first time that the incorporation of quercetin could alter the loading and release of vincristine. Quercetin incorporation not only increased vincristine loading but also reduced vincristine release from the liposomes, possibly through the formation of intermolecular hydrogen bonds which rigidified the liposomal membrane (Tsuchiya, Nagayama et al. 2002) and reduced the permeability of the liposomal membrane to vincristine during loading and release. It is worthwhile to note that despite this, the kinetics of drug release remained as first ordered, with the maintenance of

the synergistic ratio of vincristine and quercetin release over 72 hours. This is crucial in maximizing the therapeutic activity of the drug combination. The alteration of drug release by quercetin is anticipated to also apply to other membrane permeable amphipathic drugs similar to vincristine. Therefore, in addition to changing lipid composition (Waterhouse, Madden et al. 2005), the formation of drug precipitates (Drummond, Hayes et al. 2007) and changes in pH gradient (Dos Santos, Cox et al. 2004), which are traditional methods of altering drug release, the incorporation of quercetin or other compounds that can form hydrogen bonds represent a new avenue to alter drug loading and release profiles. In contrast, the observation that vincristine loading had no significant effect on quercetin release is expected, as vincristine is incorporated in the aqueous core of the liposomes (Johnston, Semple et al. 2006) and is unlikely to interfere with the release of quercetin in the lipid bilayer (Goniotaki, Hatziantoniou et al. 2004).

In this Chapter, a novel drug delivery carrier which co-encapsulated two drugs exhibiting synergism, coordinated the drug release profiles of vincristine and quercetin and prolonged the exposure times for both drugs had been developed. The fixed ratio was maintained for a sufficiently long period for synergism to be exerted as shown by the *in vitro* data, allowing for optimal anti-cancer activity to be attained in MDA-MB-231 and JIMT-1 cells.

Table 19 summarizes the CI values of irinotecan/quercetin and vincristine/quercetin liposomes in MDA-MB-231 and JIMT-1 cells from Section 6.2.7 and Section 7.2.8. From the CI values, the most active combination was the vincristine/quercetin combination in JIMT-1 cells. In view of the significant synergism of this preparation, the therapeutic efficacy of vincristine/quercetin liposomes will be assessed in the JIMT-1 breast cancer xenograft in Chapter 9.

Table 19 Summary of CI values of irinotecan/quercetin and vincristine/quercetin liposomes in MDA-MB-231 and JIMT-1 cells.

	Irinotecan/quercetin liposomes[a]	Vincristine/quercetin liposomes[b]
MDA-MB-231 cells	0.72	0.83
JIMT-1 cells	0.49	0.12

[a]Irinotecan was encapsulated in DPPC/DSPE-PEG_{2000}/Quercetin 90:5:5 molar ratio liposomes.
[b]Vincristine was encapsulated in Egg Sphingomyelin (ESM)/Cholesterol/N-palmitoyl-sphingosine-1-{succinyl[methoxy(polyethylene glycol)$_{2000}$] (PEG_{2000}-ceramide)/Quercetin 72.5:17.5:5:5 molar ratio liposomes.

In addition, the plasma elimination profiles of vincristine and quercetin will also be assessed. However, since there is no published method to simultaneously determine vincristine and quercetin in biological fluids, therefore method development and validation to determine vincristine and quercetin in plasma biological fluids will be conducted in the next Chapter.

Chapter 8

SIMULTANEOUS DETERMINATION OF VINCRISTINE AND QUERCETIN IN PLASMA AND TISSUE HOMOGENATE BY ULTRA PERFORMANCE LIQUID CHROMOTOGRAPHY (UPLC)

8.1 Introduction

As mentioned in the last Chapter, no published method is available to determine vincristine and quercetin levels together in plasma and organ homogenates. Previously, quercetin in plasma alone has been quantified by high performance liquid chromatography (HPLC) with ultra-violet (uv) detection (Jones 1998; Khaled and El-Sayed 2000; Yang 2005; Zhigaltsev, Maurer et al. 2005; Yang, Liu et al. 2007; Li, Yang et al. 2009; Tang, Yin et al. 2009) or HPLC with electrochemical detection (Chen 2005). Vincristine in plasma alone has been quantified by HPLC with uv detection (Noble, Guo et al. 2009), LC/MS (Corona, Casetta et al. 2008), LC/MS/MS (Guilhaumou, Solas et al. 2010) and radioactive methods (Boman, Mayer et al. 1993). Although a HPLC method had been described for quantifying vincristine and quercetin in nanoparticles, there was insufficient provided on the mobile phase and HPLC conditions used. Most importantly, no internal standard was used (Song, Zhao et al. 2008). The presence of an internal standard for pharmacokinetic studies allows for the correction of errors due to sample preparation, leading to more accurate values. Hence, there is a need to

develop and validate a method to simultaneously quantify vincristine and quercetin *in vivo*.

Ultra performance liquid chromatography (UPLC) is a chromatographic system which has been shown to improve the resolution, sensitivity, speed and reduce solvent consumption (Mazzeo, Neue et al. 2005; Swartz 2005; Nováková, Matysová et al. 2006). In view of these advantages, a simple, simultaneous and rapid UPLC method so as to quantify vincristine and quercetin levels in plasma for use in pharmacokinetic study in Chapter 9 has been developed.

8.2 Results

8.2.1 Optimization of analysis conditions

Apigenin was used as the internal standard (Figure 51). Initially, isocractic flow comprising of 75% milli-Q water (A) and 25% acetonitrile (B) was attempted. However, the chromatographic run time was more than 10 minutes. In addition, the vincristine peak displayed tailing. Therefore, 0.1% formic acid was added to both mobile phase A and B to reduce tailing.

Gradients that have been attempted ranged from (1) 75% A (0-3min), followed by 70% A to 50% A (3-9 min), 50% A to 5% A (9-10 min); (2) 75% A (0-3min), 70% A to 30% A (3-9 min) and 30% A to 5% A (9-10 min); (3) 75% A (0-3 min), 70% A to 30% A (3-7 min) and 30% A to 5% A (7-8 min); (4) 75% A to 5%

A (0-3.8 min), 5% A (3.81-4.1 min). For all modes, the mobile phase was reset to initial conditions of 75% A for 0.6 minutes before the next injection. Mode 4 was the optimal gradient which showed shortest run time and good separation of the analytes. Although all three compounds could be detected at 297 nm (Figure 52), quercetin was quantified at 376 nm to increase sensitivity of the method (Figure 53). At 376 nm, the vincristine peak could not be detected. The retention times of quercetin, apigenin and vincristine were 1.18, 1.35 and 1.45 minutes, respectively

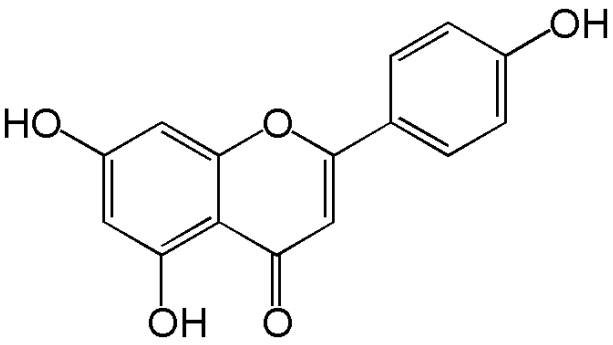

Figure 51 Structure of apigenin (internal standard).

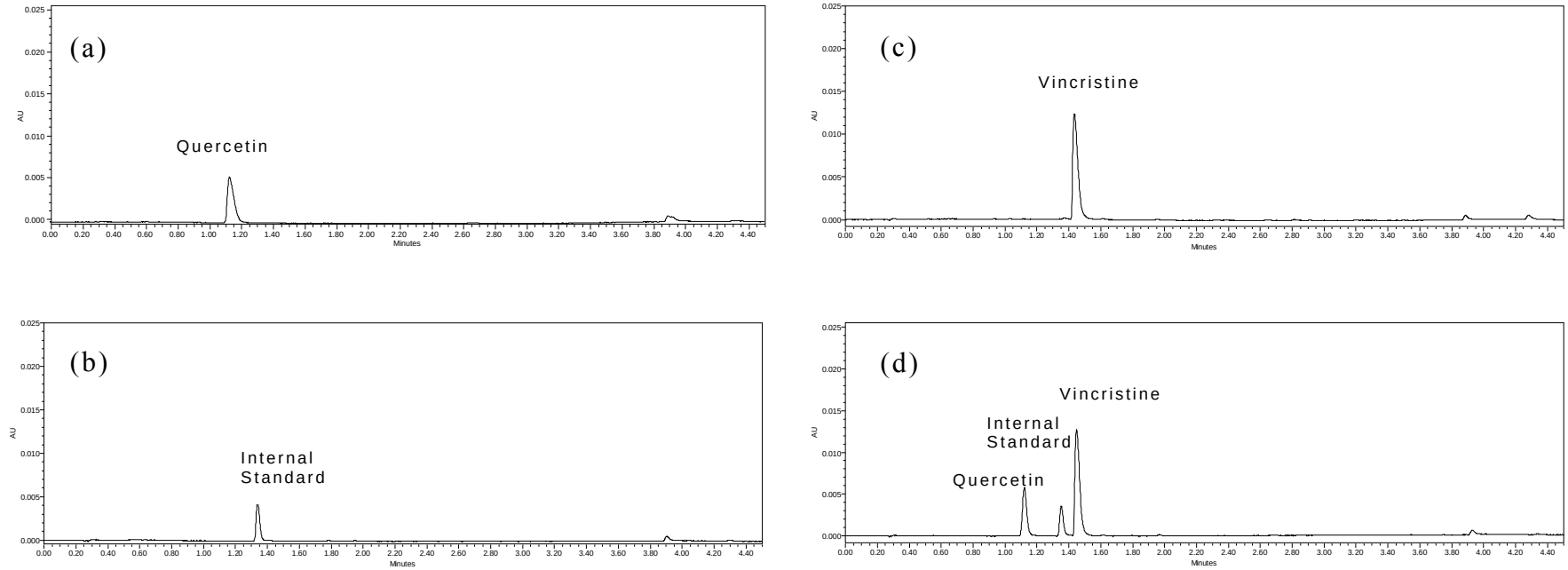

Figure 52 Representative chromatograms of (a) quercetin, (b) apigenin (internal standard), (c) vincristine and (d) mixture of quercetin, apigenin and vincristine at 297 nm.

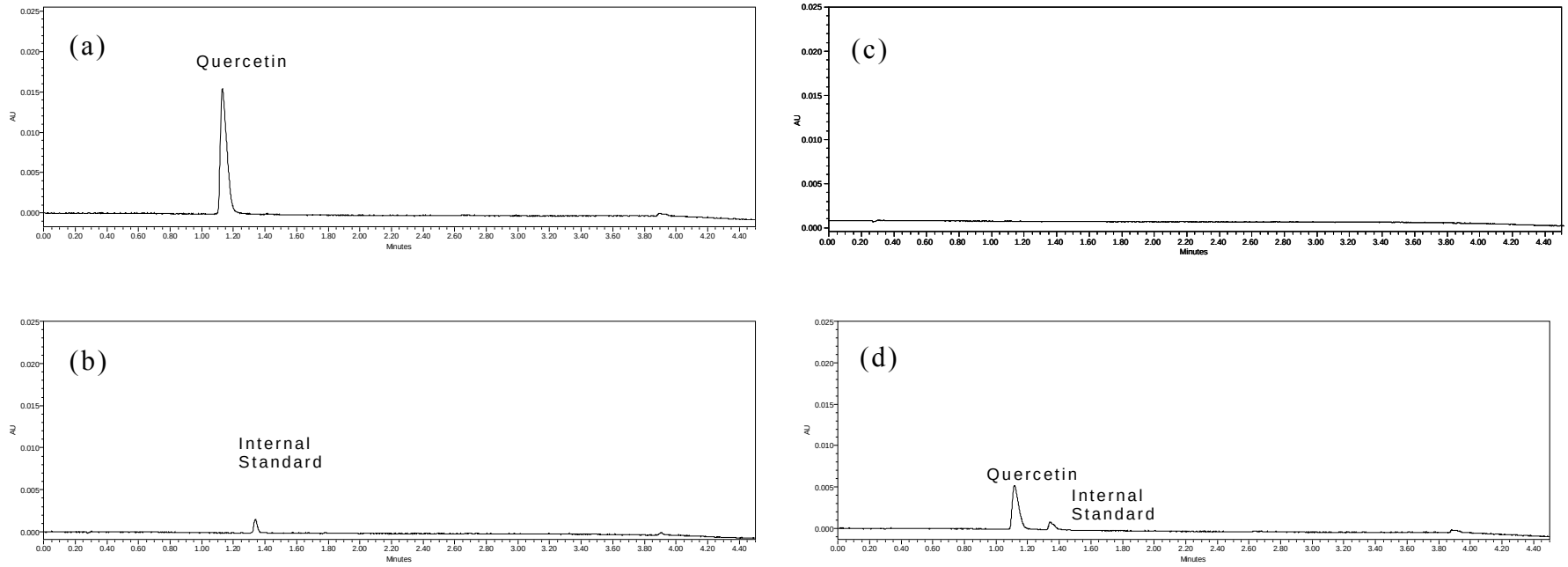

Figure 53 Representative chromatograms of (a) quercetin, (b) apigenin (internal standard), (c) vincristine (not detected) and (d) quercetin, apigenin and vincristine mixture at 376 nm.

8.2.2 Specificity in plasma samples

Figure 54 a and b show representative chromatograms of blank plasma at 297 and 376 nm, respectively. In addition, Figure 54 c and d show representative chromatograms of blank plasma spiked with quercetin, vincristine and apigenin (internal standard) at 297 nm and 376 nm, respectively, after liquid-liquid extraction with ethyl acetate. There were no peaks interfering with quercetin, apigenin and vincristine in blank mouse serum at both wavelengths.

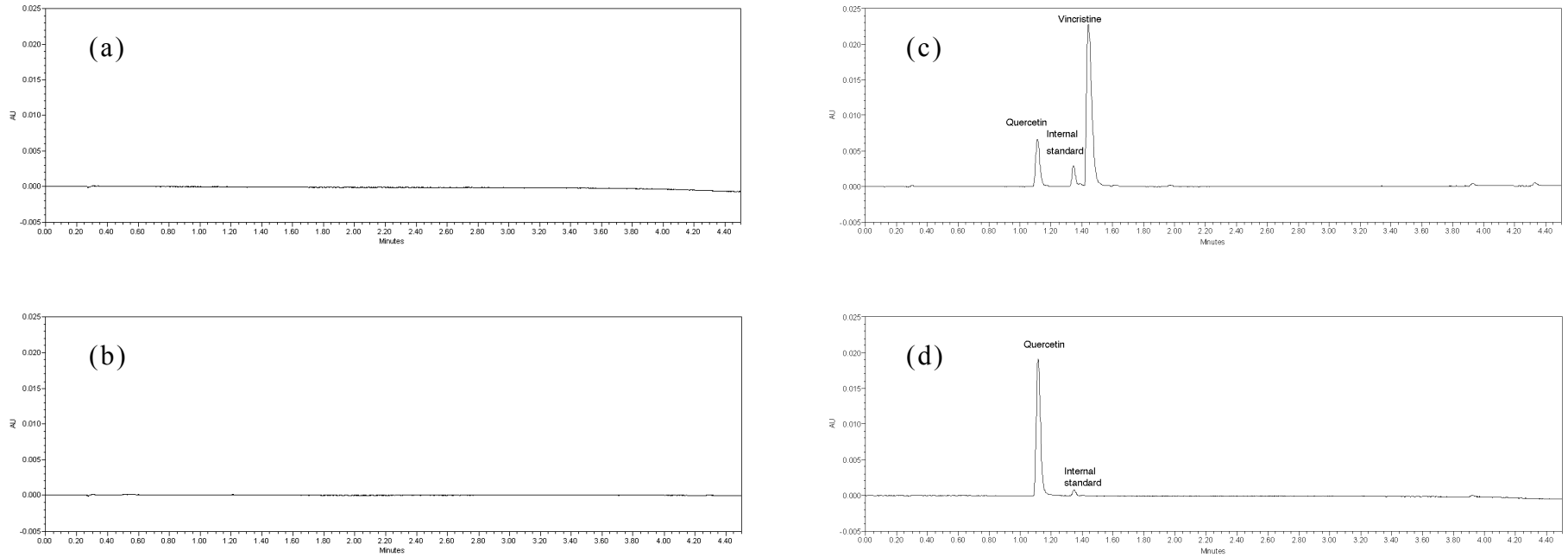

Figure 54. Chromatograms of (a) blank mouse serum at 297 nm, (b) blank mouse serum at 376 nm, (c) blank mouse serum spiked with vincristine, quercetin and internal standard at 297 nm and (d) blank mouse serum spiked with vincristine, quercetin and internal standard at 376 nm.

8.2.3 Linearity in plasma samples

The average calibration equation relating y (peak area ratio of drug:internal Standard) to x (concentration) was calculated from five analytical runs at the five concentrations cited above were as follows: (i) quercetin: y= 2.6494x – 0.1465, range of linearity from 0.22 to 17.74 nmol/mL, r^2 = 1.000 ; (ii) vincristine: y=0.34689x – 0.0056, range of linearity from 0.17 to 54.17 nmol/mL, r^2 = 0.999. The limits of detection for vincristine and quercetin were 0.11 nmol/mL and 0.06 nmol/mL, respectively. The limits of quantitation for quercetin and vincristine were 0.22 nmol/mL and 0.17 nmol/mL, respectively.

8.2.4 Accuracy and precision in plasma samples

Table 20 summarizes the intra-day analytical accuracy and precision (expressed as coefficient of variation, CV) of vincristine and quercetin. For quercetin, the intra-day accuracy ranged from 99.8% to 105.2% and its intra-day CV ranged from 2.4% to 3.3%. For vincristine, the intra-day accuracy ranged from 95.2% to 108.6% and its intra-day CV ranged from 1.5% to 14.9%. Table 21 summarizes the inter-day analytical accuracy and precision of vincristine and quercetin. The inter-day accuracy of quercetin ranged from 95.9% to 103.9% respectively and the inter-day CV ranged from 6.5% to 9.3%. For vincristine, inter-day accuracy ranged from and 98.1% to 108.8%

respectively and the inter-day CV ranged from 9.1% to 15.5%. The results indicate that the method had satisfactory accuracy and precision.

Table 20 Intra-day precision of vincristine and quercetin in plasma (n=5).

Analyte	Concentration added (nmol/mL)	Measured concentration (nmol/mL)	Accuracy (%)	CV (%)
Quercetin	14.19	14.16	99.8	2.4
	7.10	7.25	102.1	3.3
	1.77	1.84	103.7	2.5
	0.22 (LLOQ)	0.23	105.2	3.1
Vincristine	43.34	43.64	100.7	4.3
	10.83	11.27	104.1	3.5
	2.71	2.58	95.2	1.5
	0.17 (LLOQ)	0.18	108.6	14.9

CV: coefficient of variation
LLOQ: lower limit of quantification

Table 21 Inter-day precision of vincristine and quercetin in plasma (n=5).

Analyte	Concentration added (nmol/mL)	Measured concentration (nmol/mL)	Accuracy (%)	CV (%)
Quercetin	14.19	14.03	98.9	6.5
	7.10	7.38	103.9	8.5
	1.77	1.77	100.2	9.2
	0.22 (LLOQ)	0.21	95.9	9.3
Vincristine	43.34	43.12	99.5	9.1
	10.83	11.35	104.8	12.3
	2.71	2.66	98.1	13.2
	0.17 (LLOQ)	0.18	108.8	15.5

CV: coefficient of variation
LLOQ: lower limit of quantification

8.2.5 Extraction efficiency in plasma samples

Table 22 shows the absolute recoveries of vincristine and quercetin. Absolute recoveries were in the range of 96.7% to 120.0% for quercetin and 103.2% to 104.8% for vincristine. The CVs were in the range of 8.8% to 14.3% for quercetin and 12.7% to 15.5% for vincristine. Hence, simple liquid-liquid extraction from plasma with ethyl acetate is efficient for both vincristine and quercetin.

Table 22 Extraction efficiency of vincristine and quercetin (n=5).

Analyte	Concentration of analyte added (nmol/mL)	Concentration of analyte recovered (nmol/mL)	Absolute Recovery (%)	CV (%)
Quercetin	14.19	13.84	97.5	8.8
	7.10	6.87	96.7	13.9
	1.77	1.73	97.8	9.79
	0.22 (LLOQ)	0.26	120.0	14.3
Vincristine	43.34	44.86	103.5	12.7
	10.83	11.32	104.5	13.2
	2.71	2.53	104.8	14.6
	0.17 (LLOQ)	0.18	103.2	15.5

CV: coefficient of variation
LLOQ: lower limit of quantification

8.2.6 Stability in plasma samples

The stability of vincristine and quercetin in plasma samples was accessed after 24h at 4 ºC. They were stable and the CVs were in the range of 9.5% to 14.3% for quercetin and 10.5% to 15.5% for vincristine (Table 23).

Table 23 The stability of quercetin and vincristine in prepared samples stored at 4 ºC away from light at 24 h (n=5).

Analyte	Nominal Concentration (nmol/mL)	Mean detected concentration (nmol/mL)	CV (%)
Quercetin	14.19	14.07	9.5
	7.10	6.75	13.6
	1.77	1.74	12.2
	0.22 (LLOQ)	0.23	14.3
Vincristine	43.34	43.39	12.2
	10.83	11.75	10.5
	2.71	2.83	10.8
	0.17 (LLOQ)	0.17	15.5

CV: coefficient of variation
LLOQ: lower limit of quantification

8.2.7 Specificity for the liver and spleen homogenates

Figure 55 a and b show representative chromatograms of blank liver homogenate at 297 and 376 nm, respectively and Figure 55c and d show representative chromatograms of homogenate spiked with quercetin, vincristine and apigenin (internal standard) at 297 nm and 376 nm, respectively, after liquid-liquid extraction with ethyl acetate.

Similarly, Figure 56 a and b show representative chromatograms of blank spleen homogenate at 297 nm and 376 nm, respectively. Figure 56 c and d show representative chromatograms of homogenate spiked with quercetin, vincristine and apigenin (internal standard) at 297 nm and 376 nm, respectively, after liquid-liquid extraction with ethyl acetate. There were no peaks interfering with quercetin, apigenin and

vincristine in blank liver and spleen homogenate at both wavelengths.

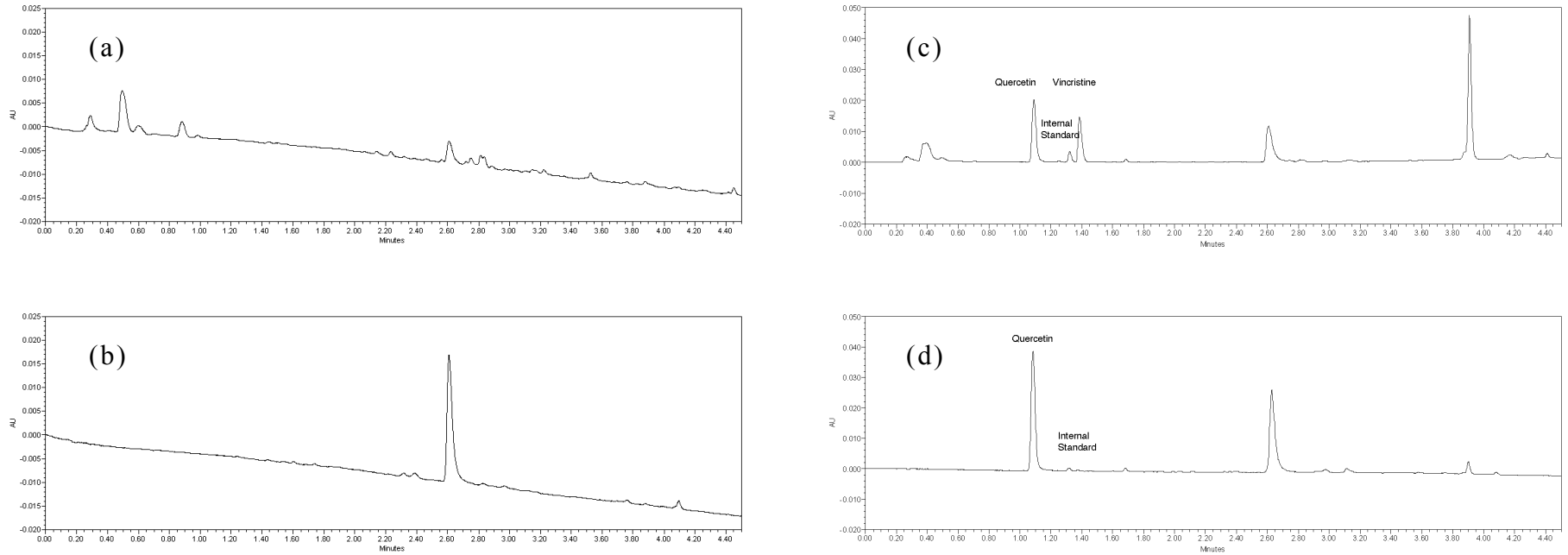

Figure 55 Chromatograms of (a) blank liver homogenate at 297 nm, (b) blank liver homogenate at 376 nm, (c) blank liver homogenate spiked with vincristine, quercetin and internal standard at 297 nm and (d) blank liver homogenate spiked with vincristine, quercetin and internal standard at 376 nm.

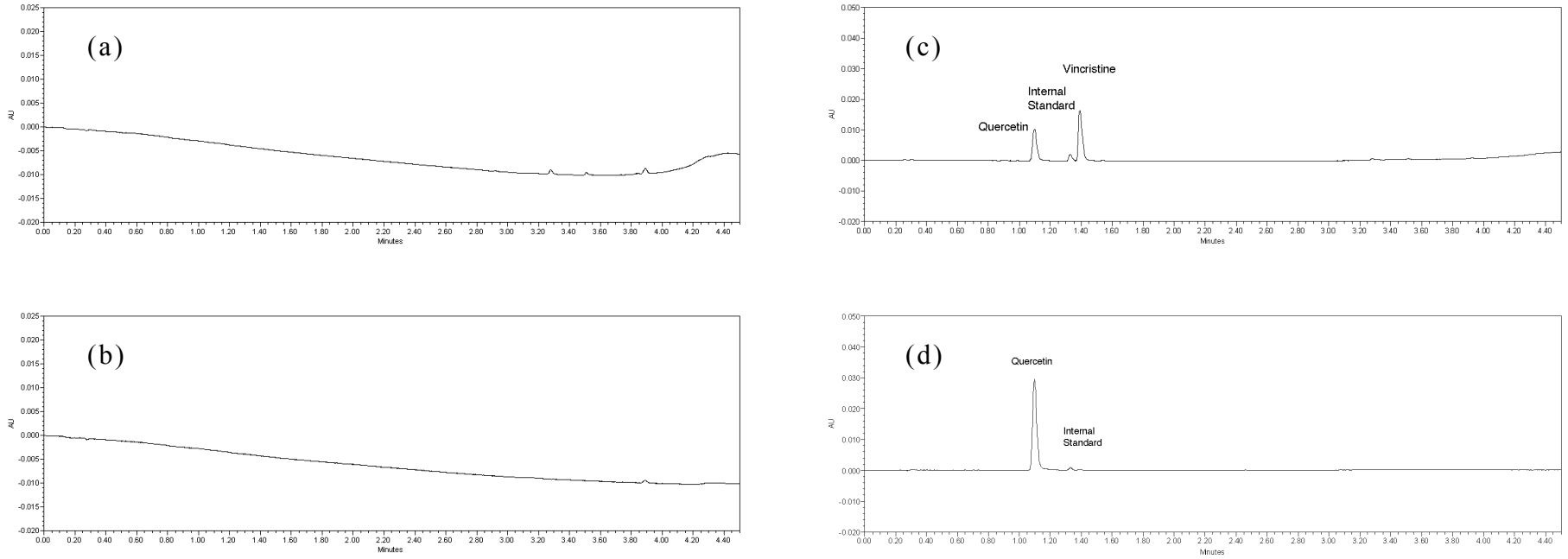

Figure 56 Chromatograms of (a) blank spleen homogenate at 297 nm, (b) blank spleen homogenate at 376 nm, (c) blank spleen homogenate spiked with vincristine, quercetin and internal standard at 297 nm and (d) blank spleen homogenate spiked with vincristine, quercetin and internal standard at 376 nm.

8.2.8 Linearity in liver and spleen homogenates

For the liver, the average calibration equation relating y (peak area ratio of drug:internal standard) to x (concentration) was calculated from five analytical runs at five concentrations as follows: (i) quercetin: y = 6.1628x + 0.4028, range of linearity from 0.22 to 17.74 nmol/mL, r^2 = 0.999 ; (ii) vincristine y = 1.3902x + 0.0521, range of linearity from 0.17 to 54.17 nmol/mL, r^2 = 0.995.

For the spleen, the average calibration equation relating y (peak area ratio of drug: internal standard) to x (concentration) was calculated from five analytical runs at five concentrations as follows: (i) quercetin: y = 6.6133x – 0.0032, range of linearity from 0.22 to 17.74 nmol/mL, r^2=0.999; (ii) vincristine y = 1.5128x + 0.1987, range of linearity from 0.17 to 54.17 nmol/mL, r^2 = 0.994. In addition, the limits of detection for quercetin and vincristine for both tissue homogenates were 0.17 nmol/mL and 0.22 nmol/mL, respectively.

8.2.9 Accuracy and precision in liver and spleen homogenates

Table 24 and Table 25 summarize the intra- and inter-day analytical accuracy and precision (expressed as CV) in liver homogenate. For the liver homogenate, the intra-day accuracy for quercetin ranged from 91.8% to 105.3% and the corresponding

CV ranged from 4.8% to 10.1%. For vincristine, the intra-day accuracy ranged from 93.6% to 115.6% and the corresponding CV ranged from 0.4% to 19.1%. In addition, the inter-day accuracy of quercetin ranged from 80.0% to 110.2% and the corresponding CV ranged from 2.9% to 9.3%. For vincristine, the inter-day accuracy of vincristine ranged from 100.2% to 109.4% and the corresponding CV ranged from 0.6% to 9.0% The results indicate that the method had satisfactory accuracy and precision.

Table 24 Intra-day precision of quercetin and vincristine in liver homogenate (n=3).

Analyte	Concentration added (nmol/g)	Measured concentration (nmol/g)	Accuracy (%)	CV (%)
Quercetin	14.19	13.03	91.8	5.0
	7.10	7.14	100.6	4.8
	1.77	1.86	105.3	6.6
	0.22 (LLOQ)	0.21	95.5	10.1
Vincristine	43.34	43.77	101.0	0.4
	10.83	11.57	106.8	6.8
	2.71	3.13	115.6	14.6
	0.17 (LLOQ)	0.16	93.6	19.1

CV: coefficient of variation
LLOQ: lower limit of quantification

Table 25 Inter-day precision of quercetin and vincristine in liver homogenate (n=3).

Analyte	Concentration added (nmol/g)	Measured concentration (nmol/g)	Accuracy (%)	CV (%)
Quercetin	14.19	13.76	97.0	2.9
	7.10	7.72	108.7	3.5
	1.77	1.95	110.2	2.5
	0.22 (LLOQ)	0.176	80.0	9.3
Vincristine	43.34	43.94	101.4	0.6
	10.83	11.84	109.4	4.7
	2.71	3.64	104.2	6.5
	0.17 (LLOQ)	0.17	100.2	9.0

CV: coefficient of variation
LLOQ: lower limit of quantification

For spleen homogenate, the intra-day accuracy for quercetin ranged from 85.0% to 112.6% and the corresponding CV ranged from 1.6% to 4.2%. The intra-day accuracy for vincristine ranged from 102.2% to 115.0% and the corresponding CV ranged from 0.6% to 2.4% (Table 26). The inter-day accuracy for quercetin ranged from 86.7% to 114.9% and the corresponding CV was in the range of 0.9% to 6.0%. For vincristine, the inter-day accuracy ranged from 102.5% to 107.2% and the corresponding CV was in the range of 1.2% to 10.3% (Table 27).

Table 26 Intra-day precision of quercetin and vincristine in spleen homogenate (n=3).

Analyte	Concentration added (nmol/g)	Measured concentration (nmol/g)	Accuracy (%)	CV (%)
Quercetin	14.19	14.78	104.3	1.6
	7.10	8.71	112.6	2.1
	1.77	1.51	85.0	2.8
	0.22 (LLOQ)	0.22	98.3	4.2
Vincristine	43.34	44.30	102.2	0.6
	10.83	12.20	112.7	1.1
	2.71	3.33	112.8	1.8
	0.17 (LLOQ)	0.20	115.0	2.4

CV: coefficient of variation
LLOQ: lower limit of quantification

Table 27 Inter-day precision of quercetin and vincristine in spleen homogenate (n=3).

Analyte	Concentration added (nmol/g)	Measured concentration (nmol/g)	Accuracy (%)	CV (%)
Quercetin	14.19	15.11	106.5	0.9
	7.10	8.87	114.9	2.7
	1.77	1.50	86.7	4.4
	0.22 (LLOQ)	0.21	95.5	6.0
Vincristine	43.34	44.42	102.5	1.2
	10.83	11.49	106.1	1.7
	2.71	2.91	107.2	10.3
	0.17 (LLOQ)	0.18	106.5	5.4

CV: coefficient of variation
LLOQ: lower limit of quantification

8.2.10 Recovery in liver and spleen homogenates

Table 28 shows the absolute recovery of quercetin and vincristine in liver, in which absolute recoveries were in the range of 98.3% to 119.7% for quercetin and 83.8% to 114.7% for vincristine. For spleen, absolute recoveries were in the range of 94.3% to 109.7% for quercetin and 106.1% to 121.2% for vincristine (Table 29). Hence, simple liquid-liquid extraction from the liver with ethyl acetate is efficient for both quercetin and vincristine.

Table 28 Extraction efficiency of quercetin and vincristine in liver homogenate (n=3).

	Concentration of analyte added (nmol/g)	Concentration of analyte recovered (nmol/g)	Absolute Recovery (%)	CV (%)
Quercetin	14.19	13.95	98.3	2.4
	7.10	7.55	106.3	2.3
	1.77	2.12	119.7	11.3
	0.22 (LLOQ)	0.22	98.7	8.7
Vincristine	43.34	44.34	102.3	1.3
	10.83	9.70	89.6	8.6
	2.71	2.27	83.8	3.8
	0.17 (LLOQ)	0.20	114.7	2.3

CV: coefficient of variation
LLOQ: lower limit of quantification

Table 29 Extraction efficiency of quercetin and vincristine in spleen homogenate (n=3).

	Concentration of analyte added (nmol/g)	Concentration of analyte recovered (nmol/g)	Absolute Recovery (%)	CV (%)
Quercetin	14.19	14.74	103.9	1.8
	7.10	7.79	109.7	12.2
	1.77	1.67	94.3	9.4
	0.22 (LLOQ)	0.22	99.6	16.3
Vincristine	43.34	45.98	106.1	5.7
	10.83	12.31	113.7	1.7
	2.71	3.28	121.2	1.3
	0.17 (LLOQ)	0.18	108.2	3.7

CV: coefficient of variation
LLOQ: lower limit of quantification

8.2.11 Stability in liver and spleen homogenates

The stability of quercetin and vincristine in homogenate samples was accessed after 24h at 4 ºC. The liver homogenate samples were stable and the CV% were in the range of 2.4% to 10.5% for quercetin and 1.6% to 5.5% for vincristine (Table 30).

Table 30 The stability of quercetin and vincristine in liver samples stored at 4 ºC away from light at 24 h (n=3).

Analyte	Nominal Concentration (nmol/g)	Mean detected concentration (nmol/g)	CV (%)
Quercetin	14.19	13.97	10.5
	7.10	7.34	2.4
	1.77	2.01	3.8
	0.22 (LLOQ)	0.18	3.5
Vincristine	43.34	43.70	2.0
	10.83	12.41	2.3
	2.71	3.18	1.6
	0.17 (LLOQ)	0.19	5.5

CV: coefficient of variation
LLOQ: lower limit of quantification

The spleen homogenate samples were stable and the CV% were in the range of 0.5% to 4.0% for quercetin and 0.8% to 9.9% for vincristine (Table 31).

Table 31 The stability of quercetin and vincristine in spleen samples stored at 4 ºC away from light at 24 h (n=3).

Analyte	Nominal Concentration (nmol/g)	Mean detected concentration (nmol/g)	CV (%)
Quercetin	14.19	14.29	0.5
	7.10	8.12	4.0
	1.77	1.58	2.5
	0.22 (LLOQ)	0.25	1.3
Vincristine	43.34	42.77	0.8
	10.83	12.25	0.6
	2.71	3.45	6.9
	0.17 (LLOQ)	0.22	9.9

CV: coefficient of variation
LLOQ: lower limit of quantification

8.3 Discussion

Due to the lack of published methods, it was necessary to develop a method to quantify quercetin and vincristine in plasma and other tissue homogenates. In addition, method validation was done to assess its reliability. Validation was necessary for the acquisition of high quality data so that meaningful conclusions can be drawn. Therefore, validation was done in accordance with Food and Drug Administration (FDA) guidelines (Administration 2001). Under these guidelines, the mean values have to be within 15% except at LLOQ, where the mean values have be within 20% for accuracy. For precision, the values should not exceed 15% CV except at LLOQ, where it should not exceed 20% CV. In addition, selectivity and stability of the method have to be determined.

The mean values and the CV% values obtained in this Chapter conformed to FDA guidelines. The chromatographs of the blank plasma and tissue homogenates show that there was no interference with endogeneous substances and the analytes was stable for 24 hours, fulfilling FDA guidelines. Results show that a simple, fast, accurate UPLC method for determination of quercetin and vincristine in mouse plasma samples and tissue homogenates has been developed and validated. The method has good calibration fit, precision, accuracy and recovery. This method will be applied to quantify quercetin and vincristine levels in the subsequent Chapter.

Chapter 9

IN VIVO STUDIES WITH QUERCETIN AND VINCRISTINE

9.1 Introduction

In Chapter 7, liposomes comprising of Egg Sphingomyelin (ESM)/Cholesterol/N-palmitoyl-sphingosine-1-{succinyl[methoxy(polyethylene glycol)$_{2000}$] (PEG_{2000}-ceramide)/Quercetin (72.5:17.5:5:5 mole ratio) were found to co-encapsulate quercetin and vincristine efficiently, display coordinated release of both drugs *in vitro*, and the formulation was active against MDA-MB-231 and JIMT-1 breast cancer cells. The aims of this Chapter are (1) to compare the plasma elimination profiles of the free drug combination with the liposome co-encapsulated formulation, (2) to determine whether the liposomal formulation can maintain the optimal synergistic ratio *in vivo*, and (3) to assess the antitumor efficacy of this formulation as compared to the free drug combination in a human xenograft model. As mentioned in Section 7.3, the JIMT-1 breast tumor xenograft model will be used because the *in vitro* data from Chapter 7 indicated that the vincristine/quercetin combination was more active against the JIMT-1 cell line as compared to MDA-MB-231. In addition, JIMT-1 also represents the ER^-, PR^- and transtuzumab-insensitive breast cancer subtype, where currently there are no effective treatment options available (Dizdar and Altundag 2010). Thus, it is worthwhile to explore

the vincristine/quercetin combination as a possible treatment regimen against this cancer subtype.

9.2 Results

9.2.1 Plasma elimination profile of free and liposomal combination of quercetin and vincristine

The plasma elimination profiles of free versus liposomal encapsulated quercetin and vincristine were determined in Balb/c mice. Figure 57 shows that free quercetin and vincristine levels were undetectable after 60 minutes and 120 minutes, respectively, whilst the levels of quercetin and vincristine in the liposome group remained detectable throughout the entire study period. In addition, quercetin and vincristine co-encapsulated in liposomes also had longer half lives, higher maximal concentration in plasma (C_{max}), higher total area under the curve (AUC_{total}), higher mean residence time (MRT_{last}), and lower clearance (Cl) as compared to the free drug combination (Table 32). In addition, Figure 58 shows that the initial encapsulated ratio of 2:1 vincristine/quercetin was maintained over the entire study period for the liposomal formulation ($p>0.05$) but not for the free drug combination ($p<0.05$).

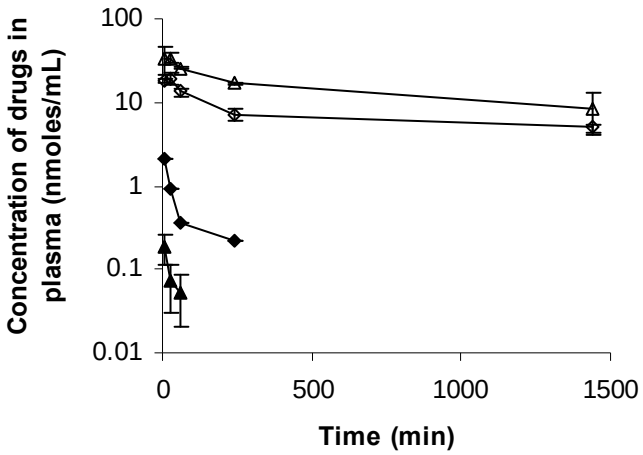

Figure 57 Concentrations of quercetin and vincristine in the plasma of Balb/c mice after intravenous administration of free combination of quercetin and vincristine or quercetin and vincristine co-encapsulated in liposomes. Concentrations of free quercetin are represented by (♦), free vincristine by (▲), liposomal quercetin by (◊) and liposomal vincristine by (Δ). Each value represents the mean ± SEM from 4 samples.

Table 32 Summary of pharmacokinetic parameters for quercetin and vincristine.

	Free		Liposomal	
	Quercetin	Vincristine	Quercetin	Vincristine
C_{max} (nmol/mL)	2.07	0.19	19.20	34.10
AUC_{last} (µmol.h/mL)	6.65	0.33	604.16	1240.54
$t_{1/2}$ (h)	1.49	0.48	14.20	16.00
Cl (mL/h)	0.47	16.90	0.01	0.01
MRT_{last} (h)	1.20	0.40	9.22	8.26
V (mL/g)	1.00	12.19	0.08	0.09
r	-0.82	-0.92	-0.84	-0.96

Mice (n=4) received the free combination of 1.33 mg/kg vincristine and 0.24 mg/kg quercetin (2:1 vincristine/quercetin mole ratio) or 1.33 mg/kg vincristine and 0.24 mg/kg quercetin co-encapsulated into liposomes. Injection volumes were 200 µL. Pharmacokinetic parameters were obtained from the pooled data from 4 mice. C_{max}: Maximum plasma concentration of drug, AUC_{last}: Area under the curve computed to the last observation, $t_{1/2}$: half life, Cl: total body clearance, MRT_{last}: Mean residence time up to the last observation,V: Volume of distribution, r: linear correlation coefficient.

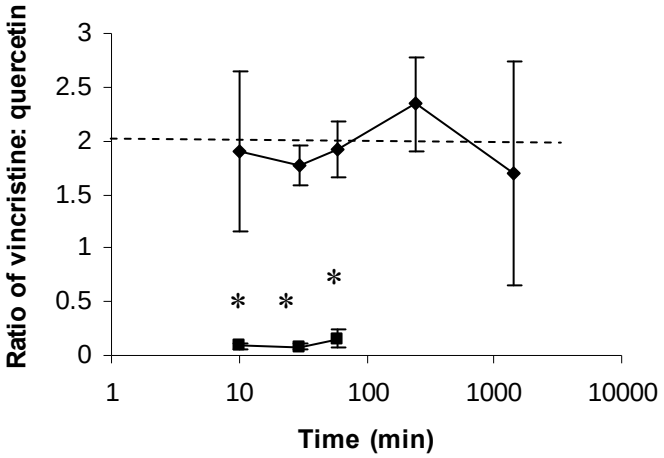

Figure 58 Comparison of the ratio of vincristine/quercetin over time for free vincristine and quercetin combination (■) and vincristine/quercetin in co-encapsulated liposomes (♦) in plasma. The dotted line represents the initial ratio of vincristine/quercetin. Each value represents the mean ± SEM from 4 samples. * $p < 0.05$.

9.2.2 Drug accumulation in the reticuloendothelial system

Liposomes are mostly eliminated by the liver and spleen- two major organs of the reticuloendothelial system (RES) (Zamboni 2005). Table 33 summarizes the accumulation of free and liposomal quercetin and vincistine in terms of C_{max} and AUC_{last}. For both quercetin and vincristine, the encapsulated drugs had higher AUC_{last} levels as compared to free drugs. However, the C_{max} values for the encapsulated drugs were lower as compared to free drugs.

Table 33 Accumulation of quercetin and vincristine in the liver and spleen after intravenous administration of free drug combination or the liposome co-encapsulated formulation.

		Free		Liposomal	
		Quercetin	Vincristine	Quercetin	Vincristine
Liver	C_{max} (nmol/g)	0.66	1.27	0.05	1.60
	AUC_{last} (μmol.h/g)	4.68	2.70	4.30	16.00
Spleen	C_{max} (nmol/g)	12.94	4.00	7.35	13.88
	AUC_{last} (μmol.h/g)	45.60	38.40	39.71	13.22

Mice (n=4) received 1.33 mg/kg vincristine together with 0.24 mg/kg quercetin (2:1 vincristine: quercetin molar ratio) as free forms or 1.33 mg/kg vincristine and 0.24 mg/kg quercetin co-encapsulated into liposomes. Injection volumes were 200 μL. Pharmacokinetic parameters were obtained from the pooled data of 4 mice.

9.2.3 *In vivo* antitumor effects against the JIMT-1 xenograft

The antitumor efficacy against the JIMT-1 xenograft was evaluated by comparing (1) vehicle control, (2) free quercetin, (3) free vincristine, (4) quercetin and vincristine combination in free form and (5) quercetin and vincristine co-encapsulated in liposomes. The dose of vincristine administered was 1.33 mg/kg, which was two-thirds of the maximum tolerated dose (MTD) of vincristine (Waterhouse, Madden et al. 2005) while the dose of quercetin was 0.24 mg/kg. This corresponded to a vincristine/quercetin molar ratio of 2:1. Figure 59 shows that although all the treated groups (groups 2-5) showed initial tumor regression, only the liposomal quercetin and vincristine

treatment group maintained the tumor regression over the entire 60 day period of the study.

Table 34 shows the time taken for the different tumors to reach 500 mm^3. One way ANOVA followed by post hoc Tukey analysis indicated that there was statistically significant difference between the liposomal quercetin and vincristine group and all the other groups ($p<0.05$). In addition, the differences in tumor volume for both the free quercetin monotherapy and free vincristine monotherapy group were not statistically significant as compared to control ($p>0.05$). Table 34 also lists tumor growth inhibition, which showed trends similar to the time taken for the tumor to 500 mm^3. According to the guidelines from the drug evaluation branch of the division of cancer treatment, National Cancer Institute considers tumor growth inhibition values equal or less than 42% as significant antitumor activity (Bissery, Guenard et al. 1991). Under this criterion, only the co-encapsulated group exhibited significant antitumor activity. Percentage weight change at nadir was used as an indicator of the toxicity of the treatment (Laster, Schabel et al. 1961). Statistical significance ($p<0.05$) was observed between the free quercetin and vincristine group as compared to the co-encapsulated liposomal quercetin and vincristine group for the percentage weight change in nadir.

Finally, Kaplan-meier survival analysis with log-rank significance test was conducted, as shown in Figure 59.

Statistical significance ($p<0.05$) was found between the co-encapsulated liposomal quercetin and vincristine group with the following: (1) vehicle control group, (2) free quercetin group and (3) free vincristine group. There was no significant difference between the co-encapsulated liposomal vincristine/quercetin group and the free vincristine/quercetin group ($p>0.05$).

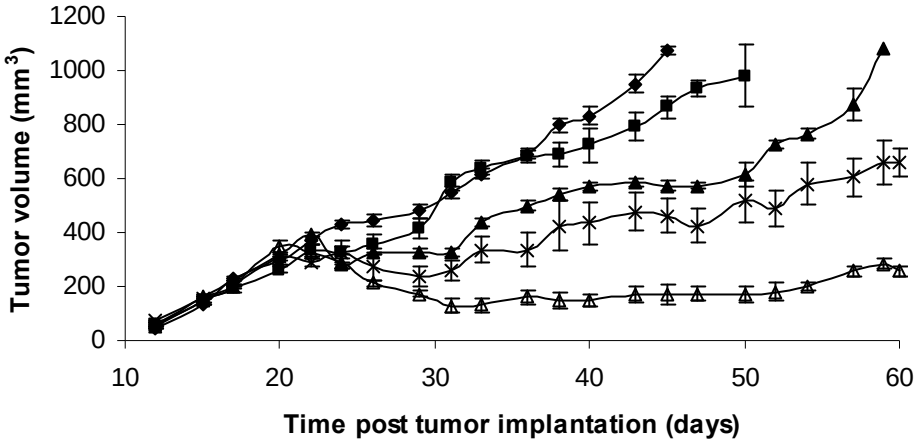

Figure 59 *In vivo* antitumor effects of the various treatment groups against JIMT-1 xenografts in SCID mice (n=5). The mice were treated via tail vein injections with vehicle buffer (♦), quercetin (■), vincristine (▲), quercetin and vincristine as free form (x) and co-encapsulated quercetin and vincristine in liposomes (Δ). The doses of vincristine were 1.33 mg/kg and that of quercetin was 0.24 mg/kg (2:1 vincristine: quercetin mole ratio). A total of 3 doses were administered on days 17, 20 and 23.

Table 34 Summary of *in vivo* antitumor efficacy studies in the JIMT-1 breast cancer xenograft in SCID mice (n=5).

Treatment group	Time taken for tumor to reach 500 mm^3 (days ± SD)	Tumor growth inhibition[a] at 500 mm^3 (%)	Percentage weight change at nadir[b]
Control	29.0 ± 3.4	NA	5.43 ± 0.28
Free quercetin	30.0 ± 1.2*	87	5.68 ± 0.55
Free vincristine	36.0 ± 2.2*	68	- 3.43 ± 0.91
Free quercetin and vincristine	50.0 ± 9.5*	49	- 4.72 ± 0.32
Co-encapsulated liposomal quercetin and vincristine	> 60 days*	36	2.75 ± 0.37

Co-encapsulated liposomal quercetin and vincristine showed statistically significant difference between the liposomal quercetin and vincristine group and all the other groups, * $p < 0.05$.

[a]Tumor growth inhibition = median tumor weight in the treated group (T)/ median tumor weight in the control group (C) x 100%.

[b]Percentage weight change at nadir = (Initial weight before treatment-weight at nadir)/initial weight before treatment x 100%.

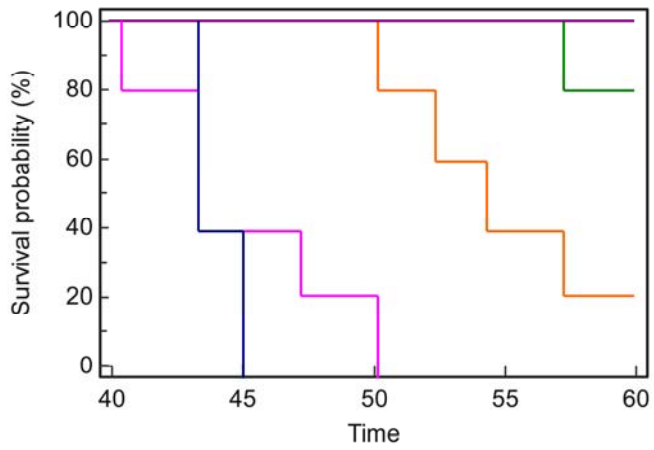

Figure 60 Kaplan-meier survival curves of the different treatment groups over time (n=5), control (blue), free quercetin (pink), free vincristine (orange), free quercetin and vincristine combination (green), liposomal quercetin and vincristine combination (purple). Log rank test was conducted.

9.2.4 *In vitro* evaluation of CI values in the ratios of free quercetin and vincristine

From Section 9.2.1, the ratios of vincristine/quercetin in plasma following the administration of free quercetin and vincristine were found to be 1:11, 1:12 and 1:6. The vincristine/quercetin ratios of 1:12 and 1:6 were tested *in vitro* and analyzed with the median-effect equation to determine CI. The CI values were 1.21 for the vincristine/quercetin ratio of 1:12 and 2.41 for the vincristine/quercetin ratio 1:6, indicating antagonism when the two agents were administered freely in the absence of a drug carrier.

9.3 Discussion

In this Chapter, it has been shown that in the absence of a drug carrier, the administration of free quercetin and vincristine led to antagonistic CIs *in vivo*. This could potentially reduce the efficacy of antitumor therapy as antagonistic drug ratios were delivered from the blood to the tumor. The results highlighted the need for a delivery vehicle for optimal antitumor efficacy. In contrast, liposomal encapsulation of quercetin and vincristine prolonged circulation half life and co-ordinated the release of the agents, maintaining the most synergistic molar ratio of the two drugs both *in vitro* and *in vivo*. Importantly, it was demonstrated that after liposomal co-encapsulation, enhanced antitumor efficacy could be achieved even at two-thirds the maximum tolerated dose (MTD) of vincristine, highlighting the potential of this formulation.

Consistent with previous studies, the pharmacokinetic study showed that free vincristine and free quercetin had short half lives (Krishna, Webb et al. 2001; Yuan, Chen et al. 2006). After liposomal incorporation, the *in vivo* half life of quercetin was increased nine-fold to 14.2h as compared to free quercetin. In addition, this liposomal formulation also showed a seven-fold increment in terms of half life *in vivo* as compared to a liposome formulation comprising of soybean lecithin, cholesterol and quercetin (Yuan, Chen et al. 2006). A possible reason for this could be because ESM, the major component of the liposomes

used in the present study, forms a more rigid lipid bilayer as compared to that of soybean lecithin, thereby slowing down quercetin release (Hillery 2000).

Similarly, liposomal encapsulation of vincristine increased its half life 30-fold to 16.0 h as compared to free vincristine. In addition, the formulation showed a four-fold increase in half life for vincristine as compared to DSPC/Cholesterol liposomes and around two-fold increase in half life as compared to ESM/Cholesterol liposomes *in vivo* (Krishna, Webb et al. 2001). This could be attributed to the liposomal bilayer rigidifying effect of quercetin through the formation of intermolecular hydrogen bonds (Tsuchiya, Nagayama et al. 2002), slowing down the release of vincristine from the liposomes. The higher C_{max}, AUC_{total}, $t_{1/2}$ and MRT_{last} and lower Cl in liposomes as compared to free drug obtained was also consistent with prior studies involving liposomes (Webb, Logan et al. 1998; Yuan, Chen et al. 2006).

Finally, liposomal encapsulation also maintained the optimal synergistic ratio of vincristine/quercetin of 2:1 in plasma over the entire study period. Although liposomes had been shown to co-ordinate drug release previously, they involved only amphipathic or hydrophilic drugs (Mayer, Harasym et al. 2006; Tardi, Gallagher et al. 2007; Tardi, Johnstone et al. 2009). Our study is the first to co-ordinate the release of an amphipathic agent (vincristine) and hydrophobic agent (quercetin) *in vivo*.

A comparison of the AUC values between the plasma and the reticuloendothelial system (RES) comprising of the spleen and liver showed that the levels of quercetin and vincristine co-encapsulated in the liposomes were lower in the RES as compared to that in plasma. This is consistent with other studies with liposomes formulated with PEG moiety, which reduced the rate of uptake of the liposomes by the RES (Allen and Stuart 1999). The low levels of quercetin and vincristine detected in the RES is beneficial because the uptake by the RES leads to the irreversible sequestering of the encapsulated drug in the RES, preventing the drug from being exposed to the tumor (Zamboni 2005). In addition, the uptake of the liposomes by the RES may result in acute impairment of the RES (Zamboni 2005); hence, the lower C_{max} observed in the liposomal system as compared to free drug suggests that the RES is unlikely to be overwhelmed.

Among the different treatment groups, the best antitumor activity was shown by co-encapsulated quercetin and vincristine, as reflected by the time taken for tumor to reach 500 mm^3 and the tumor growth inhibition values. Under the criterion set by the drug evaluation branch of the division of cancer treatment, National Cancer Institute (Bissery, Guenard et al. 1991), only the co-encapsulated formulation exhibits significant antitumor activity. Taking the pharmacokinetic data together, the increased antitumor efficacy in the co-encapsulated liposome group could be explained by (1) the longer circulation half life of quercetin

and vincristine increased the exposure duration of the tumor to the drugs resulting to an increase in antitumor activity (Jackson and Bender 1979; Horton, Houghton et al. 1988), (2) the optimal synergistic ratio of vincristine/quercetin of 2:1 was maintained in the plasma and to the tumor site. This was further supported by the antagonistic combination indices obtained from the administration of free quercetin and vincristine, which prevented the full synergistic potential to be realized. Importantly, this higher *in vivo* antitumor activity in the co-encapsulated liposomal formulation was attained even at two thirds of maximal tolerated dose of vincristine in SCID mice, which highlighted the potential of this formulation to achieve antitumor efficacy while reducing concentration dependent side effects. In addition, Kaplan-meier survival analysis with log-rank significance test was conducted on the last day of the study on Day 60, to determine if there was any statistical difference in survival among the different groups. The log rank significance test showed that there was no statistical difference between (1) the free vincristine/quercetin combination group and (2) the liposomal co-encapsulated quercetin and vincristine group. However, given that the tumor size of the free quercetin and vincristine group was double that of the co-encapsulated quercetin and vincristine liposome group, statistical difference might be attained if the study period was extended.

Finally, the percentage weight loss at nadir was used to evaluate the toxicity of the treatments (Corbett 2002). The percentage weight change between free quercetin and vincristine was statistically different ($p < 0.05$) as compared to that of liposomal quercetin and vincristine. Although higher levels of quercetin and vincristine were detected in the plasma and organs in the liposomal formulation as compared to free drug, this did not lead to an increase in toxicity. This could be explained by the high concentration of vincristine in plasma rather than the RES for the liposomal encapsulated group. In addition, given the short half life of quercetin and vincristine, most of the drug detected in plasma remained sequestered in the liposomes (Krishna, Webb et al. 2001), and were unable to exert their biological effects (Zamboni 2005; Lee, Kim et al. 2006), minimizing weight loss at nadir (Lee 2006).

The study has shown that the co-encapsulation of vincristine/quercetin in liposomes at synergistic ratio showed good antitumor efficacy and low toxicity in an estrogen and progesterone receptor negative and transtuzumab insensitive xenograft model. Importantly, enhanced antitumor efficacy could be achieved even at two-thirds the MTD of vincristine after liposomal incorporation.

Chapter 10

IMPLICATIONS, CONCLUSION AND FUTURE DIRECTIONS

The implications of this work will be discussed from the formulation and clinical perspectives. From the formulation perspective, this is the first known attempt to co-encapsulate irinotecan and quercetin in a single drug carrier. In spite of the anti-cancer synergy between irinotecan and quercetin reported in literature (highlighted in Chapter 1), this is the first time that these two synergistic compounds has been co-encapsulated in a drug carrier. This can enhance therapeutic efficacy by allowing controlled and co-ordinated release of the drug combination in their optimal synergistic ratio.

Although quercetin and vincristine have been co-encapsulated in nanoparticles (Song, Zhao et al. 2008), the present liposomal formulation coordinated the release of the two drugs which was otherwise not possible in the previous nanoparticle formulation. Coordinated release of quercetin and vincristine is crucial as the range of synergism between quercetin and vincristine is narrow, where a change from vincristine/quercetin molar ratio from 2:1 to 1:1 would lead to antagonism (Section 7.2.1). The present liposomal formulation is an improvement from the previous nanoparticle formulation as it coordinates the release of quercetin and vincristine from the liposomes to allow for optimal therapeutic efficacy to be exerted

between quercetin and vincristine, thereby a promising new therapeutic regimen against breast cancer.

The coordinated release of drugs with drug delivery systems had been attempted in the past. However, previous work had focused on the combination of conventional amphipathic chemotherapeutic drugs such as irinotecan with floxuridine (Tardi, Gallagher et al. 2007), doxorubicin with vincristine (Abraham, McKenzie et al. 2004) and fludarabine with mitoxantrone (Zhao, Wu et al. 2007). This is the first report which focused on the loading and coordinating the release of a hydrophobic substance, quercetin with amphipathic drugs such as vincristine and irinotecan, showing the feasibility of coordinating the release of hydrophobic and amphipathic drugs in liposomes.

The research project has also shown that efficient loading of both hydrophobic and amphipathic compounds, having different requirements for efficient loading into liposomes, could be attained through optimization of formulation variables. This has been illustrated by the vincristine/quercetin combination. Quercetin incorporation and solubilization was found to be most efficient either in the absence or at low levels of cholesterol but efficient and stable vincristine loading required at least 17.5 mol% of cholesterol. Finally, the formulation developed comprised of vincristine in Egg Sphingomyelin/Cholesterol/PEG_{2000}-ceramide/Quercetin

(72.5:17.5:5:5 mole ratio) liposomes and loading efficiency of both quercetin and vincristine were more than 70%. Moving forward, the combination of hydrophobic and amphipathic compounds are likely to become increasingly common because many of the new drug entities in the research pipeline are hydrophobic compounds and liposomes can potentially be used to co-encapsulate them.

In addition, quercetin has been shown to alter vincristine release in the vincristine/quercetin liposomal formulation. It could be a novel alternative to alter drug loading and release profiles from liposomes. Besides traditional avenues to change drug loading and release, such as changing lipid composition, the formation of drug precipitates and changes in pH gradient, the incorporation of quercetin or other compounds that can form hydrogen bonds represent a new avenue to alter drug loading and release.

To our knowledge, this is the first attempt to load irinotecan in cholesterol free liposomes and also the first successful attempt in the use of temperatures above the phase transition temperature (T_c) of the lipid for drug loading in cholesterol free liposomes. Importantly, drug loading efficiency and time needed for the loading of irinotecan in cholesterol free liposomes were not significantly different from cholesterol containing liposomes. Previously, drug loading into cholesterol free liposomes have been limited to the use of temperatures

below T_c. This has limited the utility of cholesterol free liposomes due to the longer drug loading times and lower drug: lipid ratio achievable as compared with conventional cholesterol containing liposomes. The project has indicated that efficient loading could potentially be attained in cholesterol free liposomes with the aid of a transmembrane gradient maintained by ionophore A23187 and could potentially be applied to other amphipathic chemotherapeutic drugs as well.

From a clinical perspective, this work represents the first attempt to explore the use of quercetin and vincristine for HER2 overexpressing breast cancer. Currently, either high dose chemotherapy (Dizdar and Altundag 2010) or the combination of various chemotherapeutic agents (Chen and Russo 2009) are being used. However, these approaches either lacked therapeutic efficacy and failed to increase disease free survival (Heinemann 2003) or were too toxic, leading to more treatment related deaths (Dizdar and Altundag 2010), thus highlighting the need to develop effective treatments. This work found that the co-encapsulated liposome formulation exhibited significant antitumor activity at two-thirds of the maximum tolerated dose of vincristine and also showed less toxicity as compared to the free drug combination. Therefore, the formulation is efficacious and with reduced toxicity, which could have further clinical potential to be developed as a possible treatment avenue for HER2 overexpressing breast cancer.

In addition, the *in vitro* data shows that the trends for synergistic and antagonistic ratios are similar against the two representative cell lines, JIMT-1 and MDA-MB-231. This could facilitate its clinical use as the same formulation is active against different cell lines, and is not specific to a particular subtype of breast cancer.

Therefore, future studies that could be conducted include testing in more cell lines to verify whether the trends for synergy and antagonism are similar across different breast cancer cell lines. In addition, this project has shown improved antitumor efficacy for the vincristine/quercetin liposomal formulation. The improved efficacy could be due to the maintenance of the synergistic ratio and the prolongation of half life. The extent of contribution by these two factors can be further determined by comparing the antitumor efficacy of liposomal quercetin alone, liposomal vincristine alone as well as an antagonistic ratio of vincristine/quercetin,

From a broader perspective, future studies can be done to

(1) Test the efficacy of this formulation against multidrug resistant cancers.

Multidrug resistance-associated protein (MRP) has been implicated in multidrug resistant cancer, a major cause of cancer resistance. Since quercetin has been shown to inhibit chemotherapeutic drug efflux from the MRP (Leslie, Mao et al.

2001), the liposomal formulation can be evaluated against MRP overexpressing cancer variants.

(2) Formulate targeted liposomes.

Liposomes can be attached with ligands against cell surface antigens so as to target the cancer cells. This has the potential to increase therapeutic efficacy. Promising target ligands include epidermal growth factor receptor (EGFR), transferrin receptor and the folate receptor. These can be incorporated onto the liposomal formulations comprising of vincristine/quercetin or irinotecan/quercetin. *In vivo* efficacy studies can be conducted to determine whether the ligands would enhance therapeutic efficacy.

(3) Determine the molecular mechanisms contributing to the synergism exhibited by the vincristine/quercetin and irinotecan/quercetin combinations.

The precise mechanism in which the drugs exhibit synergy in breast cancer cell lines remains unknown. Some possible targets to explore include tyrosine specific protein kinases, heat shock proteins and glycogen-synthase kinase-3-β, which have been shown to exhibit synergy in other cancer cell lines, as highlighted in the Chapter 1. It is also of interest to explore if the ratio of chemotherapeutic drugs would have an impact on the expression of these factors.

10.1 References

Abraham, S. A., McKenzie, C., et al. (2004). "In Vitro and in Vivo Characterization of Doxorubicin and Vincristine Coencapsulated within Liposomes through Use of Transition Metal Ion Complexation and pH Gradient Loading." Clin Cancer Res **10**(2): 728-738.

Administration, F. a. D. (2001). Guidance for industry: Bioanalytical method validation. Food and Drug Administration.

Akbas, S. H., Timur, M., et al. (2005). "The Effect of Quercetin on Topotecan Cytotoxicity in MCF-7 and MDA-MB 231 Human Breast Cancer Cells1." Journal of Surgical Research **125**(1): 49-55.

Allen, T. and Stuart, D. (1999). Liposomal pharmacokinetics. Classical, sterically-stabilized, cationic liposomes and immunoliposomes. Liposomes: rational design. Janoff AS. New York Marcel Dekker**:** 63-67.

Anderson, M. and Omri, A. (2004). "The Effect of Different Lipid Components on the In Vitro Stability and Release Kinetics of Liposome Formulations." Drug Delivery **11**(1): 33 - 39.

Andrew, R. H. and Philip, S. L. (2005). "Folate receptor-mediated drug targeting: From therapeutics to diagnostics." Journal of Pharmaceutical Sciences **94**(10): 2135-2146.

Bangham, A. D., Standish, M. M., et al. (1965). "Diffusion of univalent ions across the lamellae of swollen phospholipids." J Mol Biol **13**(1): 238-52.

Bartucci, R., Pantusa, M., et al. (2002). "Interaction of human serum albumin with membranes containing polymer-grafted lipids: spin-label ESR studies in the mushroom and brush regimes." Biochimica et Biophysica Acta (BBA) - Biomembranes **1564**(1): 237-242.

Bernard-Marty, C., Cardoso, F., et al. (2004). "Facts and controversies in systemic treatment of metastatic breast cancer." Oncologist **9**(6): 617-32.

Bissery, M. C., Guenard, D., et al. (1991). "Experimental antitumor activity of taxotere (RP 56976, NSC 628503), a taxol analogue." Cancer Res **51**(18): 4845-52.

Bliss, C. (1939). "The toxicity of poisons applied jointly." Ann Appl Biol **26**: 585-615.

Boman, N. L., Mayer, L. D., et al. (1993). "Optimization of the retention properties of vincristine in liposomal systems." Biochimica et Biophysica Acta (BBA) - Biomembranes **1152**(2): 253-258.

Bonte, F., Hsu, M. J., et al. (1987). "Interactions of polymerizable phosphatidylcholine vesicles with blood components: relevance to biocompatibility." Biochim Biophys Acta **900**(1): 1-9.

Bors, W., Heller, W., et al. (1990). "Flavonoids as antioxidants: determination of radical-scavenging efficiencies." Methods Enzymol **186**: 343-55.

Brunton, L. and Lazo, J. (2005). Goodman and Gilman's Pharmacological Basis of Therapeutics, McGraw-Hill.

Burke, T. G., Mishra, A. K., et al. (1993). "Lipid bilayer partitioning and stability of camptothecin drugs." Biochemistry **32**(20): 5352-64.

Cai, Z., Wang, Y., et al. (2010). "Nanocarriers: a general strategy for enhancement of oral bioavailability of poorly absorbed or pre-systemically metabolized drugs." Curr Drug Metab **11**(2): 197-207.

Casagrande, F. and Darbon, J. M. (2001). "Effects of structurally related flavonoids on cell cycle progression of human melanoma cells: regulation of cyclin-dependent kinases CDK2 and CDK1." Biochem Pharmacol **61**(10): 1205-15.

Casagrande, R., Georgetti, S. R., et al. (2007). "In vitro evaluation of quercetin cutaneous absorption from topical formulations and its functional stability by antioxidant activity." International Journal of Pharmaceutics **328**(2): 183-190.

Casagrande, R., Georgetti, S. R., et al. (2006). "Evaluation of functional stability of quercetin as a raw material and in different topical formulations by its antilipoperoxidative activity." AAPS PharmSciTech **7**(1): E10.

Cattel, L., Ceruti, M., et al. (2003). "From conventional to stealth liposomes: a new frontier in cancer chemotherapy." Tumori **89**(3): 237-49.

Chan, D., Yeo, W. L., et al. (2009). "Phase II study of gemcitabine and carboplatin in metastatic breast cancers with prior exposure to anthracyclines and taxanes." Invest New Drugs.

Chan, M. M., Fong, D., et al. (2003). "Inhibition of growth and sensitization to cisplatin-mediated killing of ovarian cancer cells by polyphenolic chemopreventive agents." J Cell Physiol **194**(1): 63-70.

Chen, J. Q. and Russo, J. (2009). "ER-negative and triple negative breast cancer: Molecular features and potential therapeutic approaches." Biochimica et Biophysica Acta - Reviews on Cancer **1796**(2): 162-175.

Chen, X. (2005). "Pharmacokinetics and modeling of quercetin and metabolites." Pharmaceutical Research **22**(6): 892-901.

Chollet, D. F., Goumaz, L., et al. (1998). "Simultaneous determination of the lactone and carboxylate forms of the camptothecin derivative CPT-11 and its metabolite SN-38 in plasma by high-performance liquid chromatography." J Chromatogr B Biomed Sci Appl **718**(1): 163-75.

Chou, T.-H., Chen, S.-C., et al. (2003). "Effect of Composition on the stability of liposomal irinotecan prepared by a pH

gradient method." Journal of Bioscience and Bioengineering **95**(4): 405-408.
Chou, T. C. (2008). "Preclinical versus clinical drug combination studies." Leuk Lymphoma **49**(11): 2059-80.
Chou, T. C. and Talalay, P. (1977). "A simple generalized equation for the analysis of multiple inhibitions of Michaelis-Menten kinetic systems." J Biol Chem **252**(18): 6438-42.
Chowdhury, S. A., Kishino, K., et al. (2005). "Tumor-specificity and apoptosis-inducing activity of stilbenes and flavonoids." Anticancer Res **25**(3B): 2055-63.
Chu, L., Sutton, L. M., et al. (1996). "Continuous infusion 5-fluorouracil as first-line therapy for metastatic breast cancer." J Infus Chemother **6**(4): 211-6.
clinical trials.gov, assessed on 6th June 2010
Corbett, T. H., L. Polin, B.J. Roberts (2002). Transplantable syngeneic rodent tumors: Solid tumors in mice. Tumor Models in Cancer Research. B. A. Teicher. Totowa, N.J, Humanapress.com**:** 41-73.
Corona, G., Casetta, B., et al. (2008). "Rapid and sensitive analysis of vincristine in human plasma using on-line extraction combined with liquid chromatography/tandem mass spectrometry." Rapid Communications in Mass Spectrometry **22**(4): 519-525.
Cowens, J. W., Creaven, P. J., et al. (1993). "Initial clinical (phase I) trial of TLC D-99 (doxorubicin encapsulated in liposomes)." Cancer Res **53**(12): 2796-802.
Cushnie, T. P. and Lamb, A. J. (2005). "Antimicrobial activity of flavonoids." Int J Antimicrob Agents **26**(5): 343-56.
Dancey, J. E. and Chen, H. X. (2006). "Strategies for optimizing combinations of molecularly targeted anticancer agents." Nat Rev Drug Discov **5**(8): 649-59.
Dandamudi, S. and Campbell, R. B. (2007). "Development and characterization of magnetic cationic liposomes for targeting tumor microvasculature." Biochim Biophys Acta **1768**(3): 427-38.
Date, A. A. and Nagarsenker, M. S. (2008). "Parenteral microemulsions: An overview." International Journal of Pharmaceutics **355**(1-2): 19-30.
de Gennes, P. G. (1987). "Polymers at an interface; a simplified view." Advances in Colloid and Interface Science **27**(3-4): 189-209.
de Kruyff, B., Demel, R. A., et al. (1972). "The effect of cholesterol and epicholesterol incorporation on the permeability and on the phase transition of intact Acholeplasma laidlawii cell membranes and derived liposomes." Biochim Biophys Acta **255**(1): 331-47.
Demel, R. A. and De Kruyff, B. (1976). "The function of sterols in membranes." Biochim Biophys Acta **457**(2): 109-32.

Devita, V. J., Serpick, A. A., et al. (1970). "Combination chemotherapy in the treatment of advanced Hodgkin's disease." Annuals of Internal Medicine **73**(6): 881-895.

Dinis, T. C., Maderia, V. M., et al. (1994). "Action of phenolic derivatives (acetaminophen, salicylate, and 5-aminosalicylate) as inhibitors of membrane lipid peroxidation and as peroxyl radical scavengers." Arch Biochem Biophys **315**(1): 161-9.

Dizdar, O. and Altundag, K. (2010). "Current and emerging treatment options in triple-negative breast cancer." Oncology Reviews **4**(1): 5-13.

Dos Santos, N., Allen, C., et al. (2007). "Influence of poly(ethylene glycol) grafting density and polymer length on liposomes: Relating plasma circulation lifetimes to protein binding." Biochimica et Biophysica Acta (BBA) - Biomembranes **1768**(6): 1367-1377.

Dos Santos, N., Cox, K. A., et al. (2004). "pH gradient loading of anthracyclines into cholesterol-free liposomes: enhancing drug loading rates through use of ethanol." Biochimica et Biophysica Acta (BBA) - Biomembranes **1661**(1): 47-60.

Dos Santos, N., Waterhouse, D., et al. (2005). "Substantial increases in idarubicin plasma concentration by liposome encapsulation mediates improved antitumor activity." Journal of Controlled Release **105**(1-2): 89-105.

Drewinko, B., Loo, T. L., et al. (1976). "Combination chemotherapy in vitro with adriamycin. Observations of additive, antagonistic, and synergistic effects when used in two-drug combinations on cultured human lymphoma cells." Cancer Biochem Biophys **1**(4): 187-95.

Drummond, D. C., Hayes, M. E., et al. (2007). Intraliposomal Trapping Agents for Improving In Vivo Liposomal Drug Formulation Stability. Liposome Technology. G. Gregoriadis. New York, Informa Healthcare. **2:** 149-168.

Drummond, D. C., Noble, C. O., et al. (2006). "Development of a Highly Active Nanoliposomal Irinotecan Using a Novel Intraliposomal Stabilization Strategy." Cancer Res **66**(6): 3271-3277.

Fenske, D. B. and Cullis, P. R. (2007). Encapsulation of drugs with pH gradient technique. Liposome Methods. G. Gregoriadis. New York Informa Healthcare. **2:** 27-50.

Fenske, D. B., Wong, K. F., et al. (1998). "Ionophore-mediated uptake of ciprofloxacin and vincristine into large unilamellar vesicles exhibiting transmembrane ion gradients." Biochimica et Biophysica Acta (BBA) - Biomembranes **1414**(1-2): 188-204.

Ferry, D. R., Smith, A., et al. (1996). "Phase I clinical trial of the flavonoid quercetin: pharmacokinetics and evidence for in vivo tyrosine kinase inhibition." Clin Cancer Res **2**(4): 659-68.

Food and Drug Administration (2001) Guidance for industry: Bioanalytical method validation.

Frijlink, H. W., Eissens, A. C., et al. (1991). "The effect of parenterally administered cyclodextrins on cholesterol levels in the rat." Pharm Res **8**(1): 9-16.

Fujiwara, Y., Hosokawa, Y., et al. (2007). "Blockade of the phosphatidylinositol-3-kinase-Akt signaling pathway enhances the induction of apoptosis by microtubule-destabilizing agents in tumor cells in which the pathway is constitutively activated." Mol Cancer Ther **6**(3): 1133-42.

Gabizon, A., Catane, R., et al. (1994). "Prolonged circulation time and enhanced accumulation in malignant exudates of doxorubicin encapsulated in polyethylene-glycol coated liposomes." Cancer Res **54**(4): 987-92.

Gao, Y., Wang, Y., et al. (2009). "Formulation optimization and in situ absorption in rat intestinal tract of quercetin-loaded microemulsion." Colloids and Surfaces B: Biointerfaces **71**(2): 306-314.

Godbout, J. P., Pesavento, J., et al. (2002). "Methylglyoxal Enhances Cisplatin-induced Cytotoxicity by Activating Protein Kinase Cdelta." Journal of Biological Chemistry **277**(4): 2554-2561.

Goniotaki, M., Hatziantoniou, S., et al. (2004). "Encapsulation of naturally occurring flavonoids into liposomes: physicochemical properties and biological activity against human cancer cell lines." Journal of Pharmacy and Pharmacology **56**(10): 1217-1224.

Gonzalez-Gallego, J., Sanchez-Campos, S., et al. (2007). "Anti-inflammatory properties of dietary flavonoids." Nutr Hosp **22**(3): 287-93.

Guilhaumou, R., Solas, C., et al. (2010). "Validation of an electrospray ionization LC/MS/MS method for quantitative analysis of vincristine in human plasma samples." Journal of Chromatography B: Analytical Technologies in the Biomedical and Life Sciences **878**(3-4): 423-427.

Gulati, N., Laudet, B., et al. (2006). "The antiproliferative effect of Quercetin in cancer cells is mediated via inhibition of the PI3K-Akt/PKB pathway." Anticancer Res **26**(2A): 1177-81.

Gupta, S., Moulik, S. P., et al. (2005). "Designing and testing of an effective oil-in-water microemulsion drug delivery system for in vivo application." Drug Deliv **12**(5): 267-73.

Hakimuddin, F., Paliyath, G., et al. (2004). "Selective Cytotoxicity of a Red Grape Wine Flavonoid Fraction Against MCF-7 Cells." Breast Cancer Research and Treatment **00085**(00001): 65-80.

Hanahan, D. and Weinberg, R. A. (2000). "The Hallmarks of Cancer." Cell **100**(1): 57-70.

Haran, G., Cohen, R., et al. (1993). "Transmembrane ammonium sulfate gradients in liposomes produce efficient and stable

entrapment of amphipathic weak bases." Biochim Biophys Acta **1151**: 201-215.
Harasym, T. O., Liboiron, B. D., et al. (2009). Drug Ratio-Dependent Antagonism: A New Category of Multidrug Resistance and Strategies for Its Circumvention. Multi-Drug Resistance in Cancer**:** 291-323.
Harasym, T. O., Tardi, P. G., et al. (2007). Fixed Drug Ratio Liposome Formulations of Combination Cancer Therapeutics. Liposome Technology. G. Gregoriadis. New York, Informa Healthcare. **3:** 25-48.
Heinemann, V. (2003). "Definition of An Optimal First-line Chemotherapy in Metastatic Breast Cancer." Breast Cancer Research and Treatment **81**(0): 43-48.
Hendrich, A. B. (2006). "Flavonoid-membrane interactions: possible consequences for biological effects of some polyphenolic compounds1." Acta Pharmacologica Sinica **27**(1): 27-40.
Hillery, A. M. (2000). "New liposomal formulation of vincristine for non-Hodgkin's lymphoma." Pharmaceutical Science & Technology Today **3**(3): 79-80.
Hollman, P. C. H., Gaag, M. V. D., et al. (1996). "Absorption and disposition kinetics of the dietary antioxidant quercetin in man." Free Radical Biology and Medicine **21**(5): 703-707.
Horton, J. K., Houghton, P. J., et al. (1988). "Relationships between tumor responsiveness, vincristine pharmacokinetics and arrest of mitosis in human tumor xenografts." Biochem Pharmacol **37**(20): 3995-4000.
Hristova, K. and Needham, D. (1994). "The Influence of Polymer-Grafted Lipids on the Physical Properties of Lipid Bilayers: A Theoretical Study." Journal of Colloid and Interface Science **168**(2): 302-314.
Huang, S. L. (2010). "Ultrasound-responsive liposomes." Methods Mol Biol **605**: 113-28.
Hung, H. (2007). "Dietary quercetin inhibits proliferation of lung carcinoma cells." Forum Nutr **60**: 146-57.
Ioku, K., Tsushida, T., et al. (1995). "Antioxidative activity of quercetin and quercetin monoglucosides in solution and phospholipid bilayers." Biochim Biophys Acta **1234**(1): 99-104.
Iyer, L. V., Furimsky, A. M., et al. (2006). "PI-49 Inhibition of 7-ethyl-10-hydroxy-camptothecin (SN-38) glucuronidation by dietary flavonoids
" Clin Pharmacol Ther **79**(2): P20-P20.
Jackson, D. V., Jr. and Bender, R. A. (1979). "Cytotoxic thresholds of vincristine in a murine and a human leukemia cell line in vitro." Cancer Res **39**(11): 4346-9.
Jeong, J. H., An, J. Y., et al. (2008). "Quercetin-induced ubiquitination and down-regulation of Her-2/neu." J Cell Biochem **105**(2): 585-95.

Johnson, I. S., Armstrong, J. G., et al. (1963). "The Vinca Alkaloids: a New Class of Oncolytic Agents." Cancer Res **23**: 1390-427.

Johnston, M. J. W., Semple, S. C., et al. (2006). "Therapeutically optimized rates of drug release can be achieved by varying the drug-to-lipid ratio in liposomal vincristine formulations." Biochimica et Biophysica Acta (BBA) - Biomembranes **1758**(1): 55-64.

Jones, D. J. L. (1998). "Determination of quercetin in human plasma by HPLC with spectrophotometric or electrochemical detection." Biomedical Chromatography **12**(4): 232-235.

Joseph, D. R. (1911). "On the formation of precipitates after the intravenous injection of salvarsan " The Journal of Experimental Medicine **14**(1): 83-98.

Kawato, Y., Aonuma, M., et al. (1991). "Intracellular roles of SN-38, a metabolite of the camptothecin derivative CPT-11, in the antitumor effect of CPT-11." Cancer Res **51**(16): 4187-91.

Kedar, U., Phutane, P., et al. (2010). "Advances in Polymeric Micelles for Drug Delivery and Tumor Targeting." Nanomedicine.

Keppen, M. (2010). "Chemotherapy principles for breast, prostate, colon and lung cancer." S D Med **Spec No**: 52-6.

Keshtgar, M., Davidson, T., et al. (2010). "Current status and advances in management of early breast cancer." International Journal of Surgery **8**(3): 199-202.

Khaled, K. A. and El-Sayed, Y. M. (2000). "High Performance Liquid Chromotographic Assay For The Determination of Quercetin in Plasma." Journal of Liquid Chromatography & Related Technologies **23**(3): 455 - 465.

Kirby, C., Clarke, J., et al. (1980). "Cholesterol content of small unilamellar liposomes controls phospholipid loss to high density lipoproteins in the presence of serum." FEBS Lett **111**(2): 324-8.

Kitagawa, S., Tanaka, Y., et al. (2009). "Enhanced skin delivery of quercetin by microemulsion." Journal of Pharmacy and Pharmacology **61**(7): 855-860.

Koo, O. M. Y., Rubinstein, I., et al. (2006). "Camptothecin in sterically stabilized phospholipid nano-micelles: A novel solvent pH change solubilization method." Journal of Nanoscience and Nanotechnology **6**(9-10): 2996-3000.

Krainer, M. (2003). "Efficacy of Combination Therapy Versus Monotherapy." Breast Cancer Research and Treatment **00081**(00001): 11-16.

Krishna, R., Webb, S. M., et al. (2001). "Liposomal and Nonliposomal Drug Pharmacokinetics after Administration of Liposome-Encapsulated Vincristine and Their Contribution to Drug Tissue Distribution Properties." J Pharmacol Exp Ther **298**(3): 1206-1212.

Krol, W., Dworniczak, S., et al. (2002). "Synthesis and tumoricidal activity evaluation of new morin and quercetin sulfonic derivatives." Acta Pol Pharm **59**(1): 77-9.

Kubo, T., Sugita, T., et al. (2001). "Targeted systemic chemotherapy using magnetic liposomes with incorporated adriamycin for osteosarcoma in hamsters." Int J Oncol **18**(1): 121-5.

Lamson, D. W. and Brignall, M. S. (2000). "Antioxidants and cancer, part 3: quercetin." Altern Med Rev **5**(3): 196-208.

Langer, K., Balthasar, S., et al. (2003). "Optimization of the preparation process for human serum albumin (HSA) nanoparticles." Int J Pharm **257**(1-2): 169-80.

Laster, W. R., Jr., Schabel, F. M., Jr., et al. (1961). "Experimental evaluation of potential anticancer agents. IV. Host weight loss as it relates to false positives in drug evaluation." Cancer Res **21**: 895-906.

Laughton, M. J., Halliwell, B., et al. (1989). "Antioxidant and pro-oxidant actions of the plant phenolics quercetin, gossypol and myricetin. Effects on lipid peroxidation, hydroxyl radical generation and bleomycin-dependent damage to DNA." Biochem Pharmacol **38**(17): 2859-65.

Lee, J.-C., Kim, J., et al. (2003). "The antioxidant, rather than prooxidant, activities of quercetin on normal cells: : quercetin protects mouse thymocytes from glucose oxidase-mediated apoptosis." Experimental Cell Research **291**(2): 386-397.

Lee, L. T., Huang, Y. T., et al. (2002). "Blockade of the epidermal growth factor receptor tyrosine kinase activity by quercetin and luteolin leads to growth inhibition and apoptosis of pancreatic tumor cells." Anticancer Res **22**(3): 1615-27.

Lee, R. J. (2006). "Liposomal delivery as a mechanism to enhance synergism between anticancer drugs." Molecular Cancer Therapeutics **5**(7): 1639-1640.

Lee, T. J., Kim, O. H., et al. (2006). "Quercetin arrests G2/M phase and induces caspase-dependent cell death in U937 cells." Cancer Lett **240**(2): 234-42.

Leslie, E. M., Mao, Q., et al. (2001). "Modulation of Multidrug Resistance Protein 1 (MRP1/ABCC1) Transport and ATPase Activities by Interaction with Dietary Flavonoids." Mol Pharmacol **59**(5): 1171-1180.

Leung, S.-h. S., Robinson, J. R., et al. (1987). Parenteral Products. Controlled drug delivery: fundamentals and applications. J. R. Robinson and V. H. L. Lee**:** 433-470.

Li, H., Zhao, X., et al. (2009). "Enhancement of gastrointestinal absorption of quercetin by solid lipid nanoparticles." Journal of Controlled Release **133**(3): 238-244.

Li, Y., Yang, Y., et al. (2009). "Simultaneous LC determination of quercetin, kaempferol and isorhamnetin in rabbits after

intragastric administration of an ethanol extract from Pollen Typhae." Chromatographia **69**(1-2): 117-121.
Loewe, S. (1957). "Antagonism and antagonists." Pharmacology review **9**: 237-242.
Lopez-Lazaro, M. (2002). "Flavonoids as anticancer agents: structure-activity relationship study." Curr Med Chem Anticancer Agents **2**(6): 691-714.
Maeda, H. (2002). Enhanced permeability and retention (EPR) effect: Basis for drug targeting to tumor. Biomedical aspects of drug targeting. V. Muzykantov and V. Torchilin. Massachusetts, Kluwer Academic Publishers**:** 211-228.
Matsumura, Y. and Maeda, H. (1986). "A new concept for macromolecular therapeutics in cancer chemotherapy: mechanism of tumoritropic accumulation of proteins and the antitumor agent smancs." Cancer Res **46**(12 Pt 1): 6387-92.
Maurer-Spurej, E., Wong, K. F., et al. (1999). "Factors influencing uptake and retention of amino-containing drugs in large unilamellar vesicles exhibiting transmembrane pH gradients." Biochimica et Biophysica Acta (BBA) - Biomembranes **1416**(1-2): 1-10.
Mayer, L. D., Bally, M. B., et al. (1986). "Uptake of adriamycin into large unilamellar vesicles in response to a pH gradient." Biochim Biophys Acta **857**(1): 123-6.
Mayer, L. D., Cullis, P. R., et al. (1994). "The use of transmembrane pH gradient-driven drug encapsulation in the pharmacodynamic evaluation of liposomal doxorubicin." J Liposome Res **4**: 529-553.
Mayer, L. D., Harasym, T. O., et al. (2006). "Ratiometric dosing of anticancer drug combinations: controlling drug ratios after systemic administration regulates therapeutic activity in tumor-bearing mice." Mol Cancer Ther **5**(7): 1854-63.
Mayer, L. D., Tai, L. C., et al. (1990). "Characterization of liposomal systems containing doxorubicin entrapped in response to pH gradients." Biochim Biophys Acta **1025**(2): 143-51.
Mazzeo, J. R., Neue, U. D., et al. (2005). "Advancing LC performance with smaller particles and higher pressure." Analytical Chemistry **77**(23).
Messerer, C. L., Ramsay, E. C., et al. (2004). "Liposomal irinotecan: formulation development and therapeutic assessment in murine xenograft models of colorectal cancer." Clin Cancer Res **10**(19): 6638-49.
Mosmann, T. (1983). "Rapid colorimetric assay for cellular growth and survival: application to proliferation and cytotoxicity assays." J Immunol Methods **65**(1-2): 55-63.
Movileanu, L., Neagoe, I., et al. (2000). "Interaction of the antioxidant flavonoid quercetin with planar lipid bilayers." International Journal of Pharmaceutics **205**(1-2): 135-146.

Mui, B. and Hope, M. J. (2007). Formation of large Unilamellar Vesicles by extrusion. Liposome technology. G. Gregoriadis, Informa Healthcare. **1:** 55-65.

Mulholland, P. J., Ferry, D. R., et al. (2001). Pre-clinical and clinical study of QC12, a water-soluble, pro-drug of quercetin. Ann Oncol. **12:** 245-8.

Nakayama, Y., Sakamoto, H., et al. (2000). "Tamoxifen and gonadal steroids inhibit colon cancer growth in association with inhibition of thymidylate synthase, survivin and telomerase expression through estrogen receptor beta mediated system." Cancer Lett **161**(1): 63-71.

Negishi, Y., Omata, D., et al. (2010). "Enhanced laminin-derived peptide AG73-mediated liposomal gene transfer by bubble liposomes and ultrasound." Mol Pharm **7**(1): 217-26.

Noble, C. O., Guo, Z., et al. (2009). "Characterization of highly stable liposomal and immunoliposomal formulations of vincristine and vinblastine." Cancer Chemotherapy and Pharmacology **64**(4): 741-751.

Nounou, M. M., El-Khordagui, L. K., et al. (2006). "In vitro release of hydrophilic and hydrophobic drugs from liposomal dispersions and gels." Acta Pharmaceutica **56**(3): 311-324.

Nováková, L., Matysová, L., et al. (2006). "Advantages of application of UPLC in pharmaceutical analysis." Talanta **68**(3): 908-918.

Papahadjopoulos, D., Allen, T. M., et al. (1991). "Sterically stabilized liposomes: improvements in pharmacokinetics and antitumor therapeutic efficacy." Proc Natl Acad Sci U S A **88**(24): 11460-4.

Park, K., de Oca, G., et al. (2009). "Determination of quercetin concentrations in fish tissues after feeding quercetin-containing diets." Aquaculture International **17**(6): 537-544.

Parkin, D. M., Bray, F., et al. (2005). "Global Cancer Statistics, 2002." CA Cancer J Clin **55**(2): 74-108.

Paterson, A. R. and Moriwaki, A. (1969). "Combination chemotherapy: synergistic inhibition of lymphoma L5178Y cells in culture and in vivo with 6-mercaptopurine and 6-(methylmercapto)purine ribonucleoside." Cancer Res **29**(3): 681-6.

Pawlikowska-Pawlega, B., Ignacy Gruszecki, W., et al. (2007). Modification of membranes by quercetin, a naturally occurring flavonoid, via its incorporation in the polar head group. Biochim Biophys Acta. **1768:** 2195-204.

Perez, E. A., Hillman, D. W., et al. (2004). "Randomized phase II study of two irinotecan schedules for patients with metastatic breast cancer refractory to an anthracycline, a taxane, or both." J Clin Oncol **22**(14): 2849-55.

Priprem, A., Watanatorn, J., et al. (2008). "Anxiety and cognitive effects of quercetin liposomes in rats." Nanomedicine: Nanotechnology, Biology, and Medicine **4**(1): 70-78.

Ramos, S. (2007). "Effects of dietary flavonoids on apoptotic pathways related to cancer chemoprevention." J Nutr Biochem **18**(7): 427-42.

Ramsay, E. C., Anantha, M., et al. (2008). "Irinophore C: A liposome formulation of irinotecan with substantially improved therapeutic efficacy against a panel of human xenograft tumors." Clinical Cancer Research **14**(4): 1208-1217.

Ranelletti, F. O., Maggiano, N., et al. (2000). "Quercetin inhibits p21-RAS expression in human colon cancer cell lines and in primary colorectal tumors." Int J Cancer **85**(3): 438-45.

Ratnam, D. V., Ankola, D. D., et al. (2006). "Role of antioxidants in prophylaxis and therapy: A pharmaceutical perspective." Journal of Controlled Release **113**(3): 189-207.

Ries, F. and Dicato, M. (1991). "Treatment of advanced and refractory breast cancer with doxorubicin, vincristine and continuous infusion of verapamil. a phase I-II clinical trial." Medical Oncology **8**(1): 39-43.

Rogerio, A. P., Dora, C. L., et al. (2010). "Anti-inflammatory effect of quercetin-loaded microemulsion in the airways allergic inflammatory model in mice." Pharmacological Research **61**(4): 288-297.

Rosen, L. S. (1998). "Irinotecan in lymphoma, leukemia, and breast, pancreatic, ovarian, and small-cell lung cancers." Oncology (Williston Park) **12**(8 Suppl 6): 103-9.

Saija, A., Scalese, M., et al. (1995). "Flavonoids as antioxidant agents: Importance of their interaction with biomembranes." Free Radical Biology and Medicine **19**(4): 481-486.

Sandstroem, M. C., Ickenstein, L. M., et al. (2005). "Effects of lipid segregation and lysolipid dissociation on drug release from thermosensitive liposomes." Journal of Controlled Release **107**(1): 131-142.

Scambia, G., Ranelletti, F. O., et al. (1990). "Synergistic antiproliferative activity of quercetin and cisplatin on ovarian cancer cell growth." Anticancer Drugs **1**(1): 45-8.

Scherphof, G. L., Dijkstra, J., et al. (1985). "Uptake and intracellular processing of targeted and nontargeted liposomes by rat Kupffer cells in vivo and in vitro." Ann N Y Acad Sci **446**: 368-84.

Schwartz, P. E. and Smith, J. P. (1976). "Treatment of ovarian stromal tumors." Am J Obstet Gynecol **125**(3): 402-11.

Senior, J., Crawley, J. C., et al. (1985). "Tissue distribution of liposomes exhibiting long half-lives in the circulation after intravenous injection." Biochim Biophys Acta **839**: 1-8.

Senior, J. and Gregoriadis, G. (1982). "Is half-life of circulating liposomes determined by changes in their permeability?" FEBS Lett **145**(1): 109-14.

Senior, J. H. (1987). "Fate and behavior of liposomes in vivo: a review of controlling factors." Crit Rev Ther Drug Carrier Syst **3**(2): 123-93.

Shah, M. A. and Schwartz, G. K. (2001). "Cell Cycle-mediated Drug Resistance: An Emerging Concept in Cancer Therapy." Clin Cancer Res **7**(8): 2168-2181.

Shah, M. A. and Schwartz, G. K. (2001). "Cell cycle-mediated drug resistance: an emerging concept in cancer therapy." Clin Cancer Res **7**(8): 2168-81.

Sharma, A., Upadhyay, A. K., et al. (2009). "Inhibition of Hsp27 and Hsp40 potentiates 5-fluorouracil and carboplatin mediated cell killing in hepatoma cells." Cancer Biol Ther **8**(22): 2106-13.

Sharma, H., Sen, S., et al. (2005). "Molecular pathways in the chemosensitization of cisplatin by quercetin in human head and neck cancer." Cancer Biol Ther **4**(9): 949-55.

Singh, M. (1999). "Transferrin As A targeting ligand for liposomes and anticancer drugs." Curr Pharm Des **5**(6): 443-51.

Sliutz, G., Karlseder, J., et al. (1996). "Drug resistance against gemcitabine and topotecan mediated by constitutive hsp70 overexpression in vitro: implication of quercetin as sensitiser in chemotherapy." Br J Cancer **74**(2): 172-7.

Sofou, S. and Sgouros, G. (2008). "Antibody-targeted liposomes in cancer therapy and imaging." Expert Opin Drug Deliv **5**(2): 189-204.

Song, X., Zhao, Y., et al. (2008). "Dual agents loaded PLGA nanoparticles: Systematic study of particle size and drug entrapment efficiency." European Journal of Pharmaceutics and Biopharmaceutics **69**(2): 445-453.

Song, X., Zhao, Y., et al. (2008). "PLGA nanoparticles simultaneously loaded with vincristine sulfate and verapamil hydrochloride: Systematic study of particle size and drug entrapment efficiency." International Journal of Pharmaceutics **350**(1-2): 320-329.

Souza, E. F. d. and Teschke, O. (2003). "Liposome Stability Verification by Atomic Force Microscopy." Reviews on Advanced Materials Science **5**: 34-40.

Steel, G. and Peckham, M. (1979). "Exploitable mechanisms in combined radiotherapy-chemotherapy: the concept of additivity." Int J Radiat Oncol Biol Phys **5**: 85-91.

Suzuki, R. and Maruyama, K. (2010). "Effective in vitro and in vivo gene delivery by the combination of liposomal bubbles (bubble liposomes) and ultrasound exposure." Methods Mol Biol **605**: 473-86.

Suzuki, R., Namai, E., et al. (2010). "Cancer gene therapy by IL-12 gene delivery using liposomal bubbles and tumoral ultrasound exposure." J Control Release **142**(2): 245-50.

Swartz, M. E. (2005). "UPLC: An introduction and review." Journal of Liquid Chromatography and Related Technologies **28**(7-8): 1253-1263.

Szejtli, J. (1991). "Cylodextrin in drug formulations: Part I." Pharm Technol Int. **3**: 15-23.

Szoka, F., Jr. and Papahadjopoulos, D. (1978). "Procedure for preparation of liposomes with large internal aqueous space and high capture by reverse-phase evaporation." Proc Natl Acad Sci U S A **75**(9): 4194-8.

Tang, D. Q., Yin, X. X., et al. (2009). "Gradient HPLC-DAD for the simultaneous determination of five flavonoids in plasma after intravenously administrated ginkgo biloba extract and its application in the study of pharmacokinetics in rats." Journal of Liquid Chromatography and Related Technologies **32**(14): 2065-2079.

Tardi, P., Johnstone, S., et al. (2009). "In vivo maintenance of synergistic cytarabine:daunorubicin ratios greatly enhances therapeutic efficacy." Leuk Res **33**(1): 129-39.

Tardi, P. G., Gallagher, R. C., et al. (2007). "Coencapsulation of irinotecan and floxuridine into low cholesterol-containing liposomes that coordinate drug release in vivo." Biochimica et Biophysica Acta (BBA) - Biomembranes **1768**(3): 678-687.

Torchilin, V. and Weissig, V. (2003). Liposomes: A Practical Approach Oxford ; New York : c2003, Oxford University Press.

Torchilin, V. P. (2006). "Recent approaches to intracellular delivery of drugs and DNA and organelle targeting." Annu Rev Biomed Eng **8**: 343-75.

Tsuchiya, H., Nagayama, M., et al. (2002). "Membrane-rigidifying effects of anti-cancer dietary factors." Biofactors **16**(3-4): 45-56.

Uchegbu, I. F. (1999). "Parenteral drug delivery: 1." Pharmaceutical Journal **263**(7060): 309-318.

van der Woude, H., Gliszczynska-Swiglo, A., et al. (2003). "Biphasic modulation of cell proliferation by quercetin at concentrations physiologically relevant in humans." Cancer Lett **200**(1): 41-7.

van der Woude, H., Gliszczynska-Swiglo, A., et al. (2003). "Biphasic modulation of cell proliferation by quercetin at concentrations physiologically relevant in humans." Cancer Letters **200**(1): 41-47.

Viroonchatapan, E., Sato, H., et al. (1996). "Magnetic targeting of thermosensitive magnetoliposomes to mouse livers in an in situ on-line perfusion system." Life Sci **58**(24): 2251-61.

Vlahos, C. J., Matter, W. F., et al. (1994). "A specific inhibitor of phosphatidylinositol 3-kinase, 2-(4-morpholinyl)-8-phenyl-4H-1-benzopyran-4-one (LY294002)." J Biol Chem **269**(7): 5241-8.

Vogelstein, B. and Kinzler, K. W. (1993). "The multistep nature of cancer." Trends Genet **9**(4): 138-41.

Wang, J., Sui, M., et al. (2010). "Nanoparticles for tumor targeted therapies and their pharmacokinetics." Curr Drug Metab **11**(2): 129-41.

Waterhouse, D. N., Madden, T. D., et al. (2005). Preparation, characterization, and biological analysis of liposomal formulations of vincristine. Liposomes, Part E. N. Düzgünes. San Diego, Elsevier Academic Press. **391:** 40-57.

Webb, M. S., Logan, P., et al. (1998). "Preclinical pharmacology, toxicology and efficacy of sphingomyelin/cholesterol liposomal vincristine for therapeutic treatment of cancer." Cancer Chemotherapy and Pharmacology **42**(6): 461-470.

Webb, M. S., Saxon, D., et al. (1998). "Comparison of different hydrophobic anchors conjugated to poly(ethylene glycol): effects on the pharmacokinetics of liposomal vincristine." Biochim Biophys Acta **1372**(2): 272-82.

Woo, J., Chiu, G. N. C., et al. (2008). "Use of a passive equilibration methodology to encapsulate cisplatin into preformed thermosensitive liposomes." International Journal of Pharmaceutics **349**(1-2): 38-46.

Woodle, M. C. and Lasic, D. D. (1992). "Sterically stabilized liposomes." Biochim Biophys Acta **1113**(2): 171-99.

Woodle, M. C. and Lasic, D. D. (1992). "Sterically stabilized liposomes." Biochimica et Biophysica Acta (BBA) - Reviews on Biomembranes **1113**(2): 171-199.

Wu, T. H., Yen, F. L., et al. (2008). "Preparation, physicochemical characterization, and antioxidant effects of quercetin nanoparticles." Int J Pharm **346**(1-2): 160-8.

Yang, C. Y. (2005). "Bioavailability and metabolic pharmacokinetics of rutin and quercetin in rats." Journal of Food and Drug Analysis **13**(3): 244-250.

Yang, C. Y., Hsiu, S. L., et al. (2005). "Bioavailability and metabolic pharmacokinetics of rutin and quercetin in rats." Journal of Food and Drug Analysis **13**(3): 244-250.

Yang, G.-J., Liu, P., et al. (2007). "The simultaneous separation and determination of six flavonoids and troxerutin in rat urine and chicken plasma by reversed-phase high-performance liquid chromatography with ultraviolet-visible detection." Journal of Chromatography, B: Analytical Technologies in the Biomedical and Life Sciences **856**(1-2): 222-228.

Yeh, Y. A., Herenyiova, M., et al. (1995). "Quercetin: synergistic action with carboxyamidotriazole in human breast carcinoma cells." Life Sci **57**(13): 1285-92.

Yoshida, M., Yamamoto, M., et al. (1992). "Quercetin arrests human leukemic T-cells in late G1 phase of the cell cycle." Cancer Res **52**(23): 6676-81.

Yuan, Z. P., Chen, L. J., et al. (2006). "Liposomal quercetin efficiently suppresses growth of solid tumors in murine models." Clinical Cancer Research **12**(10): 3193-3199.

Zamboni, W. C. (2005). "Liposomal, Nanoparticle, and Conjugated Formulations of Anticancer Agents." Clin Cancer Res **11**(23): 8230-8234.

Zenkevich, I. G., Eshchenko, A. Y., et al. (2007). "Identification of the Products of Oxidation of Quercetin by Air Oxygen at Ambient Temperature." Molecules **12**: 19.

Zhang, J. A., Anyarambhatla, G., et al. (2005). "Development and characterization of a novel Cremophor(R) EL free liposome-based paclitaxel (LEP-ETU) formulation." European Journal of Pharmaceutics and Biopharmaceutics **59**(1): 177-187.

Zhao, X., Wu, J., et al. (2007). "Liposomal coencapsulated fludarabine and mitoxantrone for lymphoproliferative disorder treatment." J Pharm Sci.

Zheng, Y., Haworth, I. S., et al. (2005). "Physicochemical and structural characterization of quercetin-beta-cyclodextrin complexes." Journal of Pharmaceutical Sciences **94**(5): 1079-1089.

Zhigaltsev, I. V., Maurer, N., et al. (2005). "Liposome-encapsulated vincristine, vinblastine and vinorelbine: A comparative study of drug loading and retention." Journal of Controlled Release **104**(1): 103-111.